Dissertation

Lipoprotein-associated Phospholipase A_2 in Placenta and Fetus – Effect of Obesity and Gestational Diabetes

vorgelegt von
Mag. rer. nat. Carolin SCHLIEFSTEINER

zur Erlangung des akademischen Grades
Doctor of Philosophy (PhD)

an der
Medizinischen Universität Graz
Univ. Klinik für Frauenheilkunde und Geburtshilfe

Unter der Betreuung von
Assoz. Prof. Dr. Christian WADSACK
und
Prof. Dr. Gernot DESOYE

August 2017

Statutory Declaration

I hereby declare that this thesis is my own original work and that I have fully acknowledged by name all of those individuals and organizations that have contributed to the research for this thesis. Acknowledgement has been made in the text and appendix to all other materials used. Throughout this thesis and in all related publications I followed the “Standards of Good Scientific Practice and Ombuds Committee at the Medical University of Graz“.

Graz, 21.08.2017 Carolin Schliefsteiner

Disclosures

The contents of this thesis have been published in peer-reviewed journals and permission for re-print of the Figures has been given within the Open-Access-Publication agreements of the respective publishing groups.

The thesis is based on the following two publications:

1. Human placental Hofbauer Cells maintain an anti-inflammatory M2 phenotype despite the presence of Gestational Diabetes Mellitus. Schliefsteiner C, Peinhaupt M, Kopp S, Loegl J, Lang-Olip I, Hiden U, Heinemann A, Desoye G, Wadsack C. *Front. Immunol. 2017| doi: 10.3389/fimmu.2017.00888*

2. Maternal Gestational Diabetes Mellitus increases placental and foetal lipoprotein-associated Phospholipase A2 which might exert protective functions against oxidative stress. Schliefsteiner C, Hirschmugl B, Kopp S, Curcic S, Bernhart EM, Marsche G, Lang U, Desoye G, Wadsack C. *Article re-submitted to ‚Scientific Reports' after revision.*

All co-authors gave their consent to re-use data from these publications within this thesis. The following co-authors contributed data shown in this thesis:

Jelena Lögl established and taught me the protocol for Hofbauer cell isolation.

Susanne Kopp prepared and stained the serial tissue sections in Figures 8, 9 and 10, as well as the fluorescence stainings in Figures 15 and 20.

Ingrid Lang-Olip provided the quantification of HBC in histological sections shown in Figure 10.

Miriam Peinhaupt performed the Multiplex ELISA-on-bead-assay with me and carried out all data analysis for this assay. This data is summarized in Table 5.

Eva Maria Bernhart helped establishing all ECIS set-ups and ECIS data analysis shown in Figure 21.

Sanja Curcic performed the Dihydrorhodamine assay shown in Figure 22.

This thesis project was undertaken with full financial support from the Austrian Science Fund (FWF) within the doctoral college MOLIN (Molecular Basis of Inflammation; W1421).

Zusammenfassung
Obwohl Diabetes gemeinhin eher als Stoffwechselerkrankung verstanden wird, liegen vermehrt HInweise dafür vor, dass auch Entzündungsprozesse diese Pathologie determinieren. Gestationsdiabetes (GDM) ist definiert als Diabetes, der erstmals während der Schwangerschaft auftritt und/oder diagnostiziert wird. Verschiedene Studien haben in der Vergangenheit gezeigt, dass GDM entzündliche Veränderungen in Mutter und Kind, sowie der Plazenta – dem Organ, das beide verbindet – bewirkt. Zu diesen entzündlichen Veränderungen zählen beispielsweise erhöhte Konzentrationen von pro-inflammatorischen Zytokinen aber auch Biomarkern für Vaskulopathie in mütterlichem und kindlichem Blut. In der Plazenta steigt durch GDM die Zahl der Immunzellen, und auch verschiedene inflammatorische, metabolische und anti-oxidative Moleküle werden unterschiedlich exprimiert.

In der vorliegenden Studie wurden feto-plazentare Makrophagen, sogenannte Hofbauer Zellen (HBC) verwendet. Humane Makrophagen sind sehr plastische Zellen, die für gewöhnlich in klassisch aktivierte, pro-inflammatorische Makrophagen (M1 polarisiert) und in alternativ aktivierte, regulatorische Makrophagen (M2 polarisiert) eingeteilt werden. Diese Klassifizierung beruht darauf, dass M1 und M2 Makrophagen unterschiedliche Oberflächenproteine auf der Zelle tragen und unterschiedliche Zytokine sezernieren.
Der erste Teil der vorliegenden Studie zielte darauf ab, festzustellen ob GDM, als nicht ausschließlich metabolische sondern auch entzündliche Erkrankung, dazu führt dass HBCs in der Plazenta ihre Polarisierung verändern. Dafür wurden HBC aus Kontroll- und GDM-Plazenten isoliert und hinsichtlich ihrer Oberflächenproteine – durch Histochemie und FACS – und sezernierter Zytokine durch ELISA, untersucht. Die Ergebnisse dieser Experimente deuten darauf hin, dass HBCs ihren M2 Phenotyp trotz GDM beibehalten, da kaum Unterschiede zwischen den Zellpopulationen gefunden wurden.

Im zweiten Teil der Studie wurde ein Enzym untersucht, welches vornehmlich von Makrophagen gebildet und sezerniert wird. Dieses Enzym, Lipoprotein-assoziierte Phospholipase A_2 ($LpPLA_2$), bindet im Blut an low-density lipoprotein (LDL, 80% im Erwachsenen) und high-density lipoprotein (HDL, 20%) und zirkuliert in dieser Form im Plasma. Das bevorzugte Substrat von $LpPLA_2$ sind oxidierte Phospholipide. Es ist nicht vollständig geklärt, ob $LpPLA_2$ eher entzündungsfördernde oder entzündungshemmende Wirkung besitzt. Laut Studien ist $LpPLA_2$ im mütterlichen Blut erhöht in jenen Schwangerschaften, die durch Präeklampsie oder GDM beeinträchtigt sind. Welche Bedeutung $LpPLA_2$ in Plazenta oder Fötus hat, ist weitgehend unbekannt.

Daher war es das Ziel des zweiten Teils dieser Studie, $LpPLA_2$ Aktivität sowie die Regulierung des Enzyms in den feto-plazentaren Hofbauer Zellen zu untersuchen. Zu diesem Zweck wurden HBC aus gesunden und GDM Plazenten isoliert. GDM-HBC zeigten signifikant mehr $LpPLA_2$ Aktivität als Kontrollzellen. *In vitro* wurde die $LpPLA_2$ Aktivität von HBCs positiv durch Insulin, Leptin und entzündungsfördernde Zytokine reguliert, wohingegen entzündungshemmende Zytokine die Aktivität negativ regulierten.
Da $LpPLA_2$ im Plasma zirkuliert, wurden außerdem fötale Lipoproteine (LDL und HDL) aus dem Nabelschnurplasma von gesunden und GDM Föten isoliert und hinsichtlich ihrer $LpPLA_2$ Aktivität und der Verteilung zwischen LDL und HDL untersucht. Im Gegensatz zum Erwachsenen, wurde HDL als hauptsächlicher Träger von $LpPLA_2$ Aktivität im Fötus

identifiziert. Außerdem war die HDL-$LpPLA_2$ Aktivität in der GDM Gruppe signifikant erhöht und zeigte eine positive Korrelation mit mütterlichem Body-Mass-Index (BMI), sowohl vor als auch am Ende der Schwangerschaft.
Eine Mischung oxidierter Phospholipide sowie ein spezifischer Inhibitor der $LpPLA_2$ Aktivität wurden verwendet, um die Funktionalität von HDL-$LpPLA_2$ *in vitro* zu untersuchen. Im Zellversuch mit plazentaren Endothelzellen konnte gezeigt werden, dass HDL-$LpPLA_2$ in Plazenta und Fötus möglicherweise anti-oxidative und vaskulo-protektive Eigenschaften besitzt.

Abstract

Although diabetes is generally perceived as metabolic disease, it has an additive underlying link to inflammatory mechanisms. Gestational diabetes mellitus (GDM) is defined as any form of diabetes with first on-set and/or recognition during pregnancy. In the past, several studies have shown that GDM causes inflammatory changes in mother and child, and also the placenta – the organ connecting the two. Among these changes are e.g. elevated pro-inflammatory cytokine levels and markers of vascular pathology in maternal and fetal blood, In the placenta, influx of immune cells in GDM has been demonstrated, as well as altered expression of inflammatory, metabolic and anti-oxidative molecules.

The study presented here, investigated feto-placental macrophages, so-called Hofbauer cells (HBCs). Human macrophages are very versatile cells and are usually described as either classically activated pro-inflammatory macrophages (M1 polarized) or alternatively activated tissue-remodeling macrophages (M2 polarized). M1 and M2 macrophages can be classified according to their expression of specific cell surface proteins and release of different cytokines. The first part of this study aimed to determine if GDM, being not only a metabolic but also inflammatory condition, could cause alterations in polarization of HBCs. To this extent, HBCs from control and GDM placentas were isolated, and surface proteins were investigated by histochemistry and FACS, cytokine release was measured by ELISA. The results obtained demonstrated that HBCs maintain an M2 polarized phenotype despite presence of GDM, as surface markers and cytokine release were barely changed between control and GDM-HBCs.

In the second part of this study, an enzyme produced almost exclusively by macrophages was investigated. This enzyme, lipoprotein associated phospholipase A_2 ($LpPLA_2$), once released from macrophages binds to low density lipoprotein (LDL, 80% in adults) and high density lipoprotein (HDL, 20%) and circulates in blood. It has a unique substrate preference for oxidized phospholipids. It is currently under discussion if $LpPLA_2$ has pro- or anti-inflammatory properties. In pregnancy, elevated maternal $LpPLA_2$ levels have been demonstrated in pre-eclampsia and GDM. Knowledge about $LpPLA_2$ in placenta and fetus is limited, however.

Therefore, $LpPLA_2$ activity and regulation in primary HBCs was investigated. It was found that HBCs isolated from GDM placenta released more $LpPLA_2$ activity than controls. $LpPLA_2$ activity was up-regulated *in vitro* by insulin, leptin, and pro-inflammatory cytokines, but down-regulated by anti-inflammatory cytokines. Furthermore, as $LpPLA_2$ circulates associated to lipoproteins, fetal lipoproteins from cord blood of healthy and GDM fetuses were isolated and investigated for $LpPLA_2$ activity and distribution among lipoproteins. HDL was identified as major carrier of $LpPLA_2$ in the fetus, which is in contrast to adults. Also, HDL-$LpPLA_2$ was significantly increased in GDM and positively correlated with maternal BMI. A mixture of oxidized phospholipids as well as a specific inhibitor of $LpPLA_2$ activity were employed to conduct functional assays on placental endothelial cells with native HDL and HDL with inactivated $LpPLA_2$. These results demonstrated that HDL-$LpPLA_2$ in placenta and fetus might exert anti-oxidative and vasculo-protective actions.

Table of Contents

List of Abbreviations

A

AA	Amino acid
AGEs	Advanced glycation end products
ANOVA	Analysis of variance
AOC	Anti-oxidative capacity
ATM	Adipose tissue macrophages

B

b-HCG	Human choriongonadotropin beta
BCA	Bichinonic acid
BMI	Body mass index
BSA	Bovine serum albumin

C

CCR7	Chemokine receptor type 7
CD	Cluster of differentiation
CETP	Cholesterol ester transfer protein
CK7	Cytokeratin 7
CM	Conditioned medium
CRP	C-reactive protein

D

DHR	Dihydrorhodamine
DMEM	Dulbeccos modified eagle medium

E

EBM	Endothelial basal medium
EC	Endothelial cells
ECIS	Electrical cell-substrate impedance sensing
EDTA	Ethylen-diamine-tetra-acetate
EGF	Epithelial growth factor
EL	Endothelial lipase
ELISA	Enzym linked immunosorbent assay

F

FABP	Fatty acid binding protein
FACS	Fluorescence assisted cell sorting
FCS	Fetal calf serum
FFA	Free fatty acid
FGF basic	Fibroblast growth factor
FTT	First trimester trophoblast
FV	Fetal vessels

G

GA	Gestational age
GCs	Glucocorticoids
GDM	Gestational diabetes mellitus
GLUT	Glucose transporter
GM-CSF	Granulocyte macrophage colony stimulating factor

H

HbA1c	Glycated hemoglobin
HBCs	Hofbauer cells
HCA	Histopathological chorioamnionitis
HDL	High density lipoprotein
HDL-C	HDL-cholesterol
HIV	Human immunodeficiency virus

I

IC	Immune complexes
ICAM-1	Intracellular adhesion molecule 1
ICC	Immune cytochemistry
ICH	Immune histochemistry
ICs	Immune complexes
IF	Immune fluorescence staining
IL-	Interleukin
INFɣ	Interferon ɣ

L

LDL	Low density lipoprotein
LDL-C	LDL-cholesterol
LFA-1	Lymphocyte function-associated antigen 1
LGA	Large-for-gestational age
LIF	Leukemia inhibiting factor
LPDS	Lipoprotein deficient serum
LPL	Lipoprotein lipase
LpPLA2	Lipoprotein-associated phospholipase A2
LPS	Lipopolysaccharide
LRP-1	LDL-receptor related protein 1
lysoPC	Lyso-phosphotidylcholine

M

MaM	Macrophage medium
MAPK	Mitogen activated protein kinase
MCP-1	Monocyte chemotactic protein 1
MCP-3	Monocyte chemotactic protein 3
MDA	Malondialdehyd
MM-LDL	Minimally modifed LDL
MoD	Mode of delivery
MPO	Myeloperoxidase
mTOR	Mechanistic target of rapamycin
MwCo	Molecular weight cut-off
MΦ	Macrophage

N

NFkB	Nuklear factor kappa light chain enhancer of B-cells

O

2-OHQ	2-hydroxyquinoline
oGTT	Oral glucose tolerance test
ONOO-	Peroxynitrite
oxPL	Oxidized phospholipids

P

pAECs	Placental arterial endothelial cells
PAF	Platelet activating factor
PAF-AH	Platelet activating factor- acetyl hydrolase
PAF-LL	PAF-like lipids (same as oxPL)
PAGE	Polyacrylamide gel electrophoresis
PDGF AB	Platelet derived growth factor AB
PE	Pre-eclampsia
PI	Ponderal Index
PI3K	Phosphoinositol 3 kinase
PLA2G2A	Phospholipase A2 Group 2A
PLA2G5	Phospholipase A2 Group 5
PLA2G7	Phospholipase A2 Group 7
PlGF	Placental growth factor
PON-1	Paraxonase-1
pVECs	Placental venous endothelial cells

Q

qRT-PCR	Quantitative real-time polymerase chain reaction

S

SC	Syncytiotrophoblast
SD	Standard deviation
SEL	Sub-endothelial layer
SEL	Subendoehtlial layer
SEM	Standard error of the mean
SR-BI	Scavenger receptor B1

T

T1DM	Type 1 diabetes mellitus
T2DM	Type 2 diabetes mellitus
TAM	Tumor associated macrophages
TBARS	Thiobarbituric acid reactive species
TG	Triglycerides
TGF α/β	Transforming growth factor α/β
TLR	Toll-like receptor
TNFα	Tumor necrosis factor α
Treg	Regulatory T-cells
TT	Term trophoblast

V

VCAM-1	Vascular adhesion molecule 1
VE-Cadherin	Vascular endothelial cadherin
VEGF	Vascular endothelial growth factor
VLDL	Very low density lipoprotein
VUE	Villitis od unknown etiology
vWF	Van Willebrandt factor

W

WB	Western blot

1. Introduction

1.1 The Human Placenta - Anatomy, Cell Types and Function

The placenta is a highly-specialized organ formed temporarily for the duration of pregnancy in order to connect and at the same time separate maternal and fetal circulations and ensure fetal oxygen and nutrient supply. To cater to the different needs of different species during embryonic development, huge structural and functional variability in placentas of vertebrates is observed. Surprisingly, the human placenta is more comparable to ruminant placenta (e.g. sheep's) than to those of other primate species (1).
Macroscopically, the human placenta is a round-shaped, discoidal organ measuring about 25 centimeters in diameter, 2.5 centimeters in thickness, and weighs on average 500 grams (2). Discoidal means that there is only one single contact site between the feto-placental tissue with the maternal uterine wall.
As a connective organ between mother and fetus, the placenta is considered to have a maternal and a fetal side. The maternal side is referred to as basal plate, it is sub-divided into placental lobes by grooves and clefts (Figure 1, right panel). It contains a mixture of cells, e.g. extravillous trophoblast cells (derived from fetal tissue), and maternal decidual stroma cells, e.g. decidual macrophages and natural killer (dNK) cells (2). It also contains various extracellular matrix proteins and fibrinoid (3). The fetal side is referred to as chorionic plate, it is covered by the amnion (Figure 1, left panel). The umbilical cord inserts into the chorionic plate to connect the fetal circulation to the placenta.

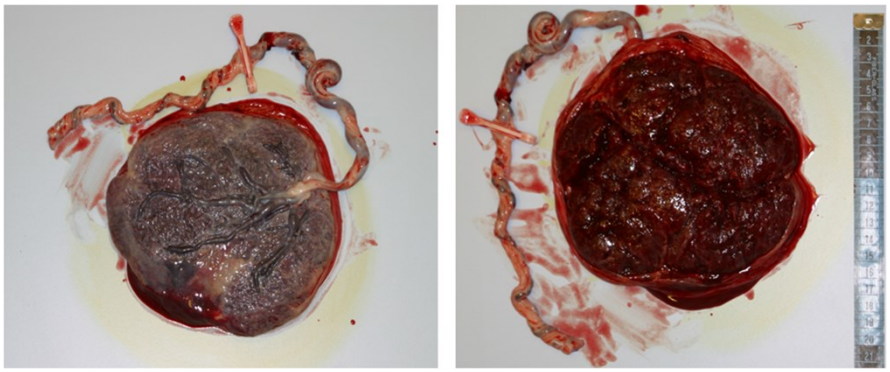

Figure 1: Macroscopic structure of the human placenta. Left panel: fetal side facing upwards, covered by the amniotic membrane. The umbilical cord and branching from it the chorionic arteries and veins are clearly visible. Right panel: maternal side facing upwards; zoning of placental tissue into lobes is visible.

Of note, the feto-placental systemic circulation has a reversed flow compared to adults, so oxygenated nutrient-rich blood is transported from the mother over the placental veins and finally the umbilical vein to the fetus. Nutrient-depleted blood is transported from the fetus back via the two umbilical arteries (Figure 2a).
Microscopically, the placenta has a hemochorial, villous-type architecture. Hemochorial means that maternal blood is in direct contact with the chorionic structures. Finally, a villus (*pl. villi*) is a structural feature of the placenta, resembling a tree with branches.

Placental villi reach into endometrial crypts and are directly surrounded by maternal blood (Figure 2b and c). Consequently, there is a multi-villous exchange surface between maternal and fetal blood flow, maximizing the available area for gas and nutrient exchange (1).

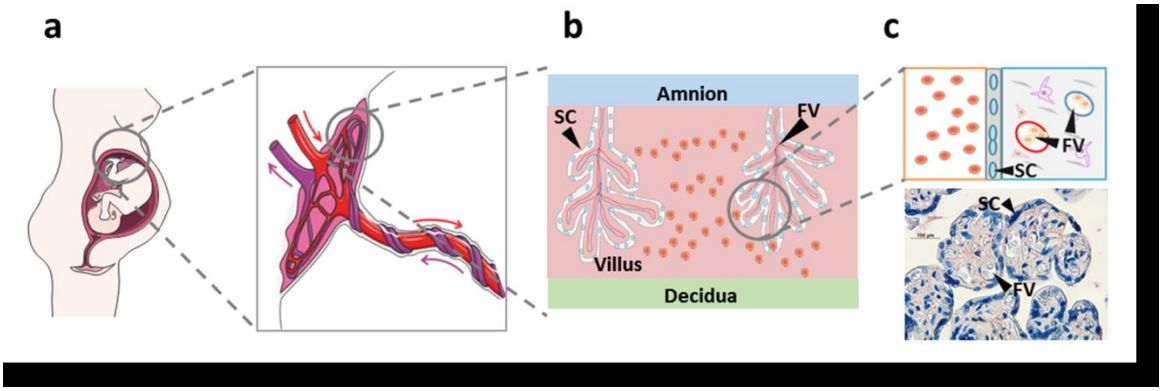

Figure 2: Microscopic architecture of the human placenta. a: The discoidal placenta is connected to the maternal uterine linings only at one single contact site. Placental blood flow is reversed compared to adult circulation: nutrient-rich, oxygenated blood is delivered within the umbilical vein (red) to the fetus, whereas nutrient-depleted blood is transported back into the placental vasculature by two umbilical arteries (blue). b: The placenta can be broken down into structural units called villi; each villus is surrounded by a syncytiotrophblast (SC) layer which is in direct contact with maternal blood (red dots). Within each villous branch, fetal vessels (blue and red lines) reside, so that nutrient and gas exchange may happen at the feto-maternal interface. Between the villi, there is the intervillous space. On the fetal side, the placenta is covered by the amnion and its membrane, on the maternal side the outmost layer of the basal plate is the decidua. c: Schematic cross-section and representative immune histochemistry through a placental villus. SC = fused multi-nucleated syncytiotrophoblast, FV = fetal vessels; the area within one villus between vessels is referred to as stroma and contains e.g. fibroblasts and macrophages.

One constituent cell type of the placenta is the trophoblast. The blastocyst, an intermediate state in embryonic development after conception but before implantation, is made of an outer trophoblast layer and the inner cell mass. The inner cell mass gives rise to the placental mesenchymal cells, umbilical cord and the fetus itself, whereas the trophoblast gives rise to the placenta and amnion. After tight attachment to the uterus (= implantation), the trophoblast fuses into one poly-nucleated layer called syncytiotrophoblast. As the placental architecture evolves, each placental villus is surrounded by the syncytiotrophoblast. It is the only cell type that is in direct contact with maternal blood, which - in absence of any vessel walls - perfuses the intervillous space (2). The syncytium surrounds the villous stroma, containing core stroma cells, such as fibroblasts and placental macrophages. Inside the villi, fetal blood runs in fetal arteries and veins: these vessels are lined with placental endothelial cells. *In vitro*, it was shown that placental endothelial cells from veins (pVECs) and arteries (pAECs) show differences in morphology and gene expression; pVECs have been described to have a more juvenile phenotype, capable of still differentiating into adipocytes and osteoblasts (4). pAECs have a more mature phenotype and show more classic endothelial morphology. Endothelial cells are crucial to placental branching angiogenesis and respond to angiogenic factors such as vascular endothelial growth factor (VEGF) and placental growth factor (5) (PlGF). Additionally, fetal vessels are supported by smooth muscle cells and pericytes (6). For this work, placental macrophages are the most relevant cell type and are therefore further reviewed in section 1.2.

Two essential main functions are achieved by the placenta and/or certain placental cell types: 1) nutrient transport and gas exchange between mother and growing fetus, and 2) induction of maternal tolerance against the semi-allogeneic fetus.

All three macronutrients, that are carbohydrates, proteins and lipids, cross the placenta to be available to the fetus. Carbohydrates in the form of glucose are specifically important, as the fetus is entirely dependent on maternal supply. Glucose flux across the placenta is achieved by facilitated diffusion and follows a maternal to fetal gradient. A sodium-independent transporter system has been found present on both the basal and apical side of the syncytiotrophoblast membrane. Glucose transporters GLUT1 (7), GLUT3 (8), and GLUT4 (9) are present in placental cells. GLUT1 is expressed by all placental cell types, GLUT3 by endothelial cells and GLUT4 by stroma cells. GLUT1 transporters apparently are not saturated and downregulated until glucose concentrations ranging between 20 and 25mM, therefore maternal hyperglycemia also affects the fetus (see section 1.3).

The growing fetus also has a high demand for proteins, i.e. amino acids (AA), as well as lipids, especially in the form of cholesterol and free fatty acids (FFA) in order to build up cell mass for organ development. Placental AA transfer is hardly studied in humans; some data indicate that the placenta can take up glutamate and serine (10) and that glutamate is further converted to glutamine (11). As serum concentrations of AA are increased in cord blood compared to maternal blood, some active transporters for AA must be expressed on the placenta (10), and has been demonstrated on mRNA level (12), however protein expression remains unclear.

Cholesterol and fatty acids are made available to the fetus from maternal lipoproteins which are taken up by the placenta via receptors and binding proteins fractionized by placental lipases. To cater to the fetal need for these nutrients, the maternal metabolism switches from an anabolic to a catabolic state throughout pregnancy and gestational hyperlipidemia develops (13). Plasma triglycerides (TG) can be elevated by about 300% and total cholesterol by about 50% in that specific physiological state (14). Similar to glucose, there is a maternal-to-fetal concentration gradient for FA across the placenta, and FA can traverse by facilitated diffusion. However, the majority of FA is packed within lipoproteins and must first be released from their esters. This is achieved in two steps: first maternal lipoproteins bind to respective receptors on the placenta. For triglyceride-rich very-low-density lipoprotein (VLDL) this is LDL receptor related protein 1 (LRP-1), for low-density lipoprotein (LDL) it is the LDL receptor (LDLR), and for high-density lipoprotein (HDL) it is scavenger receptor BI (SR-BI). VLDL and LDL are taken up by receptor-mediated endocytosis and broken down by intracellular lipases, whereas esterified fatty acids from HDL are hydrolyzed by triglyceride lipases and subsequently traverse the placenta with the help of carriers (fatty acid binding proteins, FABP) through fatty acid transporters. Both lipoprotein lipase (LPL) and endothelial lipase (EL) are expressed in syncytiotrophoblast (15), further aiding breakdown of triglycerides; similarly phospholipase activity in placental cells could support transport of phospholipids.
Transport of macronutrients is depicted schematically in Figure 3. Additionally, it is known that micronutrients such as iron and copper (16), calcium (17) and vitamins (18,19) traverse the placenta to be available to the fetus.

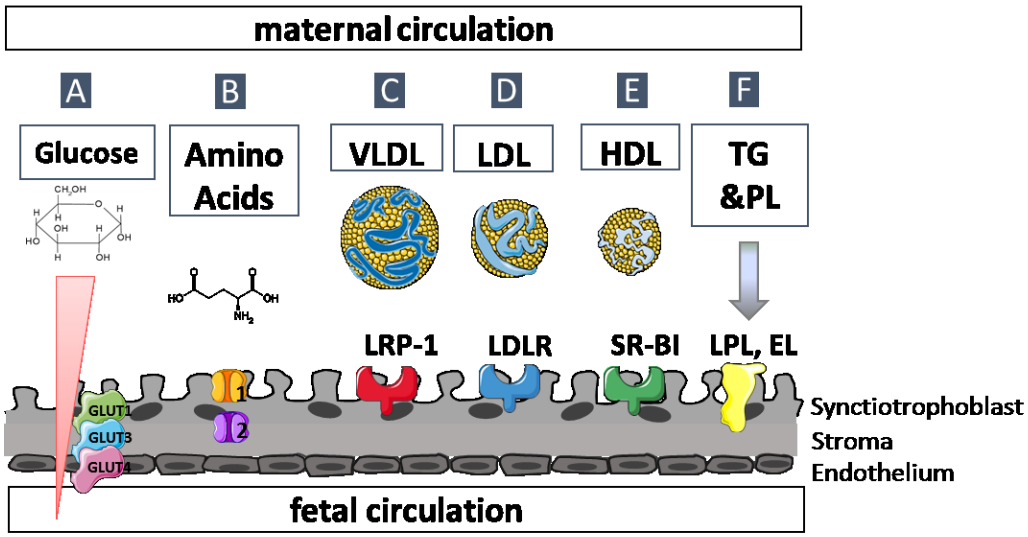

Figure 3: Macronutrient transport across the human placenta. A: Glucose transport across the human placenta follows a maternal-to-fetal gradient and is achieved by facilitated diffusion. Glucose transporters are present ubiquitously (GLUT1), in stromal cells (GLUT3) and on fetal endothelium (GLUT4). B: Transport of Amino Acids across the placenta may happen in two steps, depending on different transporters on the apical (1) and basal (2) side of the syncytial membrane. AA1 is transported through transporter 1, and reaches the endothelium after release from transporter 2. Possibly, AA1 can also be converted to AA2 within the placenta, before being released into fetal circulation via transporter 2. AA transporters can be Na^{2+}-dependent, and also exchange transporters specifically aiding influx of a certain AA1 in exchange for an AA2 exist. C and D: Triglyceride-rich lipoproteins VLDL and LDL bind to their respective receptors and are taken up by receptor-mediated endocytosis, TG are hydrolyzed by intracellular lipases, so that FFA can be released either into the fetal circulation or stored within the tissue for metabolic needs (20). E and F: Phospholipid and cholesterol-rich HDL binds to SR-BI, which facilitates transport of maternal cholesterol across the placenta. LPL, EL and putative phospholipases expressed on syncytiotrophoblast mediate release of FFA and phospholipids (PL). This figure has been adapted from (21).

1.2 Hofbauer Cells – Macrophages at the Feto-Maternal Interface

Macrophages are phagocytic cells that are recruited from the circulation as monocytes and undergo differentiation to become tissue-resident cells. They are part of the innate immune defense, and act as antigen presenting cells to T-cells, thereby contributing to the acute inflammatory response (22,23). But they are a versatile cell type, fulfilling many more functions then 'just' phagocytosis. Among the pleiotropic functions of macrophages tissue remodeling (24), wound healing (25) and promotion of vasculogenesis (= *de novo* formation of new blood vessels) and angiogenesis (= branching/sprouting of new blood vessels from existing ones) have been demonstrated (26,27). Because of this plasticity macrophages have been categorized into phenotypes called i) M1 – the classically activated, phagocytic macrophage promoting Type 1 inflammatory responses and ii) M2 – or alternatively activated macrophage, promoting Type 2 inflammatory response, wound healing and tissue remodeling; M2 macrophages have been further divided into subtypes M2a, M2b, M2c and M2d (28,29). Both M1 and the various M2 subsets are not only classified by their function, but also stimulation by and secretion of certain cytokines, as well as expression of defined

surface proteins which all act as specific markers to discriminate cellular subspecies. A summary of these respective hallmark cytokines and surface proteins is provided in Figure 4.

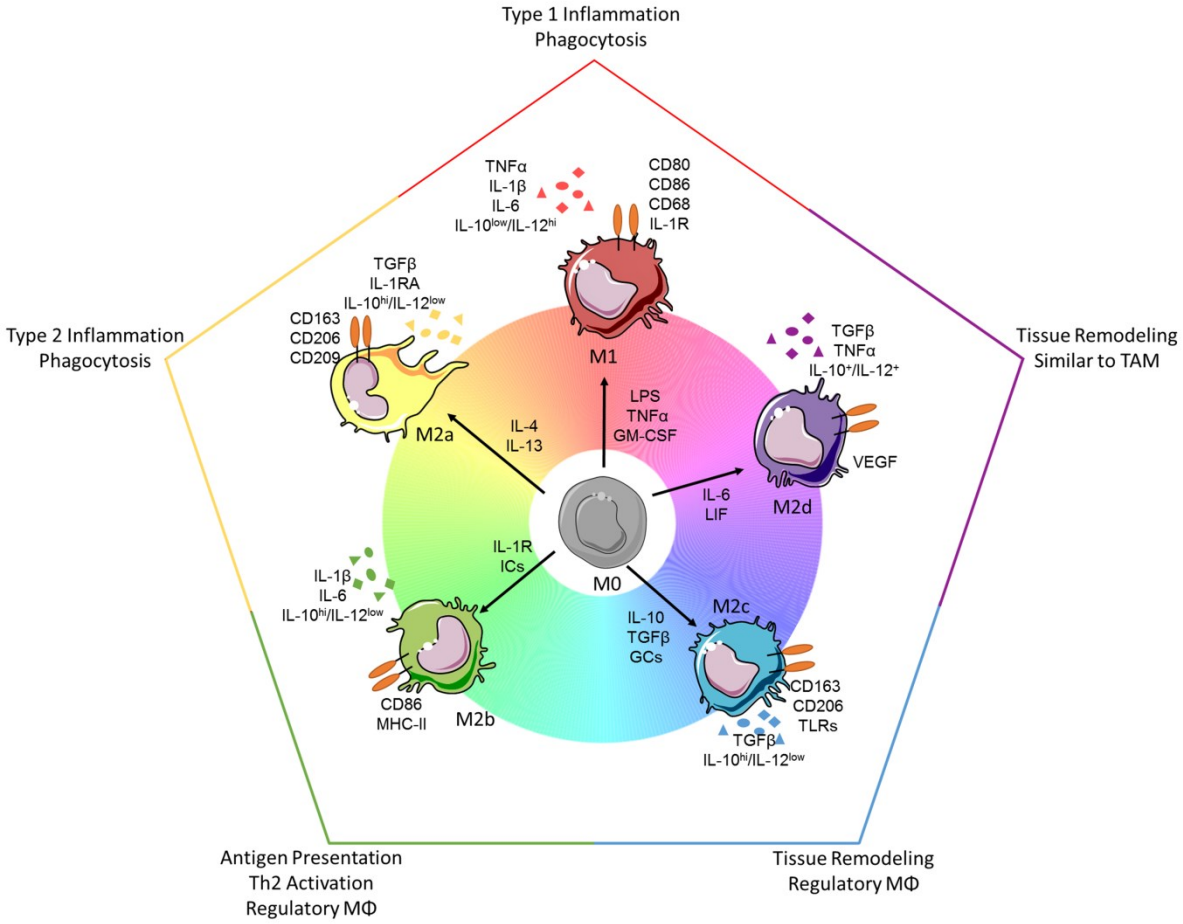

Figure 4: General concept of macrophage polarization into M1 and M2 phenotypes. Cytokines next to arrows represent the stimuli driving polarization towards a certain phenotype. Surface markers are represented by orange oval shapes and labeled accordingly. Secreted cytokines from polarized macrophages are shown next to each subtype in respective colors. Non-standard Abbreviations: ICs = immune complexes, GCs = glucocorticoids, LIF = leukemia inhibitory factor, TAM = tumor associated macrophages.

Macrophages of the feto-placental unit have been first described more than a century ago by J. Isfred Isidor Hofbauer (*1879-†1961); the cells have been termed 'Hofbauer cells' (HBCs) after their discoverer. HBCs are eosinophilic, mononuclear phagocytes. Within placental tissue, they present a round oval shape and are about 30µm in size. *In vitro*, we observed, that post-isolation the cells have a round shape, but start to stretch after 48-72h in cell culture, forming lamellopodia (see Figure 5a and b) – which has also been observed by other researchers (30). HBCs belong to the placental stroma cells and first appear as early as 5-weeks post-menstruation (31). In this early phase, it is believed that HBCs arise from mesenchymal cells (6), whereas after establishment of the fetal circulation they seem to be

recruited and differentiated from fetal monocytes (1,32). Typically, HBC cell numbers decrease from the first trimester until full-term (33).
A characteristic morphological feature is the high number of granules and vacuoles within the cells (Figure 5c and 5d). Maternal choriongonadotropin (β-hCG) is able to cross the placental barrier and enter fetal plasma through mesenchymal villi. The hormone influences male sex development. Excess β-hCG might therefore lead to irregular genital differentiation. HBCs take up excess β-hCG into their cytoplasmic vacuoles; the characteristic granulous morphology of HBCs can be induced in other macrophage cell lines by loading them with β-hCG *in vitro* (34).

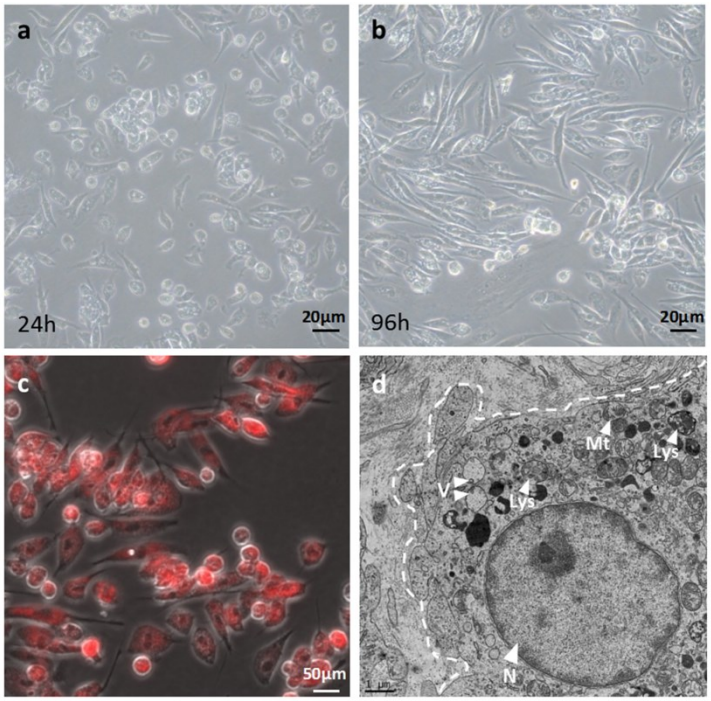

Figure 5: Hofbauer cell morphology in cell culture and ultra-structural analysis. a: Hofbauer cells in culture for 24 hours. A mixed morphology is visible, round shaped cells are characteristic early after isolation, long-stretched cells can be observed at later time points. b: After 96h in cell culture, the majority of cells shows long-stretched shapes and lamellopodia. c: Uptake of fluorescence labeled Dil-Ac-LDL is characteristic for macrophages, including HBCs. d: Ultrastructural analysis by transmitting electron microscopy (TEM. Dashed line = cell boarder, N= nucleus, V =vacuoles, Lys= phagolysosomes, Mt = mitochondria. Various vacuoles, endosomes and lysosomes are visible, characteristic for HBCs.

Similar to other macrophage populations, also HBCs seem to exert pleiotropic functions:

1. HBCs have been shown to both promote vertical transmission of maternal viral disease, e.g. infection with Zika virus (35,36), but also hinder other infections, e.g. with human immune deficiency virus (37,38) (HIV). With respect to bacterial infections, decreased numbers of HBCs have been observed in histopathological chorioamnionitis (39) (HCA) and increased HBC infiltration has been demonstrated in villitis of unknown etiology (40) (VUE). In summary, the role of HBCs in placental bacterial and viral infections therefore remains quite inconclusive.

2. HBCs have been shown to be involved placental vascular remodeling, vasculogenesis and angiogenesis. Seval et al. demonstrated close proximity of HBCs with endothelial

cells in placental tissue and found a positive correlation of HBC cell number with the number of vascular structures (41). Another study found that HBCs express some proteins of the Sprouty family, which are responsible for villous branching (42). Also, we recently demonstrated that conditioned medium of Hofbauer cells promotes in vitro tube formation of human placental endothelial cells in matrigel (43). Additionally, Hofbauer cells numbers have been shown to be decreased in pre-eclampsia, a condition characterized by aberrant spiral artery remodeling (44) indicating the physiological relevance to tissue remodeling of these cells *in vivo*.

3. HBCs have been shown to mediate maternal tolerance towards the fetus. As it carries 50% paternal genes, the fetus is semi-allogeneic, so major adaptation of the maternal immune system is required. Immunologic adjustment to pregnancy is achieved via cross-talk of maternal and fetal cells (45), and also hormonal changes (46). Hofbauer cells as well as T_{reg}-cells contribute to the immunologic environment needed for successful pregnancy (47). Inflammatory activated Hofbauer cells, on the other side, have been associated with miscarriage (48).

Within the concept of M1/M2 polarized macrophages, Hofbauer cells have generally been perceived to belong to the M2 phenotype. This is underpinned by 1) surface expression of M2 markers, such as CD163, CD206, and CD209 (49); 2) induction via anti-inflammatory cytokines such as IL-10 (50); 3) their functionality – angiogenic properties have only been described in M2 macrophages (51); and 4) epigenetic profiling demonstrating hypo-methylation of M2 associated genes (52).
Although studies have shown that HBCs maintain their M2 phenotype despite e.g. maternal allergy or chorioamnionitis (53), recent studies have challenged this claim, suggesting that HBCs might undergo a switch to a pro-inflammatory M1 phenotype, e.g. in pregnancies affected by Type 1 Diabetes (54).

1.3 Gestational Diabetes Mellitus – Nine Months and Beyond

Gestational Diabetes Mellitus (GDM) is defined as any on-set or first recognition of maternal hyperglycemia during pregnancy. Actually, maternal hyperglycemia is a physiological feature of pregnancy; the maternal metabolism switches from an anabolic to a more catabolic state to ensure the fetal energy supply. Most women adapt to these alterations however, in some GDM develops. Prevalence of the condition ranges from 3 to 20% of pregnancies, depending on the population – in central Europe about 5% of pregnancies are affected by GDM (55).
GDM is usually diagnosed after an oral glucose tolerance test (oGTT) at 24 to 28 weeks of gestation. In Austria, this test is a standard procedure within the 'Mutter-Kind-Pass' examinations. In other countries, there is no universal screening for GDM, but only women at specific risk for GDM undergo the oGTT. Risk factors include maternal pre-pregnancy overweight and obesity, hyperglycemia in previous pregnancies, family history of diabetes, advanced maternal age, and ethnicity. Whereas South-/East Asian women are at much higher risk for developing GDM compared to Caucasian women (56) independent of maternal BMI, whereas obesity is the strongest predictor of GDM in the Caucasian population (57).

GDM leads to changes in placental structures and function, causes altered nutrient transport to the fetus, and imposes in both maternal and fetal perinatal and long-term health. All of these topics are discussed in the following sections.

1.3.1 GDM- induced changes in placental morphology

Several studies have showed that placental architecture is changed in pregnancies affected by GDM. These studies employed mostly histological techniques and microscopy.
In a study comparing placentas from type 1, type 2 and GDM patients, it was found that GDM is associated with villous immaturity, fetal vasculopathy and inflammatory changes in placental tissue (58).
Another study found that capillary branching and as a consequence capillary bed surface area is higher in GDM placentas (59). At the same time, vascular barrier function seems to be impaired, as indicted by reduced expression of adherens junction proteins like VE-cadherin (60). In line with increased capillary branching, proteins related to placental angiogenesis were found to be increased in GDM placenta, e.g. receptors for vascular endothelial growth factor (61) (VEGF), and fibroblast growth factor (FGF) 2 (62).
Placental hypervascularization in GDM seems to be driven – at least in part- by insulin levels. Theoretically, the placenta is susceptible to maternal and fetal insulin signaling acting on trophoblast and endothelium respectively. Throughout gestation, a spatio-temporal shift occurs and fetal insulin signaling on endothelium becomes more relevant (63). Although maternal insulin can't cross the placenta, fetal hyperinsulinemia has been observed in diabetic pregnancy as a consequence of maternal hyperglycemia leading to fetal hyperglycemia (64). As a result, the feto-placental metabolism switches from anaerobic to aerobic state; therefore, oxygen demand rises. This is reflected by upregulation of VEGF receptors in the placenta (61) and erythropoietin in the fetus (65), leading to a hypoxic, pro-angiogenic environment. Additionally, the angiogenic properties of insulin on placental endothelial cells have been demonstrated using in vitro assays of tube formation and network formation (66).

1.3.2 GDM-induced changes in placental nutrient transport

In pregnancies affected by GDM, a higher proportion of children is born large-for-gestational age (LGA) or macrosomic, suggesting excessive nutrient transport across the placenta. From placenta perfusion studies, there is evidence that glucose transport is altered in GDM placenta, at least if women receive insulin therapy (67). Also expression of receptors of the insulin signaling pathway, PI3K and GLUT4 glucose transporter are changed in GDM placenta (68). Amino acid transfer is apparently unchanged in GDM pregnancies (69,70). In GDM, maternal dyslipidemia is characterized by increased plasma remnant lipoproteins and small, dense, atherogenic LDL. No concomitant changes in placenta and fetus have been demonstrated conclusively (71). However, increased levels of fatty acid binding proteins (FABP) 1, 3 and 4 have been found in GDM placenta (72), as well as upregulation of placental genes involved in lipogenic pathways (73), suggesting increased placental lipid delivery to the fetus.

1.3.3 Inflammation, Oxidative Stress and Endothelial Dysfunction

Gestational Diabetes has been associated with chronic low-degree inflammation in mother, placenta and fetus. Several studies have pointed in this direction, however, most of them focused on mRNA levels of inflammatory proteins. For instance, one microarray study found upregulation of several inflammatory pathway genes, such as IL-1, TNFα and its receptors and leptin (74) in GDM placenta. Others found increased mRNA levels of IL-6, TLR-4 and TGFβ, along with markers of macrophages and T-cells in GDM placenta, suggesting infiltration with immune cells (75). Protein data on inflammatory markers is limited and inconclusive if available. One meta-analysis including 22 studies measuring maternal plasma cytokine levels in GDM, showed trends towards increased IL-6 and TNFα in maternal plasma in GDM pregnancies, but no convincing significant changes (76). Data on inflammatory markers in newborn fetuses is limited: C-reactive protein (CRP) tended to be higher in cord blood of GDM fetuses compared to controls (77), and increased pro-inflammatory INF gamma levels have been found (78,79) as well as decreased levels of anti-inflammatory IL-10 (78).

In addition to inflammation, markers of oxidative stress have been found to be altered in GDM placenta, mother and fetus. Oxidative stress is an imbalance between the (unregulated) production of reactive oxygen species and the systems capability to detoxify these compounds, e.g. by enzymatic actions. Using placental tissue explants from normal and GDM pregnancies, it was demonstrated that in GDM placenta there is increased release of 8-isoprostane and increased activity of superoxide dismutase, both indication oxidative stress (80). In maternal and cord blood plasma, increased xanthine oxidase activity was found along with accelerated oxidative reactions and increased malondialdehyde levels (81).

1.3.4 Maternal and fetal long-term health

While gestational diabetes mellitus is a transient form of hyperglycemia and usually wears off after pregnancy, a clinical history of GDM has long term implications for maternal health. Specifically, a higher risk for transition to Type 2 diabetes mellitus (T2DM) later in life has been demonstrated by follow-up studies (82). In a Caucasian population from Sweden, for instance, a 35% higher risk of development of T2DM over a 15-year follow-up was found in women with history of GDM (83). Meta-analysis of different studies with varying follow-up duration ranging from 5 months to 15 years demonstrated that the risk for progression to T2DM increased the longer the follow-up period was (84). Co-morbidities alongside T2DM are also more frequent in women with history of GDM, e.g. cardiovascular disease (85), arterial stiffness (86), and hypertensive disorders (87).

Gestational diabetes does not only alter maternal susceptibility towards metabolic disorders, but also imposes risks in the offspring, both perinatal and long-term. As already mentioned, children born to GDM pregnancies are often bigger than average at birth. The two terms large-for-gestational-age (LGA) and macrosomia are commonly used to describe this feature, and are often used interchangeably: LGA is usually referred to if babys' length, weight, and/or had circumference lie above the 90th percentile for that gestational age (which is not necessarily full-term). Macrosomia literally translates to big body and is usually referred to if baby's weight at birth is higher than 4000-4500g, not relating the weight to gestational age. However, it is not only length and weight, or fetal ponderal index (relating the two parameters similar to body mass index in adults) that should be considered, but rather body composition. Anthropomorphic measurements have shown that newborns from GDM

pregnancies – despite similar birth weight – have decreased lean body mass but increased body fat compared to control newborns (88). Additionally, both LGA and macrosomia are linked to an increased risk for shoulder dystocia at birth, birth trauma of head and neck, and need for cesarean section (reviewed in (89,90)).
Long-term health outcome of children born to GDM pregnancies is characterized by increased BMI and central fat deposition in childhood and adolescence (91,92), and increased risk of progression to T2DM and cardiovascular disease which was corroborated by discordant sibling studies (91,93). Underlying epigenetic mechanisms contributing to increased risk for adult T2DM and obesity in children born to GDM mothers have been described (reviewed in (94)).
Considering that statistically half of the children born to GDM mothers are females having a higher risk for obesity and diabetes in their own pregnancies, a vicious cycle affecting future generations evolves. This vicious cycle is not only detrimental to a populations' health, but also is a burden to a society's economic wealth and productivity. Although no such data could be found for Europe, US economists have evaluated annual health costs of gestational diabetes and also projected healthcare costs because of diabetes in the future.
One study showed that GDM caused health costs of $636 million in 2007, of which approximately one third was covered by US Medicare (95)– in Europe, where medical care is primarily provided in a public manner, these costs would have to financed almost entirely with tax payers money. Another study looking at diabetes in general, found that in 2012 total estimated cost for diabetes in the US was $245 billion, a sum which included $69 billion of loss in work force productivity due to absence from or lower productivity at work, unemployment due to disease-related disabilities and lost capacity due to early mortality (96). Finally, an expenditure-projection-study found that until 2034 the number of people with diagnosed and undiagnosed diabetes will almost double, which will lead to a 3-fold increase in diabetes-related health cost spending (97). These numbers emphasize our need to understand gestational diabetes and its impact on mother and fetus in depth, to be able to provide not only treatment but also preventive measures against the disease.

1.4 Maternal Obesity – Foundation for a Fatty Future

Maternal pre-gravid obesity is not only a major risk factor for the development of gestational diabetes, but contributes by itself to peripartal complications (98), and maternal and fetal long-term health (99). For European countries, obesity prevalence in women ranges from 6 to 37% (100) and it is estimated that about 20% of pregnant women are overweight or obese (101).
Obesity is defined as a body-mass-index (BMI) higher than 30 kilograms per squared body length (kg/m^2). Overweight is defined as BMI higher than 25 kg/m^2 but lower than 30 kg/m^2. A BMI between 19 and 25 kg/m^2 is defined as lean, normal weight. Not only does BMI have to be considered, but also anthropomorphic data, such as e.g. waist circumference and distribution of fat mass (visceral/omental fat versus subcutaneous fat).
During the mid-nineties, it was established that adipose tissue itself is large endocrine organ, able to release certain cytokines, referred to as 'adipokines' as signaling molecules to other cells throughout the entire body (102,103). Alterations in adipokine production and secretion in adipose tissue of obese subjects have been observed (104,105) suggestive of inflammation of this tissue in obesity. Inflammation of adipose tissue has also been related to increased insulin resistance (106).

With respect to pregnancy, similar pathophysiological findings as in gestational diabetes (which is often accompanied by overweight/obesity) have been made. Obesity affects placenta, as well as mother and fetus. In plasma of obese pregnant women, increased levels of circulating CRP, leptin (107) and IL-6 (108,109) have been found as well as higher ICAM-1 levels (110), indicating both inflammation endothelial dysfunction (111).
In placental tissue of obese mothers, several changes have been found: on mRNA level, expression of IL1, TNFα, IL6 was found increased (112) as well as IL-8 and MCP-1 (108). Whereas the former study showed increased histochemical staining of macrophage markers CD68 and CD14, the latter did not find any infiltration of leukocytes in placental villi. Also changes affecting placental nutrient transport, especially lipids and fatty acids have been observed, e.g. increased expression of FABP4 on trophoblast (113), and of the phospholipase genes PLA2G2A and PLA2G5 which are known to be activated by adipokines TNFα and leptin (114). Changes in insulin signaling pathways have been observed, e.g. increased expression of IRS-2, and lower expression of PI3K and GLUT4 in obese placenta (68). Other studies found reduced mTOR signaling (115) as well as decreased AMPK but increased NFkBp65 expression, and an impaired total antioxidant capacity (116). However, it has also been reported that in obese placenta a switch from oxidative to nitrative stress occurs (117) . Also, it has been proposed that the observed changes in placental gene and protein expression are due to the placentas adaption to a hostile metabolic environment, probably protecting itself and the fetus (118,119).
Similar to GDM, also babies of obese mothers are often born bigger than average, imposing the same perinatal complications as described in section 1.3.4. Also, long-term health outcome regarding increased risk for T2DM and obesity is comparable (99) and can be explained in part by genetic and environmental factors (120) as well as epigenetic mechanisms (121).

1.5 Lipoprotein-associated Phospholipase A_2 – Friend or Foe?

1.5.1 $LpPLA_2$ – structure and function

Inflammatory responses, if regulated, are part of physiological defense mechanisms to maintain cellular homeostasis. Unregulated responses, however, can have detrimental effects, further exacerbating inflammation. A key mediator involved in both regulated and unregulated response is 1-alkyl-2-acetyl-*sn*-glycero-3-phosphocoline, or platelet activating factor (PAF). Also, several PAF analogues, so-called PAF like lipids (PAF-LL) have been identified. Activating inflammatory signal transduction through the PAF receptor (PAFR), to which PAF and PAF-LL bind with varying affinity, these molecules are important mediators of inflammation. In 1981, Blake et al. identified an enzyme specifically cleaving PAF and PAF-LL that was therefore called platelet activating factor acetylhydrolase (PAF-AH) (122). Later it was found that the enzyme, although sharing relevant enzymatic features with neutral lipases and esterases (123), is part of the phospholipase A_2 (PLA_2) superfamily and was termed PLA2G7 within the nomenclature of the superfamily.
Structurally, the enzyme has a Ser-Asp-His catalytic triad, that's positioned similarly to other esterases in an α/β-hydrolase conformation (Figure 6). The enzyme is 441 amino acids long, and has a molecular weight of 45kDa which is variable however, due to the heavy degree of N-glycosylation(124,125). Unlike other lipases, its activity is Ca^{2+}-independent.
PAF-AH is now more commonly called lipoprotein-associated phospholipase A_2 ($LpPLA_2$), as it circulates in plasma bound to lipoproteins. In normolipidemic adults, the majority (75-80%)

of $LpPLA_2$ is associated with low-density lipoprotein (126) (LDL) via apoB100, the remainder is bound to high-density lipoprotein (HDL) via ApoA1. In hyperlipidemic subjects, whose plasma Lp(a) levels are increased, however, it was found that almost 10% of PAF-AH activity might associate with Lp(a) instead of LDL (127).
Using mutation/deletion, residues Trp115, Lys116 and Tyr205 have been identified as crucial for $LpPLA_2$ association with LDL (Figure 6). Additionally, the carboxyl terminus of apoB100 apparently plays a key role in the interaction with the $LpPLA_2$ enzyme(128). Less is known about the association with HDL, but a stretch of amino acids at the carboxyl terminus of $LpPLA_2$ seems necessary for binding to HDL(129) (Figure 6).

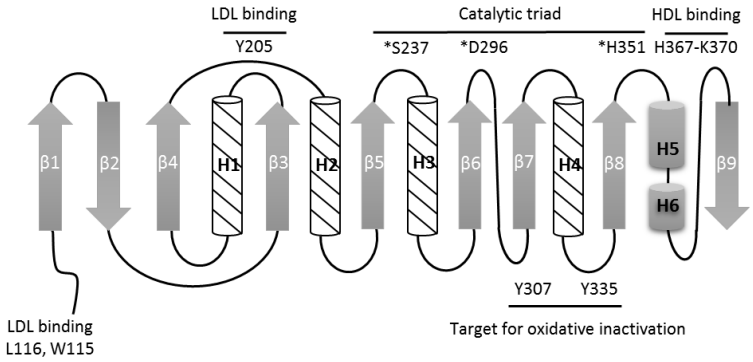

Figure 6: Structure of lipoprotein associated phospholipase A_2. $LpPLA_2$ has a classical α/β-hydrolase scaffold common to serine esterases. The catalytic triad as well as LDL and HDL binding sites and target sites for oxidative inactivation are depicted.

The cellular source of $LpPLA_2$ are monocytes and macrophages, which depending on their degree of differentiation produce the enzyme and secrete it into the circulation (130).
The substrate preference of $LpPLA_2$ is unique; the enzyme catalyzes the removal of an acetyl group at the sn-2 position of PAF to abrogate inflammation. In addition, it cleaves PAF-LL, which are generated in an unregulated manner in situations of oxidative stress such as i) oxidized phospholipids (oxPL), releasing an oxidized fatty acid and lyso-phosphatidylcholine (lysoPC), ii) long chain phospholipid hydroperoxides, releasing hydroperoxy fatty acids and lysoPC, and iii) esterified isoprostanes, releasing free isoprostane and lysoPC (Figure 7) (131).

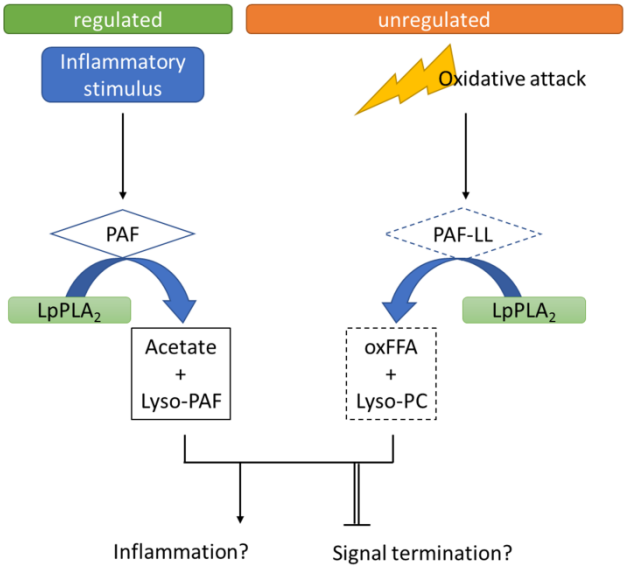

Figure 7: Action of $LpPLA_2$ in regulated and unregulated settings generating inflammation and oxidative stress.

Common to these substrates is that all of them are distorted molecules able to affect membrane fluidity and integrity, and may cause derivatization of surrounding proteins. This underpins the need to detoxify these molecules in order to maintain cellular homeostasis, and led to the general assumption that $LpPLA_2$ is an anti-oxidative, anti-inflammatory enzyme, limiting PAF and PAF-LL action.

Interestingly, $LpPLA_2$ expression is not regulated, but constitutive. There is no TATA box in proximity of the transcriptional start site, but instead, GC-rich motifs are present which is characteristic for housekeeping genes. Sp1 and Sp3 transcription factors have been shown to be involved in transcriptional regulation of the enzyme expression (132). Constitutive activity in combination with independence of Ca^{2+}-levels might threaten the integrity of the phospholipid membrane and lipoproteins; however, the exclusive substrate preference ensures protection of undamaged, structurally relevant phospholipids from hydrolysis. Despite the constitutive nature of $LpPLA_2$ expression, certain cytokines, e.g. TNFα, INFɣ and IL-1, IL-10 but also glucocorticoids and bacterial endotoxin (LPS) have been shown to influence $LpPLA_2$ expression in macrophages (133–135). Of note, although $LpPLA_2$ action is supposed to limit cellular oxidative attacks, the enzyme itself is susceptible to oxidative inactivation (136) e.g. by peroxynitrite species ($ONOO^-$).

1.5.2 $LpPLA_2$ in metabolic disease

Although considered anti-inflammatory, recently discussion has been raised if $LpPLA_2$ could contribute to inflammation via its reaction products (Figure 7) since lysoPC has been demonstrated to promote pro-inflammatory cytokine secretion (137) , monocyte attraction (138) and atheroma formation (139) . As a matter of fact, increased $LpPLA_2$ levels have been found to be associated with various metabolic pathologies, e.g. familial hypercholesterolemia (140), atherosclerosis (141,142), insulin-dependent and -independent diabetes (143,144) and obesity (145). In contrast, $LpPLA_2$ deficiency is also linked to poor health prognoses; 4% of the Japanese population carries a mutation in the PLA2G7 gene that encodes $LpPLA_2$, changing valine 279 to phenylalanine (V279F), resulting in absent plasma

$LpPLA_2$ activity (146,147). The mutation is associated with exacerbated asthma (148), and predisposition for atherosclerosis (149), and stroke (150). Independent of individual risks transferred by a certain genotype, decreased $LpPLA_2$ levels have also been found in systemic lupus erythematosus (151), myocardial infarction (152), sepsis (153) and anaphylactic shock (154). Because of these conflicting observations, it is unclear if $LpPLA_2$ activity is causal to inflammation itself, or rather a (bio)marker secondary to inflammatory processes.

In consideration of this ambiguity, it is also being debated if $LpPLA_2$ function might depend on its lipoprotein carrier in plasma (155), with LDL-$LpPLA_2$ having pro-inflammatory and HDL-$LpPLA_2$ exerting benefical, anti-inflammatory properties. Several studies point into this direction. First, it was shown that $LpPLA_2$ on HDL protected LDL against oxidative modification (156) and formation of minimally modified LDL (MM-LDL), which is the first step in atherogenesis. Subsequent studies revealed that overexpression of HDL-$LpPLA_2$ protected $ApoE^{-/-}$ mice from endothelial dysfunction (157) and atherosclerosis (158). In humans, decreased HDL-$LpPLA_2$ activity was found in patients suffering from (pre-)diabetes (159) and metabolic syndrome (160). Increased LDL-$LpPLA_2$ mass and activity, on the contrary, have been established as prognostic marker for cardiovascular disease (161–163).
Noteworthy, despite promising animal studies employing overexpression of $LpPLA_2$, recombinant $LpPLA_2$ treatment in patients did not have any beneficial effects (157,158), e.g. on survival of septic shock (164). Likewise, inhibition of LDL-$LpPLA_2$ to improve cardiovascular health by pharmacological means (a specific $LpPLA_2$-inhibitor called Darapladib) did not prove efficient in humans (165,166) despite previous effects in various animal models (167,168).

1.5.3 $LpPLA_2$ in pregnancy

During pregnancy, major adaptation of maternal body functions is needed to adapt to 'hosting' a fetus for the coming 40 weeks; specifically immunological changes occur. Whereas these adaptations were long believed to be immune-suppressive, current evidence suggests referring to these changes as immune-modulatory (169). Consequently, levels of $LpPLA_2$ might be modulated during pregnancy too. $LpPLA_2$ levels in maternal plasma have been shown to drop throughout gestation in various species and there is evidence that female sex hormones can regulate enzyme expression (170). Additionally, intracellular PAF-AH is expressed in maternal uterine cells and fetal tissues. Apparently, control of PAF levels by PAF-AH is important for embryo implantation as well as parturition. These mechanisms have been extensively reviewed by Tiemann (171).
Observational studies on humans have shown that pre-eclampsia leads to increased $LpPLA_2$ activity not in pre-eclamptic mothers but their neonates (172). Likewise, a study showed that GDM increased $LpPLA_2$ levels in plasma of GDM mothers but not in fetal cord blood (173). In a prospective birth cohort, early pregnancy $LpPLA_2$ levels in maternal plasma were identified as prognostic marker for the development of hypertension later in pregnancy (174). In follow-up studies of mothers with a history of GDM, $LpPLA_2$ levels were identified as prognostic markers for the development of T2DM, and metabolic syndrome (175,176). Apart from the two cited Chinese studies, no research on $LpPLA_2$ in the fetal circulation, its lipoprotein distribution and physiological functions exists to the best of our knowledge.

1.5.4 Fetal Lipoprotein Metabolism

The lipoprotein profile at birth differs significantly from the lipid profile established within the first week after delivery and later in life (177,178). In the newborn, HDL-C/LDL-C ratio is about 2:1, reflecting that HDL is the predominant lipoprotein fraction in the neonate. Using shotgun proteomics approaches, our lab could show that neonatal HDL carries different proteins than maternal HDL with respect to quantity and quality, and might therefore fulfil other functions than maternal adult HDL (179). Also fetal HDL differs in size, suggesting particle characteristics of the light HDL_2 sub-fraction, whereas maternal HDL appears more dense (HDL_3 sub-fraction). Comparing neonatal HDL from control and GDM pregnancies, we further identified differences in HDL composition and functionality in health and disease, e.g. lower PON-1 mass and activity in GDM leading to impaired anti-oxidant capacity, and lower CETP levels and impaired cholesterol uptake in efflux experiments (180). We speculated that GDM might also affect HDL-$LpPLA_2$ mass and activity, thereby affecting neonatal HDL function.

2. Hypothesis & Research Questions

We hypothesized that chronic low-grade inflammation in GDM might alter macrophage polarization of fetal Hofbauer cells. Also, we speculated that $LpPLA_2$ activity in Hofbauer cells and fetal circulation might be altered in GDM and/or obesity and wanted to investigate regulatory mechanisms and to understand functional consequences in late pregnancy.
Therefore, we phrased the following research questions:

1) *Does GDM cause a switch from M2 to M1 polarized macrophages in fetal Hofbauer cells and which are the metabolic drivers of potential polarization?*
2) *Is $LpPLA_2$ present in placental tissue and does it derive from Hofbauer cells?*
3) *Is $LpPLA_2$ activity affected by GDM and/or obesity?*
4) *Which stimuli of the diabetic/obese environment might contribute to $LpPLA_2$ activity?*
5) *Is $LpPLA_2$ activity on fetal lipoproteins altered in GDM?*
6) *Do $LpPLA_2$ enzyme alterations change lipoprotein functionality?*

3. Material and Methods

To aid fluid legibility it has been omitted to list suppliers of reagents, kits, antibodies, and consumables in the text. Instead, information on suppliers, as well as detailed lists of antibody dilutions, have been provided in the Appendix starting on page 85. Instruments and software packages are referred to in the running text were appropriate.

3.1 Patient Epidemiology

This study was performed at the Department of Obstetrics and Gynecology, Medical University of Graz and had been approved by the Institutional Ethics Board (24-529 ex 11/12). All patients enrolled in the study, gave written informed consent. Women underwent an oral glucose tolerance test (oGTT) at 24 to 28 weeks of gestation and GDM was diagnosed according to the criteria of the American Diabetes Association (181). For this study, only women with mild hyperglycemia (classified White A), manageable by lifestyle interventions and not requiring insulin administration, were enrolled.
Placentas of healthy and hyperglycemic women were used for isolation of Hofbauer cells; their patient characteristics are summarized in Table 1.

Table 1: Patient characteristics of women whose placenta was used for isolation of Hofbauer cells. CS= cesarean section, SP= spontaneous delivery.

	Control group (N=20)	**GDM group (N=12)**	**p-value**
Maternal age (years)	31.0±5.6	35.7±3.7	0.02
Maternal pre-gravid BMI (kg/m^2)	23.3±3.2	27.8±6.5	0.01
Maternal BMI (kg/m^2) at term	27.8±4.0	32.5±5.6	0.01
Gestational weight gain (kg)	12.4±6.0	12.2±7.0	n.s.
Gestational age (weeks+days)	39+3	38+3	n.s.
Mode of delivery	CS=10, SP=10	CS=10, SP=2	n.s.
Placental weight (g)	576.2±84.3	622.0±133.6	n.s.
Fetal Ponderal index (kg/m^3)	2.6±0.2	2.5±0.3	n.s.
Fetal Sex	11 ♀ 9 ♂	5 ♀ 7 ♂	n.s.

Importantly, the data in Table 1 were obtained by combining patient data of HBCs isolated for two different sub-studies, i) the phenotypical characterization of HBCs and ii) the $LpPLA_2$

study. Although HBCs were isolated for both studies, individual isolations were used in different experiments. In this dissertation, results from both studies are presented, so that the patient data were combined for a better overview. As a consequence, maternal age and pre-gravid as well as term BMI became significantly different between Control and GDM group. In the patient sub-set for the phenotypical characterization, gestational age at delivery was significantly different, as GDM mothers are often delivered pre-term by obstetricians recommendations and guidelines (182), but all other factors were matched (183). In the patient sub-set of the $LpPLA_2$ study, maternal pre-gravid BMI was significantly higher in GDM, and also tended to be higher at term; all other parameters were matched for. Fetal parameters, most importantly fetal ponderal index (PI), were not significantly between the groups.

PI is used as a measure of body composition which takes body volume into account rather than body area, thereby better reflecting the typical proportion of head-to-body size in neonates. PI is calculated as

$$PI = \left(\frac{bodyweight\ (g)}{body\ lenght\ (cm)^3}\right) * 100$$

Well matched PI between the groups indicates that fetuses in both groups were similar in their development. PI does however, not tell anything about body composition, e.g. lean versus fat tissue.
For isolation of lipoproteins, cord blood was collected as mixed blood from umbilical vein and arteries of both control and GDM neonates immediately after birth. Plasma was harvested from EDTA tubes by centrifugation and stored at -80°C until isolation of lipoproteins. Patient characteristics of mothers and neonates whose cord blood plasma was used in this study are summarized in Table 2.

Table 2: Characteristics of mothers and neonates whose cord blood was used to isolate lipoproteins.

	Control (N=21)	**GDM (N=21)**	**p-value**
Maternal pre-gravid BMI (kg/m^2)*	22.7±3.4	31.5±7.7	<0.001
Maternal BMI at term (kg/m^2)	28.6±4.0	34.9±6.2	<0.001
Gestational weight gain (kg)*	15.9±9.7	9.3±9.6	0.05
Maternal age (years)	32.8±6.3	32.6±5.5	n.s.
Gestational age at delivery (weeks+days)	39±3	39±2	n.s.
Mode of Delivery	CS18, SP3	CS18, SP3	n.s.
Placental weight (g)*	672.3±218.8	737.8±169.2	n.s.
Fetal ponderal index (kg/m^3)	2.6±0.3	2.6±0.2	n.s.
Fetal Sex (female ♀/male ♂)	♀11 ♂10	♀10 ♂11	n.s.
Neonatal Cholesterol (mg/dl)	67.4±22.8	71.4±16.4	n.s.
Neonatal Triglycerides (mg/dl)	38.8±20.6	36.2±16.2	n.s.
Neonatal Phospholipids (mg/dl)	114.6±30.5	122.7±19.6	n.s.
Neonatal Apo A1 (mg/dl)	72.4±17.9	76.3±12.3	n.s.
Neonatal ApoB (mg/dl)	20.4±7.9	22.3±7.6	n.s.

.

In addition, for the comparison of the $LpPLA_2$ distribution between LDL and HDL in adults and fetuses, expired plasma donations of healthy, non-pregnant, female donors at child-bearing age (N=4) was obtained from the Blood Bank at the University Hospital of Graz.
All experimental methods were performed in accordance with the approved study protocol.

3.2 Isolation of Hofbauer Cells

For isolation of Hofbauer cells the protocol of Tang and colleagues was followed with minor modifications (30). In brief, placental tissue was obtained within 30min after delivery. To avoid contamination with decidual macrophages all membranes on the maternal side of the placental disk were removed. Placenta was diced, washed in cold physiological saline solution and the tissue was scraped off the vessels. 60 to 100 gram of finely minced tissue was used for isolation. Tissue was digested in two steps; 1) a Trypsin-DNase digest and 2) a Collagenase A digest. Trypsin was used at a final concentration of 0.25%, DNase I at a final concentration of 0.08mg/ml, and Collagenase A at a final concentration of 1mg/ml. The cell suspension yielded from the digestion steps was applied onto a Percoll gradient and centrifuged for 30min, 2300g, brake off. Hofbauer cells are floating in the density layer between 30 and 35% Percoll after centrifugation. Cells were aspired from the gradient, washed and further purified in a negative immune selection step employing magnetic beads coupled with antibodies against epithelial growth factor receptor (EGFR) and CD10. After immune purification, cells were counted and plated at a density of 1x10^6 cells/ml in appropriate culture ware. Cells were cultivated in macrophage media (MaM) at 21% oxygen and 37°C.

3.3 Immune Cytochemistry

Immune cytochemistry was used routinely as purity control of Hofbauer cells. Cells were plated onto 4-well glass chamber slides suited for microscopy at a density of 250.000cells/well and cultivated for 7 days. Thereafter, cells were washed twice and fixated using ice cold aceton. Incubation against CD163, CD68, CD90, smooth muscle actin (SMA) and desmin (Des) was done for 30min in Dako Antibody diluent. CD163 and CD68 are macrophage markers, with CD163 particularly described as Hofbauer cell marker. CD90 allows to detect contamination with fibroblasts, SMA with smooth muscle cells, and Des with cells of mesenchymal origin. Contamination with fibroblasts could not be completely omitted, but was low (<2%), contamination with smooth muscle cells was not observed and mesenchymal cell contamination was also usually absent or below 2%. Cells were incubated for 10min with Dako Antibody Enhancer Solution. After a washing step in TBE, cells were incubated with Dako Large HRP Polymer solution for 30min, followed by incubation with Dako AEC Chromogen Solution for 10min. Cells were counterstained using haemalaun and mounted with glycerin. In addition to purity control, immune cytochemistry was used to determine expression of certain surface markers of the M1 (CD11b, CD11c, CD14) and M2 phenotype (CD206, CD209) on macrophages, and $LpPLA_2$ expression in different cells types. A complete list of antibodies and their respective dilutions is provided in the Appendix on pages 89 and 90. Cell photographs were taken using AxioVision Software v8.0 (Zeiss, Jena, DE) on an Olympus BX53 light microscope with an AxioCam MRc5 (Zeiss, Jena, DE).

3.4 FACS

Fluorescence assisted cell sorting was used to quantify cell populations expressing M1 and M2 polarization markers in HBC. After 7 days, cells were carefully harvested using Trypsin and gentle scraping. A minimum of 3x10^5 cells per antigen was used for FACS preparation. Cells were resuspended in 3% BSA-HBSS solution to block unspecific binding sites for 10min at RT. As only staining of surface molecules was desired, a permeabilization-fixation-step was omitted. Cells were washed in PBS and incubated with antibodies against CD11b, CD11c, CD206, CD209, CD80, CD86, CD45, CD40 and CD163 for 30min in the dark. A complete list of antibodies and their respective dilutions is provided in the Appendix on pages 89 and 90. Cells were washed thoroughly, and taken up in 200ul PBS for sorting. Sorting was performed on a LSR-II device (Becton Dickinson-BD, San Jose, CA, USA) using FACSDiva v.8 software (BD, San Jose, CA, USA) for data acquisition and analysis.

3.5 Immune Histochemistry

Tissue pieces were cut from central regions of the placental disk, the tissue piece was divided in half and the piece corresponding to the fetal side was paraffin-embedded. Serial sections of 5µm thickness were cut with a microtome and mounted onto glass slides. Paraffin was removed from tissue by xylene treatment and tissue was rehydrated using an ethanol dilution series. Antigen retrieval was performed using 1mM EDTA. For immune histochemistry, the Dako UltraVision LP Detection System was used: tissue was incubated for 15min in Hydrogen Peroxide Block, followed by thorough washing in TBE buffer. Thereafter, tissue was incubated with UltraV Block for 5min. Samples were incubated with the primary antibodies and subsequently an antibody enhancer, for 30 and 10min respectively. A complete list of antibodies and their respective dilutions is provided in the Appendix on pages 89 and 90. After TBE washing, HRP Polymer solution was applied for 30min, followed by incubation with AEC chromogen solution. Tissue was counterstained with haemalaun and slides mounted using glycerin. All photographs were taken on an Olympus BX53 light microscope with an AxioCam MRc5 (Zeiss, Jena, DE) using AxioVision Software v8.0 (Zeiss, Jena, DE). Quantification of Hofbauer cells in placental serial sections was performed using Visiopharm Stereotopix™ software platform (Visiopharm, Hoersholm, DK).

3.6 Immune Fluorescent Double-Staining

Placental tissue was prepared in the same way as for immune cytochemistry. Antigen retrieval was omitted to avoid destruction of placental villus structure. Blocking of unspecific binding sites was done in 3% BSA-TBE. Antibodies were diluted in a mix of Antibody Diluent and Background Reducing Component. Incubation with the primary antibody was carried out overnight at 4°C in a humidified chamber. A complete list of antibodies and their respective dilutions is provided in the Appendix on pages 89 and 90. After thorough washing, tissue was incubated with fluorescence labeled secondary antibody for 2h in the dark at room temperature. Prolong Gold Antifade Reagent with DAPI was used to simultaneously stain nuclei and mount slides with coverslips. All photographs of cells were taken with a LSM510 – AxioVert200M microscope (Zeiss, Jena, DE), pictures were acquired using Zen Software (Zeiss, Jena, DE).

3.7 Multiplexed ELISA-on-bead Assay and Validation

To quantify levels of 23 cytokine, chemokines, and growth factors in parallel, a custom-tailored multiplexed ELISA-on-bead approach was employed. Control (N=5) and GDM (N=6) HBC were cultivated in MaM, samples were collected every 24h for four days. Supernatant was concentrated 4-fold in Amicon Ultra Spin Filters (MwCo 3kD). The multiplex assay was carried out according to manufacturer's instructions. Bead signals were quantified using a FACSCalibur instrument (BD, San Jose, CA, USA). Analysis was carried out using FlowCytomixPro software (eBioscience, San Diego, CA, USA) to calculate standard curves and sample concentrations. For data normalization, total protein content was measured in supernatant samples by bichoninic acid assay. Cytokine levels were normalized to total protein levels.
According to differences in cytokine release between control and GDM samples in the multiplex assay, TNFα, IL-1β, IL-6, IL-10, ICAM-1, VEGF, MCP-1, and IL-1RA were further validated by conventional ELISA. ELISA kits are listed in the Appendix on page 88. Additionally, TGFβ was measured by ELISA only, as TGFβ detection requires acidification of samples to unfold and access the epitope.

3.8 Endothelial Activation Assay

Control and diabetic HBCs were cultivated in MaM medium for 6 days, and supernatant was collected. Supernatant was mixed 1:1 with endothelial basal medium (EBM) without growth supplements and only 2% FCS, to obtain macrophage conditioned medium. Human placental arterial endothelial cells (pAECs) were exposed to macrophage conditioned medium from control and GDM HBCs. EBM only was used as untreated control, MaM that had not been in contact with macrophages was mixed 1:1 with EBM to generate an unconditioned control. Additionally, a mix of TNFa (1.5ng/ml), IL-1b (0.2ng/ml) and IL-6 (1ng/ml) was added to unconditioned medium as positive control. After two days of cultivation at 37°C, 5% CO_2 and 12%O_2, cells were harvested and lysed using cell lysis buffer. A custom Quantibody array (see Appendix page 88) was carried out according to manufacturer's instructions, fluorescence scanning was performed on an Agilent Microarray Scanner G2565CA (Agilent, Santa Clara, CA, USA). Proteins detected in the array were ICAM-1, VCAM-1, VE-Cadherin, M-CSF, P-Selectin and E-Selectin; data extraction and analysis, standard curve calculation and sample quantification was carried out using GenePix Pro v6.0 (Molecular Devices, Sunnyvale, CA, USA) and a software plugin for MS Excel provided by the manufacturer.

3.9 Quantitative Real-Time PCR

RNA was extracted from total placental tissue, HBCs, endothelial cells, and trophoblasts using RNeasy Mini Kit according to manufacturer's instructions. RNA quantity was measured using ScanDrop device (Jena Analytics, Jena, DE), RNA quality was assessed by 260/280nm ratio, only samples with a ratio between 1.8 and 2.2 were used for cDNA synthesis. cDNA Synthesis was carried out using random hexamer primers and SuperScript II Reverse Transcriptase, 0.5 to 1µg of RNA was transcribed to cDNA which was thereafter diluted 10-fold. qRT-PCR was performed using Universal Master Mix and Taqman probes (against *PLA2G7* and *RL30* and *PPIA* as a housekeeping genes). Data Analysis was carried out with SDS 2.2 software (Applied Biosystems, Darmstadt, DE) using the 2^ΔΔCt method. Placental trophoblasts and endothelial cells used for RNA isolation were isolated as described

previously(4,184). Trophoblasts were cultured at 21% oxygen, in DMEM supplemented with 10% FCS and 2.5% HEPES, pH 7.4. Venous and arterial endothelial cells were cultured in EBM supplemented with EGM-V Bullet kit and 5% FCS at 21 and 12% oxygen, respectively.

3.10 Stimulation of Hofbauer cells

For all experiments using HBCs that measured $LpPLA_2$ activity as endpoint in HBC supernatant, cells were cultivated in MaM, with macrophage growth supplements, but addition of FCS was omitted. Instead, 5% of lipoprotein deficient serum (LPDS) was added to the medium, so that intrinsic $LpPLA_2$ activity in the medium was kept at a minimum. LPDS was prepared as follows: healthy human donor plasma was obtained from the Blood Bank at the General Hospital of Graz. To precipitate fibrinogen, 0.37g of calcium chloride were added per 100ml of plasma and incubated at 30°C in a water bath until plasma was fully coagulated. Using a spatula, the resulting jelly was stirred up, and centrifuged at 15.000rpm for 20min. Supernatant (= serum) was collected for further use. Density of the serum was adjusted to 1.24g/ml by addition of potassium bromide. Serum was centrifuged in an ultracentrifuge at 48.000rpm for 48. The resulting supernatant containing lipoproteins was discarded, and the bottom layer was dialysed extensively against isotonic sodium chloride solution at 4°C, over 48h, changing the dialysis solution at least 5 times daily. The dialysate was filled up to 80% of its original serum volume with isotonic sodium chloride solution, sterile filtered and stored in aliquots at -20°C until use in cell culture.

3.10.1 Time-course experiments

Hofbauer cells isolated from control and diabetic placentas were cultivated in 6-well plates at a density of $3x10^6$ cells per well in MaM up to 6 days, a sample was collected every 24 hours. Additionally, control HBCs were also exposed to 250nM Darapladib, a specific inhibitor of $LpPLA_2$ activity for 24, 72 or 120 hours. Activity released into supernatant was measured using a commercially available kit.

3.10.2 Diabetic Stimuli

For all treatments HBCs were seeded at a density of 3x10^6 cells per well into 6-well plates. An untreated control was included in every experiment. HBCs were serum starved for 12h before treatment. *Glucose treatment:* HBCs were exposed to 5, 15, and 25mM of D-glucose for 72 hours, glucose was added daily. Equimolar controls with L-glucose were included. *Insulin treatment:* HBCs were exposed to 5, 10, 20, 30, and 50nM of insulin daily for 72h. *Leptin treatment:* HBCs were exposed to increasing concentrations of Leptin (500, 1000 and 3000pg/ml) for 72h, leptin was added daily. *Cytokine treatments:* HBCs were exposed to increasing concentrations of TNFα (50, 150 and 250pg/ml) and adhesion molecules ICAM-1 and VCAM-1 (both 500, 1000 and 3000pg/ml) in different concentrations each day for 72 hours. The concentration range for leptin, cytokines and adhesion molecules was chosen according to initial results obtained in the multiplex assay, thereby mimicking physiological levels of possible autocrine stimulation in macrophages.

3.10.3 Anti-inflammatory Stimuli

HBCs were exposed to increasing concentrations of IL-4 and IL-13 (both 200, 600, and 1000pg/ml) for 72h, IL-4 and IL-13 were added daily.
After all treatments, supernatants were collected for activity assay; cells were washed twice with 1x HBSS and lysed using RIPA buffer supplemented with proteinase inhibitor cocktail. Cell lysates were incubated for 30min on ice, centrifuged at 16000g for 20min and stored at -20°C. Protein concentration of lysates was determined using bichinonic acid (BCA) method.

3.11 Enzyme-linked immunosorbent assay (ELISA)

All ELISAs performed on either Hofbauer cells supernatant or neonatal plasma were carried out according to manufacturer's instructions; all measurements were performed in duplicates. A complete list of ELISA kits used for this work is provided in the Appendix on page 88.

3.12 Isolation of fetal lipoproteins

Fetal cord blood was collected from umbilical vein and arteries into EDTA tubes, plasma was obtained by centrifugation, aliquots were prepared and stored at -80°C until further use. For isolation of fetal lipoproteins, 8ml of plasma were thawed and density was adjusted to ρ=1.24g/ml with potassium bromide. Plasma was transferred into tubes suited for ultracentrifugation and potassium bromide solution with a density of ρ=1.006g/ml was layered on top of the plasma. Samples were centrifuged at 15°C and 90.000rpm for 4h in a table-top ultracentrifuge (Optima TLX100; Beckman Coulter, Brea, CA, USA).
The LDL layer on the very top of the tube was collected, the interphase was aspired and discarded and the central HDL layer was collected. Lipoproteins were stored at 4°C, protected from light, underneath a layer of argon gas to prevent oxidation. Each sample was concentrated in Vivaspin tubes (MwCo 5kD) and excess potassium bromide was removed by PD10 columns. Purity of HDL was determined as ratio of Protein to Cholesterol (>2:1 were used), therefore protein was measured using bichinonic acid method and cholesterol was measured using a commercial kit.

3.13 $LpPLA_2$ activity assay

PAF-AH assay was obtained from Cayman Chemical. It is a colorimetric assay employing cleavage of 2-thio PAF by intra- or extra-cellular PAF-AH; freed thiols are detected via their reaction with DTNB ((5,5'-dithio-bis(2-nitrobenzoic acid)). Two assay buffers are provided with the kit, here only assay buffer 1, for extra-cellular PAF-AH (=$LpPLA_2$) was used. The assay was carried out according to manufacturer's instructions to measure LpPLA2 activity released from macrophages and LpPLA2 activity on neonatal lipoproteins. Intra-assay variance of this assay is 3.5%, inter-assay variability is 10%, as reported by the manufacturer.

3.14 Western Blots

Cell lysates of HBC or placental tissue lysates were subjected to polyacrylamide electrophoresis (TGX System; Biorad, Hercules, CA, USA); 15µg per lane were loaded onto 4-

20% gradient bis-acrylamide gels. Proteins were transferred onto nitrocellulose membranes using the TransBlot Turbo system from Biorad (Biorad, Hercules, CA, USA).
Membranes were blocked for 1h in 5% non-fat milk in TBE buffer and incubated against proteins of interest over night at 4°C. A complete list of antibodies and respective dilutions is available in the appendix on pages 89 to 90. The next day, membranes were washed in TBE and incubated with the secondary antibody. Membranes were developed using ECL chemiluminescence substrate in a Biorad LSA-400 camera (Biorad, Hercules, CA, USA). For normalization, membranes were also blotted against β-Actin. Densitometric analysis was performed using DigiDoc 1000 software (Alpha Innotech Corp., San Leandro, CA, USA).

3.15 Electrical Cell Substrate Impedance Sensing (ECIS)

Human feto-placental endothelial cells were plated onto electrode chamber slides suited for endothelial barrier function assays; 90.000 cells/well were used in 8-well chamber slides. Cells were cultivated for 24h in complete EBM medium. Medium was switched to EBM without growth supplements and only 2% FCS. A baseline was recorded at 4000Hz for 4 to 6 hours on an ECIS Z instrument (Applied BioPhysics, Troy, NJ, USA). To assess the effect of LpPLA2 on HDL functionality, a mixture of oxidized phospholipids (oxPL-mix consisting of POV-PC, PAz-PC and PG-PC, final concentration 15ug/ml) plus neonatal HDL (200ug/ml), plus either Darapladib (250nM) or DMSO (vehicle control) – which had been pre-incubated for 1h at 37°C – was added to cells. Additionally, cells were exposed to oxPL only, Darapladib only, and endothelial basal medium only (EBM; untreated control). Impedance was monitored over 40h at 4000Hz. Analysis of experiments was done using ECIS software (Applied BioPhysics, Troy, NJ, USA).

3.16 Assays of HDL anti-oxidative function

3.16.1 ClickIT Lipid Peroxidation assay

To test if LpPLA2 on HDL prevented lipid peroxidation in placental cells, human placental endothelial cells were plated onto chamber slides suited for fluorescence microscopy. Cells were grown in complete EBM medium to 80% confluence. Neonatal HDL was used in its native form or pre-incubated with 250nM Darapladib. Cells were exposed to HDL (200ug/ml) with or without inhibitor for 2h at 37°C. Cells incubated with oxPL-mix only (15ug/ml) served as positive control, addition of BSA (200ug/ml) was used as negative control. Subsequently, cells were incubated with linoleamide alkyne (LAA) for 2h. For cell fixation, permabilization and visualisation by Alexa488 fluorophore, the kit was carried out according to manufacturer's instructions. Laser scanning microscopy (LSM510 AxioVert200M - Zeiss, Jena, DE) was used to detect peroxidation-induced fluorescence in the cells, pictured were acquired using Zen software (Zeiss, Jena, DE).

3.16.2 Dihydrorhodamine 123 assay

A cell-free assay was employed to measure individual contribution of HDL anti-oxidative enzymes $LpPLA_2$ and PON1; fetal HDL was used either in its native form or pre-incubated for 1h at 37°C with either Darapladib (250nM) or 2-hydroxy-quinoline (400uM). HDL samples (10ug total) were added to 384-well plates with 15µl of 50 µmol/L Dihydrorhodamine 123

reagent containing 1 mmol/L 2,2'-azobis-2-methyl-propanimidamide-dihydrochloride. The increase in fluorescence (538nm) per minute was determined over 30 minutes. Dihydrorhodamine decays upon oxidation, releasing auto-fluorescence; HDL addition is supposed to prevent DHR oxidation, thereby the assay yields lower fluorescence levels for samples than for blank wells. By setting blank to zero, percentages of DHR oxidation can be calculated as a measure of HDL anti-oxidative capacity.

3.17 Statistical Analysis

All statistical analysis was done using GraphPad Prism v7.0 (Graphpad, La Jolla, CA, USA). Normality was tested by Shapiro-Wilks-test. If only two groups were compared, two-tailed t-test was used; where applicable (e.g. comparison of matched LDL and HDL samples from the same individuals) paired t-test was used. If more than two groups were compared, one-way ANOVA with Dunnetts post-hoc test for multiple comparisons was carried out. If more than two groups were compared at different time-points, two-way ANOVA with Sidaks post-hoc test for multiple comparisons was performed. If normality test failed i) Mann-Whitney test was performed instead of t-test and ii) ANOVA on ranks with Dunns post-hoc test instead of one-way ANOVA was performed. Pearson or Spearman Correlation was calculated for correlation analyses, depending on normality of the data. All data are presented as mean±SD (Dot plots and Tables) or minimum to maximum (box plots) unless indicated differently; graphs were drawn in Prism v7.0. Post-hoc power analysis was conducted using G*Power 3.1., available for download at the University of Duesseldorf, DE (http://www.gpower.hhu.de/).

4. Results

4.1 Hofbauer cells carry markers of both M1 and M2 polarization

4.1.1 Immune Histochemistry

Cell surface markers typical for M1 and M2 polarized macrophages were investigated *in situ* in paraffin embedded tissue from control and GDM placentas by immune histochemistry. Serial sections were prepared for better comparability. Human spleen and lymph node tissue was used as positive control to test antibody specificity.
As M1 markers, CD80 and CD86 were used. Both markers were completely absent in Control placenta (Figure 8A). In GDM placenta, limited CD80 staining was observed but was non-specific compared to the typical distribution of macrophages in placental stroma (Figure 8B). CD86 staining was absent (Figure 8B). In spleen (Figure 8C) and lymph node tissue (Figure 8D), both CD80 and CD86 positive cells were detected.

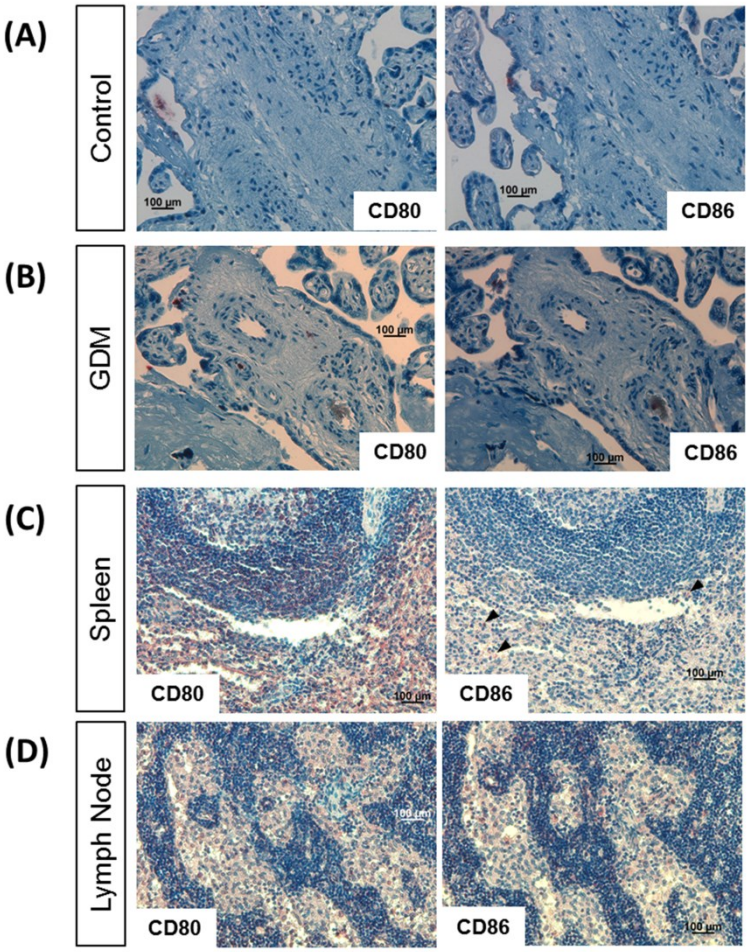

Figure 8: M1 markers in placental tissue. A: Staining of Control Placenta against CD80 and CD86 in serial sections. B: Staining of GDM Placenta against CD80 and CD86 in serial sections. C and D: Spleen and lymph node tissue were used as positive control; some cells in both tissues stained positive for

CD80 and CD86. Images representative of n=4 placentas/group, scale bar = 100um. This figure has previously been published in (183).

Furthermore, the M1 markers CD40, and CD11b in conjunction with CD11c have been investigated. While CD11b is a marker present on most macrophages and appears to be independent of polarization, in adipose tissue macrophages it has been demonstrated that presence of CD11b and CD11c at the same time points towards macrophage activation.
Neither CD40 (Figure 9 A), nor CD11b (Figure 9B) or CD11c (Figure 9C) showed a positive staining in either control or GDM placentas. However, all antibodies showed positive reactions in either spleen or lymph node tissue.

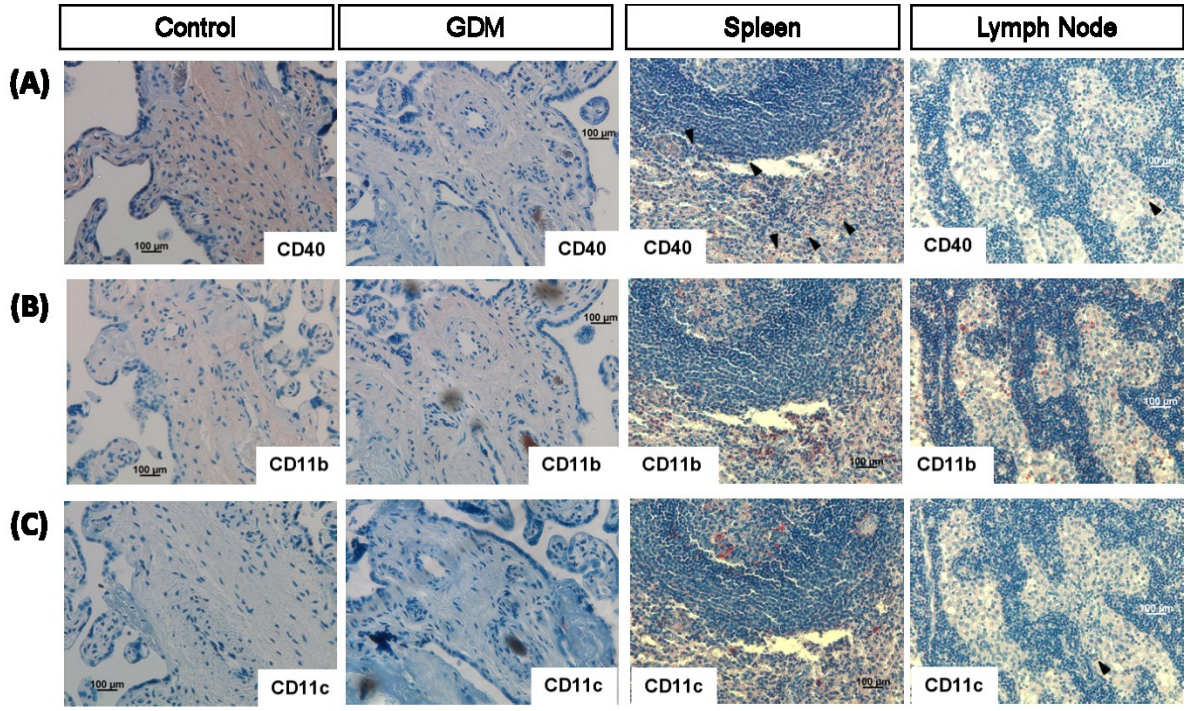

Figure 9: M1 markers in placental tissue. A: CD40 staining in serial sections of Control and GDM placenta, spleen and lymph node. B: CD11b staining in Control and GDM placenta, spleen and lymph node. C: CD11c staining in Control and GDM placenta, spleen and lymph node. Spleen and lymph node, used as positive control, showed positive reaction against respective antibodies. Images representative of n=4 placentas/group, scale bar = 100um. This figure has previously been published in (183).

On the contrary, several markers typical for M2 polarized macrophages were detected in Control and GDM placenta. Although considered the classical pan-macrophage marker, CD68 gave only limited staining in human placenta. While staining against both CD68 and CD163 was observed in Control and GDM placenta (Figure 10A), localized to the villous stroma of stem villi but distant from blood vessels and connective tissue surrounding vessels, areas were observed were CD163 was present but CD68 was absent (black arrowheads, Figure 10A). Therefore, CD163 appears to be a better marker to detect HBCs in placental tissue by immune histochemistry and it is generally described as M2 markers. Also, CD206 and CD209 positive cells were present in Control and GDM placenta. Quantification of the cell populations revealed equal numbers of CD163 positive cells in Control and GDM placenta (Figure 10B). Using CD163 as the most abundant marker of HBCs, CD206 and CD209 were

quantified relative to CD163. The number of CD209 positive cells was significantly increased in GDM placenta (Figure 10C). CD206 positive cell numbers were unchanged relative to CD163 (Figure 10C), but significantly decreased relative to the number of CD209 positive cells (Figure 10D).

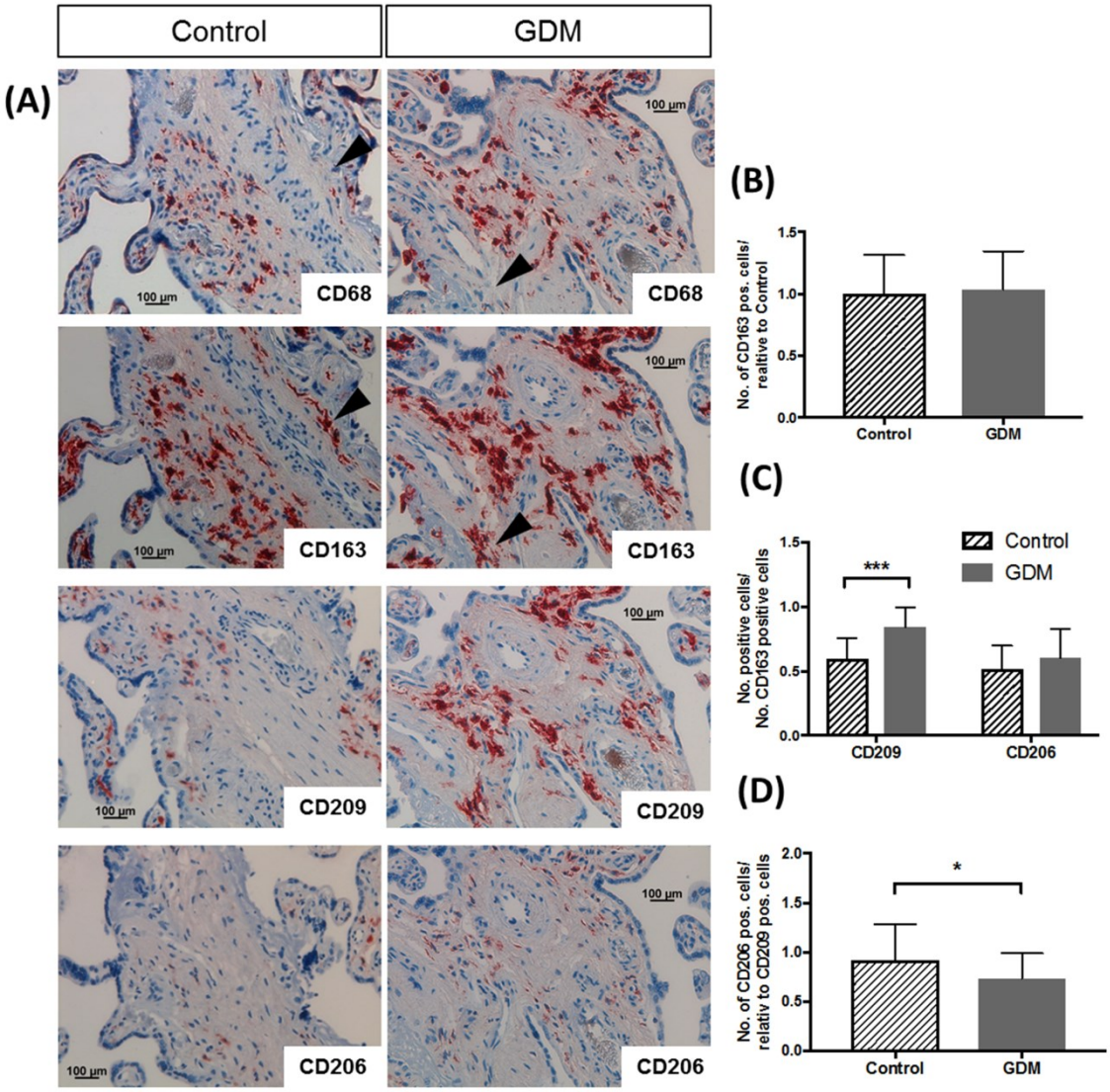

Figure 10: M2 markers in placental tissue. A: Staining of serial sections of Control and GDM placental tissue against CD68 (top), CD163 (second from top), CD209 (second from bottom) and CD206 (bottom). Arrowheads in CD68 and CD163 images indicate areas of divergent presence of CD68 and CD163. Images representative of n=4 placentas /group, scale bar = 100um. B: Quantification of CD163 in Control and GDM placenta. C: Quantification of CD209 and CD206 levels relative to CD163 levels in Control and GDM placenta. D: Quantification of CD206 levels relative to CD209 levels in Control and GDM placenta. For B, C and D images from 3 placentas per group and 10 different areas in each placenta were quantified, mean±SD, t-test in B and D, one-way ANOVA in C. This figure has previously been published in (183).

4.1.2 Immune Cytochemistry

In addition to immune histochemistry in intact placental tissue, immune cytochemistry on isolated placental Hofbauer cells was performed. Independent of GDM, Hofbauer cells were positive for the surface markers CD68 as pan-macrophage marker, CD163 and CD209 as M2 markers, CD11b and CD11c, which when co-expressed are associated with activated i.e. M1 macrophages, and also CD14, whose role as M1 or M2 marker is ambiguous.

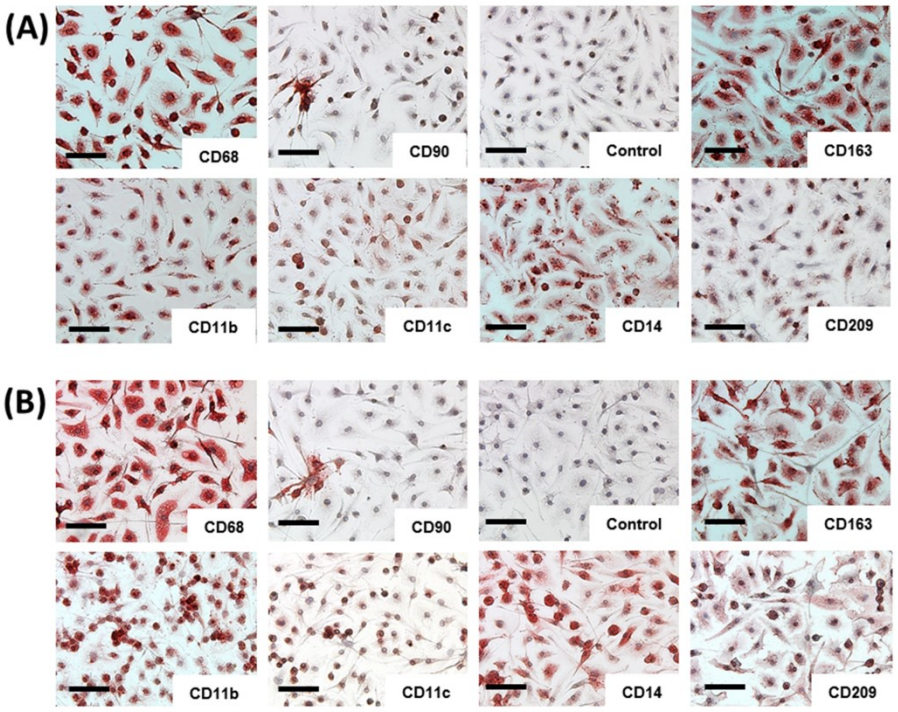

Figure 11: Immune cytochemistry of M1 and M2 markers on isolated Hofbauer Cells. A: HBCs isolated from Control Placenta. B: HBCs isolated from GDM placenta. As M1 markers CD11b and CD11c were used, CD14 is ambiguous in its role as M1 or M2 marker. CD163 and CD209 served as M2 markers. CD68 was used as pan-macrophage marker and CD90 was used to test for contamination with fibroblasts. Images representative of six different HBC isolations per group; scale bar = 200um. This figure has been modified from (183).

4.1.3 FACS

As immune cytochemistry is a more qualitative approach (although some cell biologists claim it can be quantified), Fluorescence assisted cell sorting (FACS) was used to quantify cell populations carrying either M1 or M2 surface markers (Table 3). CD45 is a marker staining all cells of the hematopoietic lineage, and stained Control and GDM-HBCs equally. Whereas levels of CD163 were comparable, the M2 markers CD206 and CD209 were both elevated on GDM-HBCs ($p=0.043$ and $p=0.003$, respectively). At the same time, also the M1 markers CD86 and CD40 were increased on GDM-HBCs ($p=0.001$ and $p=0.008$, respectively). Levels of CD11b, CD11c, the ratio of the two and levels of CD80 were unchanged in GDM.

Table 3: M1 and M2 markers on isolated Control and GDM HBCs quantified by FACS. The number of cells positive for respective markers is expressed as percentage of the total population. All data are presented as mean ±SD; p-values were calculated by χ2-test for proportions. This table has been modified from (183).

	Surface marker	Control (n=4) % population	GDM (n=4) % population	p-value χ^2-test
M2	**CD163**	85.0±21.3	97.3±3.3	n.s.
	CD206	42.8±19.6	85.0±7.6	0.043
	CD209	15.3±9.7	87.4±11.8	0.003
M1	**CD11b**	62.1±32.8	87.8±5.0	n.s.
	CD11c	72.8±23,9	97.4±2.6	n.s.
	CD11b/CD11c ratio	0.8±0.4	0.9±0.05	n.s.
	CD80	3.9±2.1	6.8±5.9	n.s.
	CD86	31.3±26.4	64.5±8.2	0.001
	CD40	19.3±4.6	44.7±30.9	0.008
	CD45	99.2±1.5	96.6±4.3	n.s.

4.1.4 Hyperglycemia and Insulinemia do not trigger an M2 → M1 switch

To test if high glucose or insulin levels were able to modify surface marker expression on HBCs, Control HBCs were exposed to 25mM D-glucose, 10nM insulin, or a combination of both. Equimolar L-glucose controls were included. Cells were lysed and subjected to Western Blot against CD86 (Figure 12A), CD209 (Figure 12B) and CD163 (Figure 12C). No difference in surface marker expression was observed.

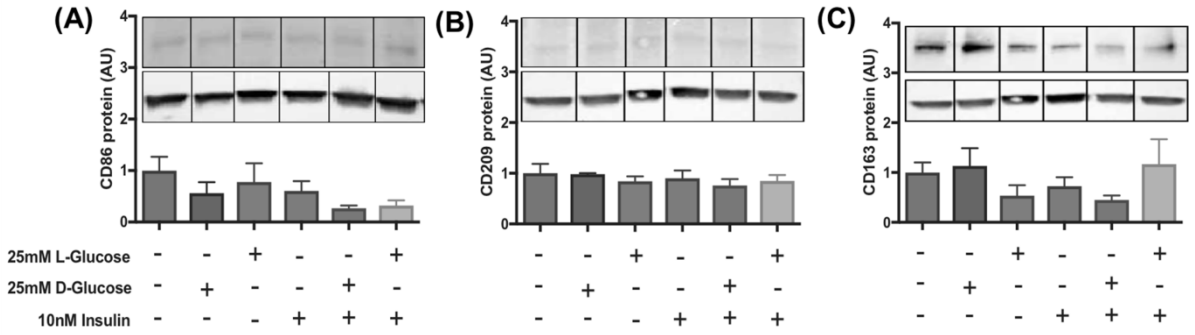

Figure 12: Effect of glucose and insulin on surface marker expression. A: Protein expression of M1 marker CD86 in HBCs after exposure to glucose and insulin. B: Protein expression of M2 marker CD209 in HBCs after exposure to glucose and insulin. C: Protein expression of M2 marker CD163 in HBCs after exposure to glucose and insulin. Beta-Actin was used as loading control for normalization of protein levels. Densitometric quantification was performed using DigiDoc 1000 (Alpha Innotech); Western Blot representative of three individual experiments, bar charts mean ±SEM from three individual experiments, one-way ANOVA. This figure has previously been published in (183).

4.2 Control and diabetic Hofbauer cells secrete the same pattern of cytokines, chemokines and growth factors

In addition to differential expression of surface marker on M1 or M2 macrophages, it is known that these cells also secrete different cytokines, chemokines and growth factors depending on their polarization. By using a multiplexed ELISA-on-bead approach, 23 relevant molecules were measured in the cell culture supernatant of Control and GDM HBCs at 4 different time points (24/48/72/96h after isolation). Results of this multiplex-experiment are summarised in Table 4.

Table 4: Release of Cytokines and Growth Factors from Control and GDM-HBC as measured by Multiplex Array. All 23 parameters measured in the ELISA-on-bead approach are listed, physiological relevance (pro-/anti-inflammatory action) is provided in the second column. All concentrations are provided as pg/mg of total protein, mean±SD, significance was calculated by ANOVA on ranks; † p≤0.09, # p≤0.05, ¶ p≤0.01. Bold print indicates factors that were validated by conventional ELISA. This table has previously been published as supplemental information in (183)

Cytokines/ Growth factors	**Physiological Relevance**	**Control (n=5)**				**GDM (n=6)**			
		24h	**48h**	**72h**	**96h**	**24h**	**48h**	**72h**	**96h**
IL-1α	pro-inflammatory, M1	N/A	0.6±1.1	0.7±1.2	2.2±3.2	1.22±0.8	2.48±0.3	1.99±0.3	1.96±0.2
IL-1β	**pro-inflammatory, apoptotic**	**1.4±0.7**	**5.8±9.3**	**5.4±6.0**	**10.4±8.3**	**8.2±8.0**	**14.9±15.9**	**15.6±19.8**	**14.6±18.8**
IL-1RA	**anti-inflammatory**	**2776.0± 1279.1**	**3344.2± 1751.5**	**4216.8± 554.9**	**4449.5± 526.5**	**2307.8± 475.4**	**3534.2± 953.7**	**4138.5± 821.9**	**4058.8± 1438.0**
IL-4	anti-inflammatory, M2	N/A	N/A	N/A	N/A	N/A	N/A	N/A	N/A
Il-6	**pro- /anti-inflammatory**	**101.9± 50.8**	**520.9± 822.8**	**645.6± 873.4**	**905.0± 1139.4**	**508.2± 548.5**	**897.6± 956.4**	**816.2± 961.5**	**622.5± 740.4**
IL-8	**NP attraction, angiogenesis**	**3076.8± 422.0**	**3039.5± 606.0#**	**3706.2± 312.2**	**3841.7± 709.0**	**2889.1± 434.9**	**4161.8± 369.4#**	**4003.8± 604.1**	**4010.3± 395.4**
IL-10	**anti-inflammatory, M2**	**2.2±1.5**	**3.0±4.0**	**2.0±2.2**	**1.5±1.8**	**4.4±2.9**	**5.5±4.9**	**2.9±3.4**	**1.9±1.9**
IL-12p70	anti-angiogenic, M1	0.2±0.3	0.3±0.3	0.3±0.3	0.2±0.3	0.4±0.3	0.5±0.4	0.3±0.4	0.3±0.4
Il-13	**anti-inflammatory, M2**	**48.7±23.5**	**63.7±48.6**	**85.7±32.1**	**83.6±46.8**	**59.5±26.8**	**97.7±47.2**	**85.7±51.1**	**103.6± 64.0**
EGF	proliferation, cell survival	N/A	N/A	N/A	N/A	N/A	N/A	N/A	N/A

FGF basic	angiogenesis, wound healing	20.8±27.5	18.4±23.1	30.3±17.5	37.6±27.0	30.0±16.1	47.8±26.0	36.8±17.5	26.8±31.2
PDGF AB	angiogenesis, mitogen	1318.0± 821.9	1981.3± 1166.2	2423.3± 1266.0	2386.8± 1188.3	1403.1± 562.3	2557.7± 1365.2	1587.9± 1519.3	2952.5± 1755.1
VEGF	**angiogenesis, vasculogenesis**	**449.2± 147.1#**	**667.6± 387.6†**	**848.9± 305.5**	**792.8± 435.7**	**663.1± 96.9#**	**1028.3± 188.7†**	**988.9± 313.7**	**933.2± 343.1**
TGFα	mitogen, proliferation	45.1±28.8	61.4±30.6†	123.3± 107.9	194.0± 222.6	62.0±23.6	93.9±21.9†	64.7±46.4	218.0± 147.5
ICAM-1	**Adhesion, pro-inflammatory**	**844.1± 238.4**	**1002.4± 344.4¶**	**1094.6± 97.1**	**1275.7± 121.5**	**868.6± 163.2**	**1904.2± 687.4¶**	**1152.5± 520.1**	**1260.1± 352.2**
VCAM-1	Adhesion, pro-inflammatory	144.3± 37.3	162.5± 57.9	175.9± 30.4	171.5±2.7	120.4± 28.1	180.3± 26.4	156.9± 54.2	165.62± 40.3
MCP-1	**Adhesion, pro-inflammatory,**	**511.7± 236.7**	**298.9± 119.4**	**730.3± 61.5**	**558.2± 142.6**	**569.3± 85.7**	**625.5± 263.1**	**589.4± 285.6**	**644.8± 247.4**
MCP-3	monocyte attraction,	89.6± 110.4	136.3± 107.8	127.7± 99.6	133.9±89.8	67.2±66.9	173.8± 156.8	90.5± 128.9	158.7± 180.0
GM-CSF	**Neutrophil attraction, MΦ differentiation**	**54.5±42.7**	**88.2±76.7**	**80.5±52.7**	**115.6± 65.6†**	**39.1±11.1**	**60.1±32.9**	**44.8±30.0**	**44.0± 28.0†**
TNFα	**pro-inflammatory, M1**	**7.0±4.5**	**14.9±28.6**	**5.6±8.9**	**6.2±8.0**	**28.1±27.5**	**10.7±13.4**	**6.3±8.5**	**2.7±3.0**
INFɣ	M1, pro-inflammatory	N/A	N/A	N/A	N/A	N/A	N/A	N/A	N/A
Leptin	energy homeostasis	666.5± 376.2	933.0± 165.0†	991.5± 233.3	938.5± 510.1	855.0± 108.2	1181.28± 195.8†	794.5± 416.2	1145.4± 287.5
MPO	ROS production	0.6±0.2#	0.7±0.3	0.7±0.2	0.8±0.3	0.4±0.1#	0.6±0.2	0.5±0.1	0.6±0.1

† p≤0.09, # p≤0.05, ¶ p≤0.01

Out of 23 parameters, four molecules (IFNγ, EGF; IL-1α, IL-4) could not be quantified due to the lower limit of detection-, two compounds (MCP-1, IL-1RA) were out of the assay range because of the upper limit of detection.

Post-hoc power analysis had shown that the initial multiplex array approach had little statistical power (<50% for most parameters, data not shown) as large intra-individual variation between HBC primary isolations was observed. Nevertheless, for some parameters, e.g. IL-1β and GM-CSF (granulocyte macrophage colony stimulating factor), a statistical power >99% was achieved also in multiplex. Combining results from ANOVA on-ranks (Table 5), post-hoc power analysis and analysis of the 95% confidence intervals of each parameter of the multiplex array, suitable cytokines and chemokines for validation by conventional ELISA were chosen. Also, MCP-1 and IL-1RA, which were out of assay range in multiplex, were validated by conventional ELISA.

Figure 13 shows M1 and M2 markers validated by conventional ELISA. TNFα secretion appeared to be increased in GDM-HBCs, but only at 48 and 72h time points, and non-significantly (Figure 13A). IL-1β (Figure 13B) and IL-6 (Figure 13C) secretion was consistently higher in GDM-HBCs (+ ~25% and + ~50%, respectively) but also non-significant. GM-CSF secretion was comparable between Control and GDM-HBCs (Figure 13D) and also secretion of MCP-1 was unchanged between the two (Figure 13E). TNFα, IL-1β and IL-6, as well as MCP-1 are well described cytokines characteristic for the M1 phenotype; also GM-CSF has mostly been associated with the M1 phenotype, but studies also demonstrated that it aids wound healing and tissue remodeling. Consequently, GM-CSF has also been connected to the M2b phenotype (185).

Transforming growth factor β (TGFβ) was only measured by ELISA and not by multiplex; detection of TGFb requires acidification of samples to make the epitope available to the antibody, so it can only be detected by its own, but not in a multiplex panel. Although much higher in GDM-HBCs at the 24h time point (p=0.06), TGFβ secretion was not different at later time points between Control and GDM-HBCs (Figure 13F). IL-10 (Figure 13G) secretion was similar in Control and GDM-HBCs at all time points. Of note, IL-12 secretion was 10-fold lower in multiplex than IL-10 (Table 5), and could not be validated by ELISA; therefore, Control and GDM-HBCs can be considered IL-10^{hi}/IL-12^{lo} macrophages, which is typical for M2 polarization. ICAM-1 secretion from GDM-HBCs was increased at all time points compared to controls; however, the increase was not significant (Figure 13H). VEGF and IL-1RA secretion did not differ between control and GDM-HBCs (Figure 13I and 13J, respectively). TGFb and IL-10 are hallmark cytokines of the M2 phenotype. Also IL-1RA, the antagonist for the IL-1 receptor, which abrogates IL-1 signaling and thereby inflammation, is a well described M2 cytokine. ICAM-1 and VEGF are not classic secretory markers within the M1/M2 concept; however soluble ICAM-1 antagonizes the effects of ICAM-1/LFA-1 signaling, promoting angiogenesis (186,187) and can therefore be considered an M2 marker. Also, VEGF is associated with the M2 phenotype, due to its pro-angiogenic nature.

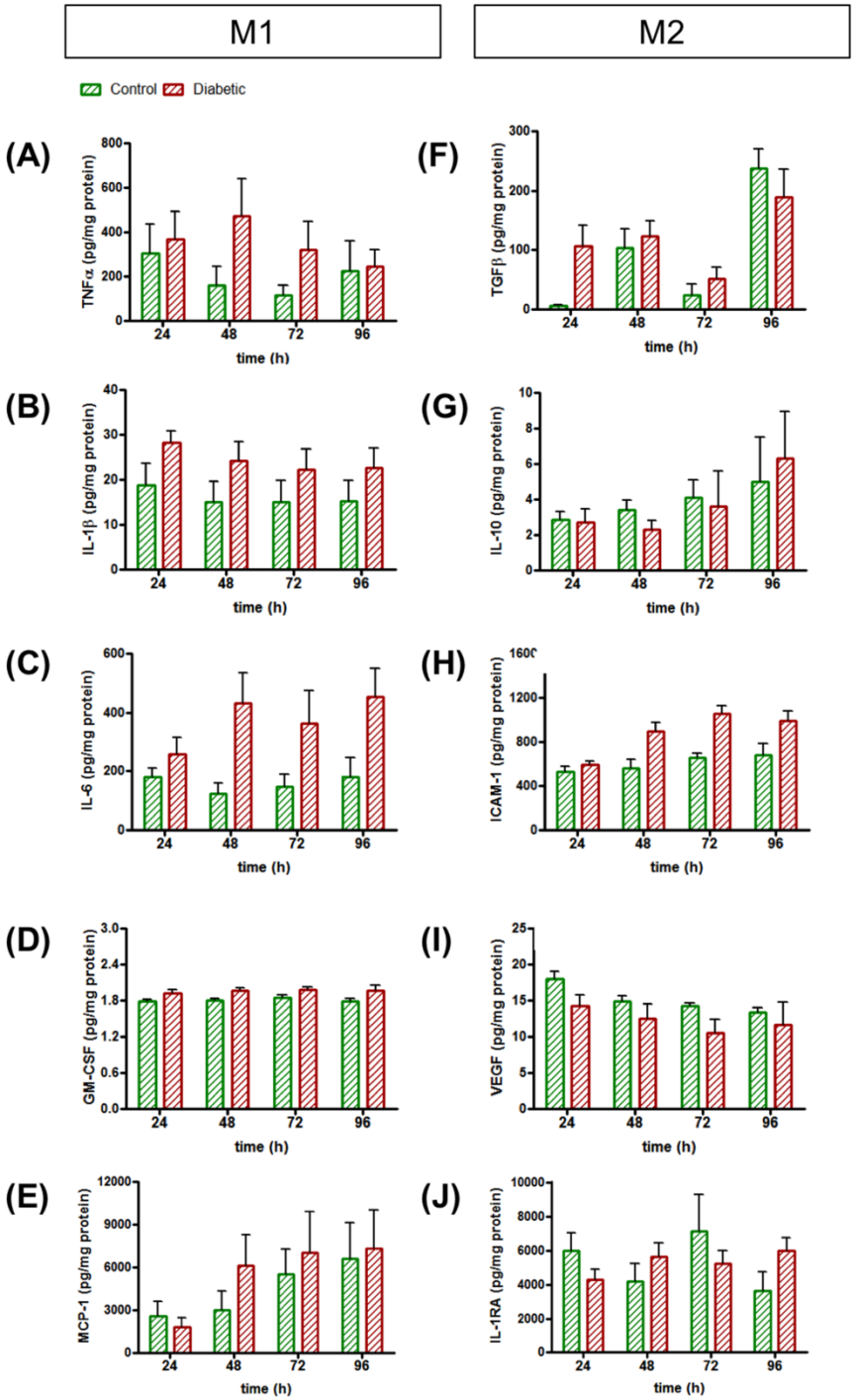

Figure 13: Validation of selected cytokines and growth factors from multiplex by conventional ELISA. A-E: M1 markers; G-J: M2 markers. Pooled data: n=5 control HBCs, n=6 GDM-HBCs, ANOVA on ranks, mean ±SEM. This figure has been modified from (183).

Post-hoc power analysis of the parameters validated by ELISA revealed that for most parameters a power >70% was reached (Table 5). Whereas 80% power is the gold standard for clinical studies, some statisticians suggest that in biological *in vitro* studies lower power is also tolerable (188).

Table 5 Post-hoc power analysis using G*Power 3.1. Column 1 gives the parameter validated by ELISA, the achieved power based on our data (mean, SD and sample size) is provided in Column 2, effect size calculated by the program is given in Column 3, and sample size per group (case-control) for 80% power calculated using the given effect size is provided in Column 4.

	G*Power 3.1 Post-hoc power analysis		
	Power achieved (%)	Effect size d	Sample size for b-error 0.8
MCP-1	11	0,50	64
IL-1β	**100**	**3,60**	**3**
IL-6	**99,80**	**3,40**	**3**
TNFα	**70,70**	**1,70**	**7**
TGFβ	30,40	0,75	48
IL-10	10,00	0,37	83
IL-1RA	8,80	0,44	116
VEGF	**65,00**	**1,60**	**8**
ICAM-1	**77,00**	**1,80**	**6**
IL-8	35,00	1,05	16
GM-CSF	**99,00**	**3,30**	**3**

Of note, with the exception of IL-8, for those parameters where a power below 65% was reached, the sample size per group needed to achieve 80% power, would have been unreasonably high, suggesting that rather than a lack in power, there really was no difference between Control and GDM-HBCs for those parameters, so the null-hypothesis can be rejected.
Nevertheless, with respect to achieved power in Multiplex and ELISA validation, and due to the small sample size, this study was claimed a pilot-study.

4.3 Endothelial Cells are not activated differently by interaction with control and diabetic Hofbauer cells

Interaction between macrophages and endothelial cells is well studied and it is known that macrophages can induce endothelial cell activation, e.g. in atherosclerosis (189). Endothelial dysfunction in mother, placenta, and fetus has been demonstrated in GDM pregnancies (190,191). Therefore, activation of placental endothelial cells by conditioned medium form Control and GDM-HBCs was investigated. Unconditioned blank macrophage medium was used as negative control, a mixture of IL-1β, IL-6 and TNFα was used as positive control. After incubation with conditioned medium and controls for 48h, cells were lysed and levels of ICAM-1, VCAM-1, VE-Cadherin, E-Selectin, P-Selectin and M-CSF were measured.

ICAM-1 protein was increased in endothelial cells after incubation with GDM-HBC conditioned medium, compared to Control-HBCs (+12%, $p<0.05$) but not compared to the negative control (Figure 14A). The cytokine mix induced ICAM-1 protein in endothelial cells (Figure 14A). VCAM-1 was only induced by the positive control ($p<0.01$), but no other treatment (Figure 14B). E-Selectin protein was not changed by any treatment (Figure 14C), whereas P-Selectin was only induced by the positive control ($p<0.05$), but no difference

between Control and GDM-HBC conditioned medium was observed (Figure 14D). VE-Cadherin was not induced by any treatment, including the positive control (Figure 14E). M-CSF was significantly induced by all treatments, positive control ($p<0.0001$), Control ($p<0.01$) and GDM-HBC ($p<0.001$) conditioned medium alike (Figure 14F).

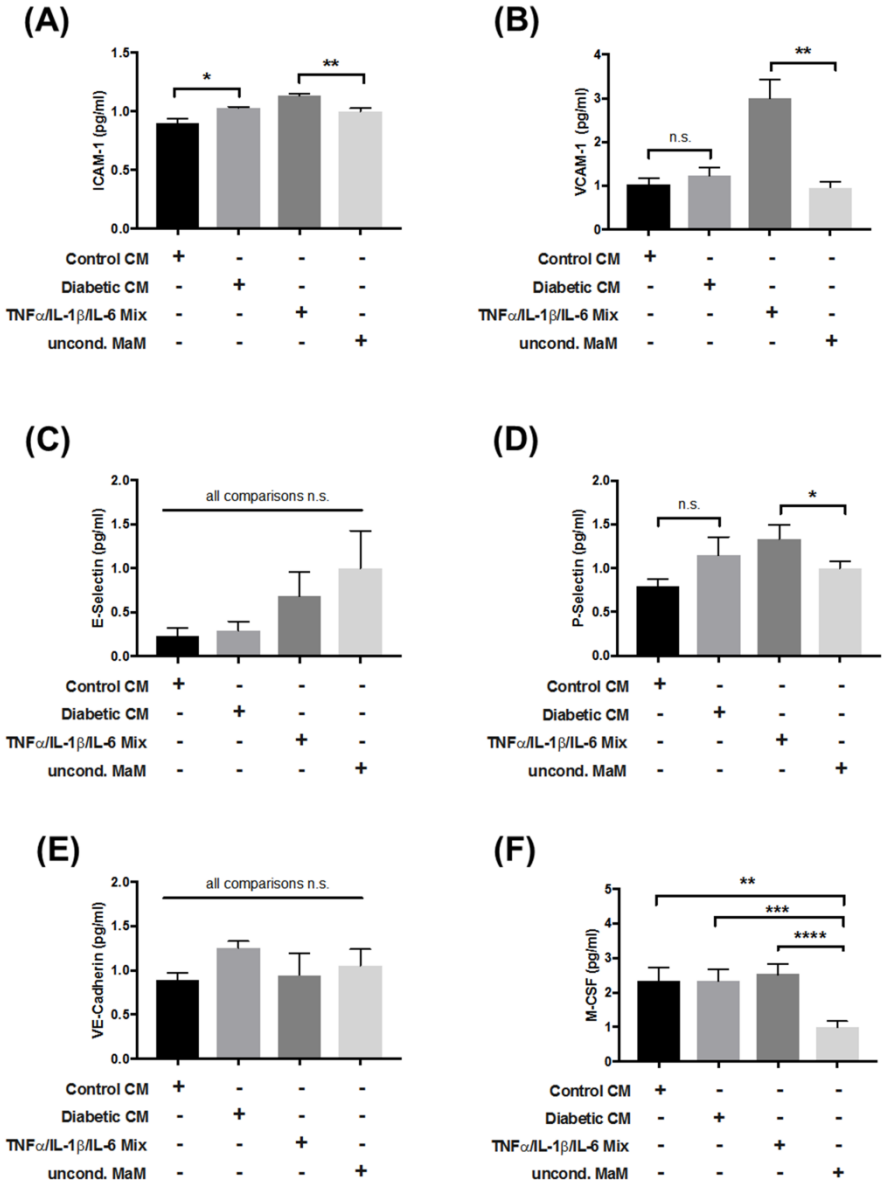

Figure 14: Adhesion molecule expression in endothelial cells in response to stimulation with macrophage conditioned medium. Placental arterial endothelial cells (pAECs) were incubated with HBC conditioned medium (CM) from control and GDM -HBC, and appropriate positive (TNFα/IL-1β/IL-6 mix) and negative controls (uncond. MaM) were included. Production of ICAM-1 (A), VCAM-1 (B), E-Selectin (C), P-Selectin (D), VE-Cadherin (E), and M-CSF (F) in response to treatment was measured. Pools of supernatant from three macrophage isolations were used to prepare CM, the experiment was performed with n=3 different primary AEC isolations. One-way ANOVA. Data are shown as mean ± SEM. This figure has previously been published in (183).

4.4 $LpPLA_2$ originates from Hofbauer cells and its expression is higher in GDM placenta

Immune cytochemistry of isolated Hofbauer cells, placental endothelial cells (ECs) and trophoblast showed that $LpPLA_2$ was present almost exclusively on HBCs (Figure 15A, left panel); some reaction against $LpPLA_2$ was present on ECs (center panel). In trophoblast, $LpPLA_2$ was completely absent (right panel). CD163 was used as marker of Hofbauer cells, van Willebrandt factor (vWF) as marker of ECs, and Cytokeratin 7 (CK7) as marker for trophoblast. These same markers were also used in immune fluorescence stainings, to further verify the results from immune cytochemistry by co-localization of $LpPLA_2$ with respective markers. LpPLA2 co-localized with CD163 only, in immune fluorescence (Figure 15B, left), but not with vWF (Figure 15B, center) or CK7 (Figure 15B, right).

Real-time quantitative PCR also demonstrated on the mRNA level, that HBCs are the only placental cell type expressing PLA2G7 mRNA, coding for $LpPLA_2$ protein, in relevant levels (Figure 15C). Expression was absent in arterial and venous ECs, and trophoblast. Only in first trimester trophoblast, some PLA2G7 mRNA was detected. This might be because of the tight balance between PAF and PAF-AH action needed at the time of implantation (171). Additionally, it was found that in GDM placenta, PLA2G7 mRNA was increased 40-fold compared to control placenta (Figure 15D).

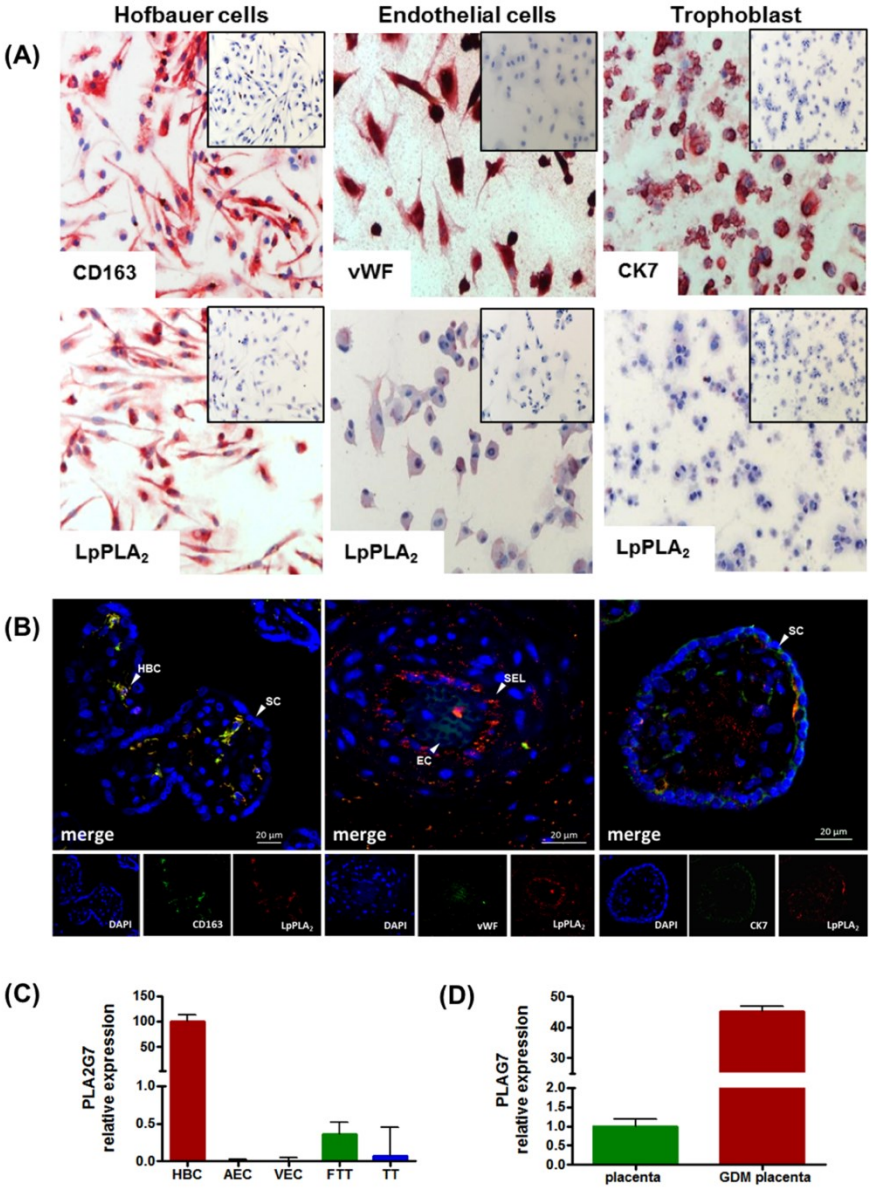

Figure 15: Hofbauer cells are the major cell type expressing $LpPLA_2$ protein and mRNA. A: Immune cytochemistry of Hofbauer cells, endothelial cells and trophoblast. CD163 was used as marker of HBCs, van Willebrandt factor (vWF) as marker of ECs, and Cytokeratin 7 (CK7) as marker of trophoblast. All three cell types were stained against $LpPLA_2$. Negative controls are shown as inserted boxes in the upper right corner of each picture. B: Immune fluorescence co-localization of $LpPLA_2$ with CD163, vWF or CK7. Blue = DAPI nuclear staining, green = CD163/vWF/CK7, red = $LpPLA_2$; HBC= Hofbauer cell, SC= syncytium, EC=endothelial cells, SEL= subendothelial layer. C: Expression level of PLA2G7 mRNA coding for $LpPLA_2$ in HBCs, arterial ECs (AEC), venous ECs (VEC), first trimester trophoblast (FTT) and term trophoblast (TT); n>4 per cell type. D: PLA2G7 mRNA levels in placenta from control and GDM placenta (n=6/group).

4.5 Diabetic Hofbauer cells secrete significantly more $LpPLA_2$ activity than controls

Whereas almost no difference between Control and GDM-HBCs was found with respect to their phenotypic polarization, differences in the activity of the macrophage-specific enzyme

$LpPLA_2$ were observed. Control and GDM-HBCs were kept in culture for a time course of 6 days, and a daily sample was collected every 24h.
Only 48h after isolation, GDM-HBCs secreted more $LpPLA_2$ activity than controls (Figure 16A; p=0.06); the increase became significant at 72h and persisted until the end of the experiment (144h/6 days).
To demonstrate the specificity of $LpPLA_2$ activity detected by the assay, Darapladib as a specific inhibitor of $LpPLA_2$ activity was used. Cells were incubated with Darapladib at a final concentration of 250nM; an equal volume of DMSO was added to untreated cells as vehicle control. Darapladib completely abolished (-93%) LpPLA2 activity secreted from HBCs (Figure 16B), proving that the right enzyme was detected by the assay. Finally, an ELISA against $LpPLA_2$ demonstrated that protein mass and activity were closely correlated (r=0.78, p<0.0001; Figure 16C).

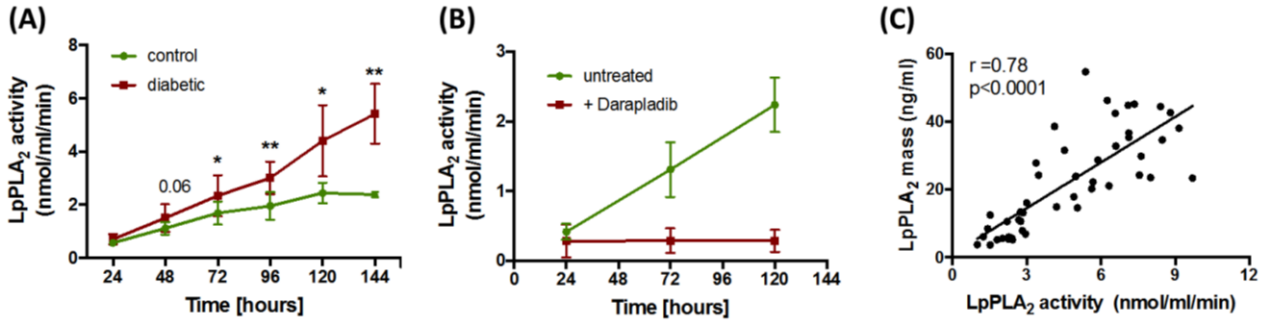

Figure 16: $LpPLA_2$ activity in vitro in Hofbauer cell culture. A: $LpPLA_2$ activity secreted from control (green) and GDM (red) macrophages over a time course of 6 days; n=5/group, one-way ANOVA. B: $LpPLA_2$ activity after incubation with the specific $LpPLA_2$-inhibitor Darapladib; n=4/condition. C: Pearson correlation of $LpPLA_2$ mass and activity in cell culture supernatant of HBCs.

4.6 Insulin and leptin increase $LpPLA_2$ activity *in vitro*

Hyperglycemia is the most obvious feature of GDM, and is countered by maternal and fetal hyper-insulinemia. Therefore, glucose and insulin were identified as possible stimuli regulating $LpPLA_2$ activity in HBCs. Exposure of Control-HBCs to supra-physiological levels of D-glucose, and equimolar L-glucose as controls, did not have an effect on $LpPLA_2$ activity (Figure 17A) or protein measured by Western Blot (insert in Figure 17A). Insulin, on the other hand, increased $LpPLA_2$ with increasing concentration (Figure 17b), peaking at 20nM (+22%, p<0.01). Also, an increase on protein level was observed (see insert, Figure 17B).
Finally, the obesity-associated hormone leptin was investigated, as many GDM mothers are also overweight or obese. Exposure of Control-HBCs to leptin only caused moderate increases in $LpPLA_2$ activity (Figure 17C) but a more pronounced increase in protein was observed (see insert, Figure 17C).

4.7 Pro-inflammatory cytokines stimulate $LpPLA_2$ activity *in vitro*

As GDM is also characterized by an inflammatory component, pro-inflammtory cytokines and adhesion molecules were investigated as possible stimulators of $LpPLA_2$. TNFα caused a dose-dependent increase in $LpPLA_2$ activity and protein (Figure 17D), with a peak at 100pg/ml TNFα (+23%, p<0.01). The adhesion molecules ICAM-1 and VCAM-1 (Figure 17E) both caused a moderate yet significant increase in $LpPLA_2$ activity (+9%, p<0.05, resp.).

Although small by themselves, *in vivo* all these molecules might be present at the same time, thereby having greater impact on $LpPLA_2$ protein and activity.

4.8 Anti-inflammatory cytokines decrease $LpPLA_2$ activity *in vitro*

Strikingly, the biggest effect on $LpPLA_2$ activity was achieved by exposure to anti-inflammatory cytokines, i.e. IL-4 and IL-13. These anti-inflammatory cytokines regulated $LpPLA_2$ activity negatively, leading to decreases in $LpPLA_2$ activity and protein. IL-4 addition decreased $LpPLA_2$ activity and protein in a dose-dependent manner, leading to a decrease in activity by 24% ($p<0.001$, Figure 17F). IL-13 had the same effect, but decreased activity even further (-41%, $p<0.001$, Figure 17F). Decreases could also be observed on protein level (see respective inserts).

As a prove-of-concept, HBCs were also stimulated with a mixture of oxidized phospholipid species. These are the main substrate for $LpPLA_2$ and should regulate its activity in a kind of positive feedback loop. It was observed that lower concentrations of oxPL (5 and 10ug/ml) increased $LpPLA_2$ activity in HBCs (+36%, $p<0.01$), whereas higher concentrations (25ug/ml) caused a decrease in activity and protein (Figure 17G). This is in line with reports demonstrating that $LpPLA_2$ is susceptible to oxidative inactivation (136,192).

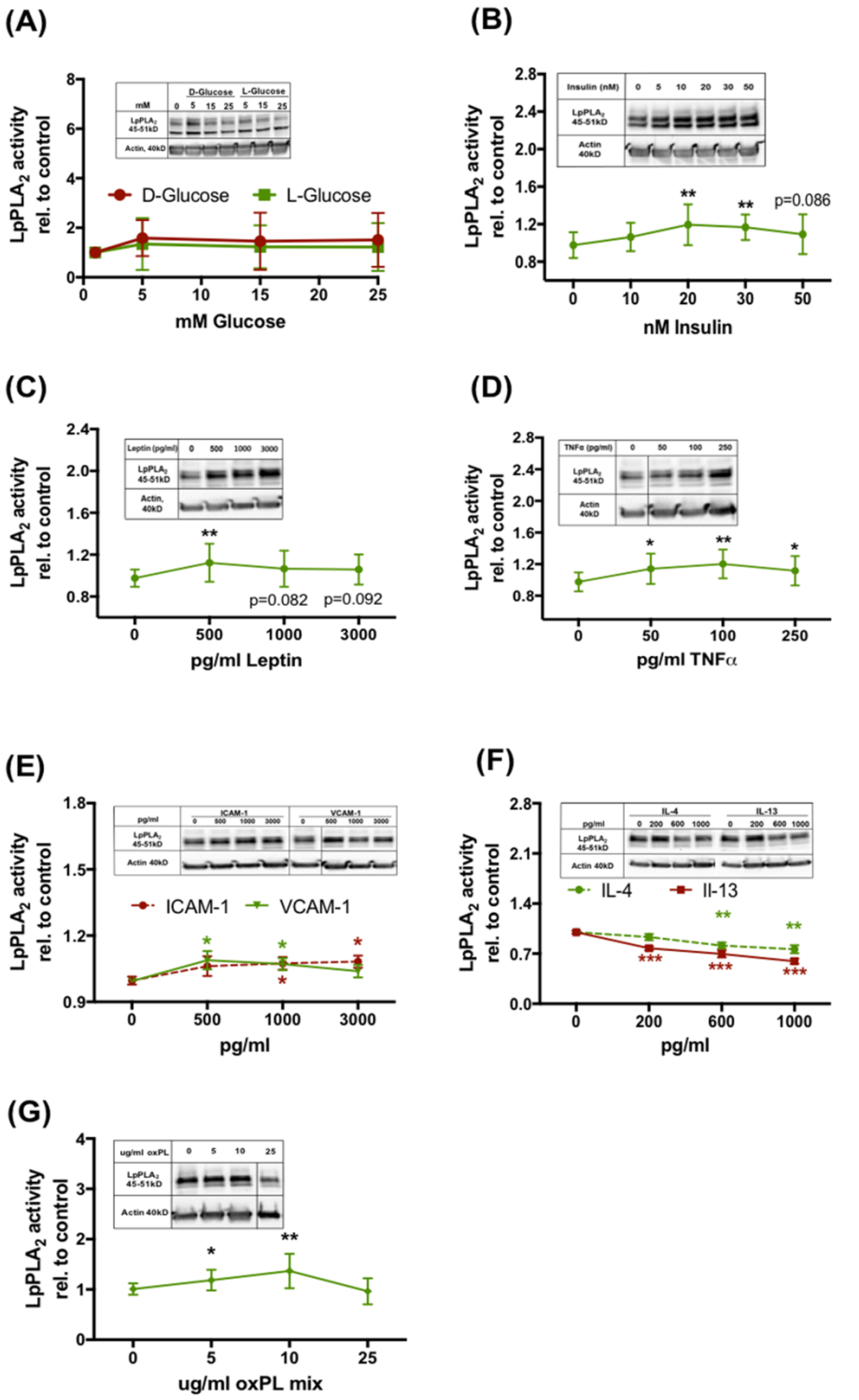

Figure 17: Hormones and cytokines regulate $LpPLA_2$ activity in HBCs *in vitro*. A: Stimulation of $LpPLA_2$ activity by D-glucose; equimolar amounts of L-glucose were used as control. B: Stimulation of $LpPLA_2$ activity by insulin. B: Stimulation of $LpPLA_2$ activity by leptin. D: Effect of TNFa on $LpPLA_2$ activity. E: Stimulation of $LpPLA_2$ activity by ICAM-1 and VCAM-1. F: Effect of IL-4 and IL-13 on $LpPLA_2$ activity. G: Effect of oxidized phospholipids (oxPL) on $LpPLA_2$ activity. All activity data were pooled from 5 individual experiments each; one representative Western Blot shown for each condition. Activity expressed as mean ±SD, one-way ANOVA.Vertical lines indicate were Western Blots were cropped.

4.9 $LpPLA_2$ enzymatic activity is mainly associated with fetal HDL and increased in children born to GDM pregnancies

LDL and HDL isolated from plasma of healthy adult non-pregnant donors and from cord blood plasma of healthy fetuses was used to study the distribution of $LpPLA_2$ on lipoproteins. It is known that the majority of $LpPLA_2$ activity in adults is associated with the LDL fraction (131) which also is the predominant lipoprotein fraction in grown-ups. In the fetus, however, HDL is the major lipoprotein fraction, similar to rodents. In rabbits, it has been demonstrated that 95% of plasma $LpPLA_2$ activity is associated with the HDL fraction (193). Consequently, it seemed likely that also in the human fetus the majority of $LpPLA_2$ activity would be associated with HDL. Indeed, it was found that about two thirds of $LpPLA_2$ activity in the fetal circulation was bound to HDL, and only one third circulates bound to LDL (Figure 18A). In contrast, in adults about 80% of $LpPLA_2$ was associated with LDL, and only 20% was associated with HDL (Figure 18A).
Comparing $LpPLA_2$ activity on LDL and HDL particles isolated from both healthy and GDM pregnancies, it was found that HDL-associated $LpPLA_2$ is specifically increased in GDM ($p=0.002$; Figure 18B). No difference in LDL-associated $LpPLA_2$ activity between the two groups was observed (Figure 18B). In addition, $LpPLA_2$ mass on fetal lipoproteins was measured by ELISA and close correlation of $LpPLA_2$ protein mass and activity was demonstrated (Figure 18C).

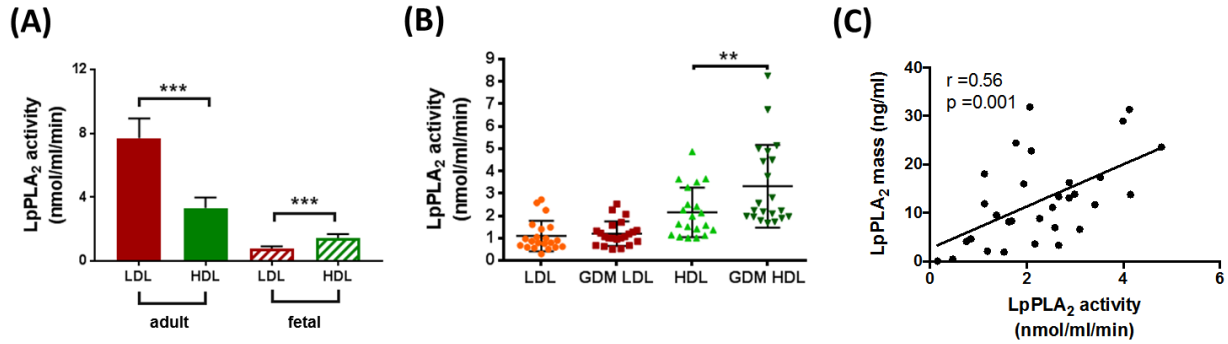

Figure 18: $LpPLA_2$ on fetal lipoproteins. A: Distribution of $LpPLA_2$ activity among adult (solid bars) and fetal (striped bars) lipoproteins. N=4/group, one-way ANOVA. B: Activity of $LpPLA_2$ on lipoproteins isolated from Control and GDM cord blood plasma. N=21/group, one-way ANOVA. C: Pearson correlation of $LpPLA_2$ activity and mass on fetal lipoproteins.

4.10 $LpPLA_2$ activity in fetal circulation correlates with maternal pre-pregnancy obesity

To investigate BMI as confounding factor in this study on gestational diabetes, correlations between maternal pre-gravid and term BMI as well as gestational weight gain with fetal $LpPLA_2$ activity were calculated. As both in the Control and the GDM group, three mothers each had not reported pre-gravid weight, only those individuals where both pre-gravid and term BMI were available, were included in the calculations (n=18/group). Pearson correlation (for non-normally distributed data) showed that LDL-associated $LpPLA_2$ activity correlated neither with pre-gravid BMI (Figure 19A) nor BMI at term (Fig 19B). On the other hand, HDL-associated $LpPLA_2$ activity – the major proportion of LpPLA2 in the fetal circulation - was significantly correlated with pre-gravid BMI ($r=0.5$, $p<0.01$; Figure 19C) and moderately correlated with maternal BMI at term ($r=0.4$, $p<0.05$; Fig 19D).

Mothers, who already enter pregnancy overweight or obese, often put on less weight during pregnancy (194). As a consequence, gestational weight gain was lower (p=0.05) in the GDM group, and HDL-LpPLA$_2$ activity was inversely correlated with maternal gestational weight gain (r = -0.35, p=0.05; Figure 19E).

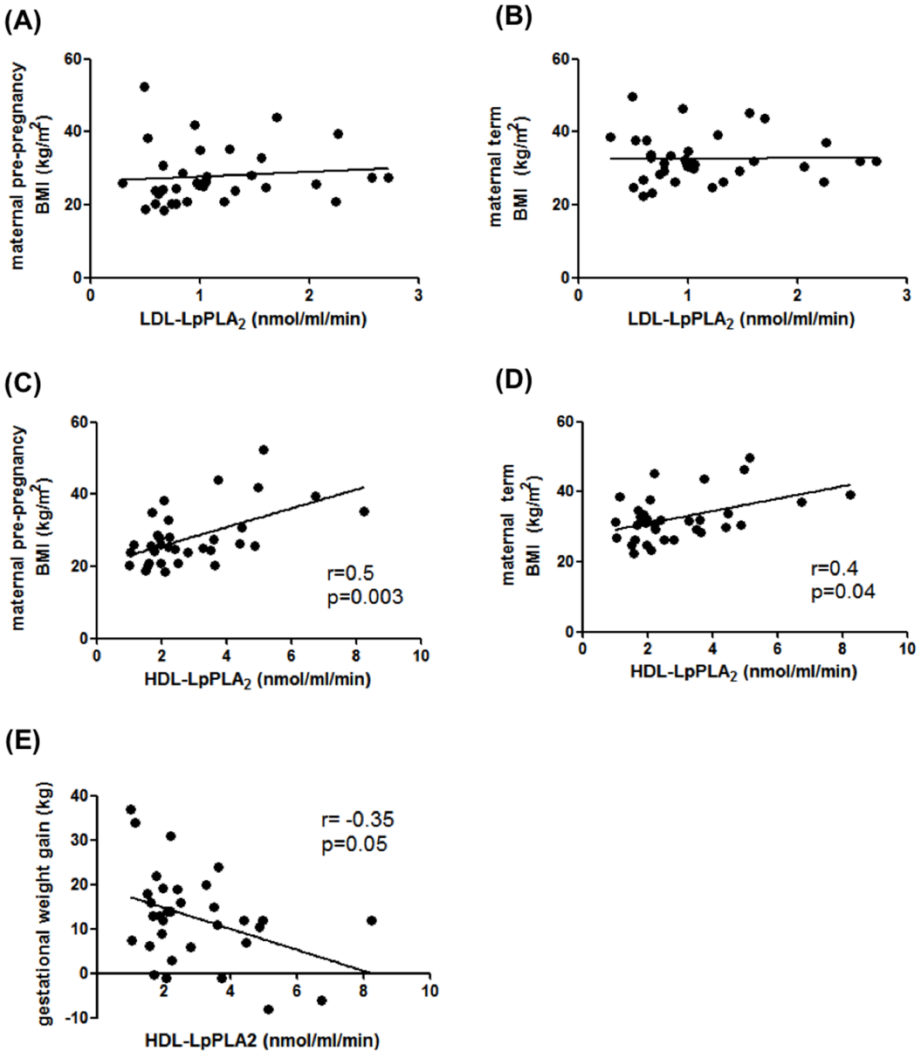

Figure 19: Spearman Correlation of LDL- and HDL-associated fetal LpPLA$_2$ activity with maternal BMI. A: Relationship of LDL-LpPLA$_2$ and maternal pre-gravid BMI. B: Relationship between LDL-LpPLA$_2$ and maternal BMI at term. C: Relationship of HDL-LpPLA$_2$ and maternal pre-gravid BMI. D: Relationship between HDL-LpPLA$_2$ and maternal BMI at term.E: Relationship between maternal gestational weight gain and HDL-LpPLA$_2$.

4.11 Parameters regulating LpPLA$_2$ activity *in vitro*, are also increased in the fetal circulation *in vivo*

To test if those stimuli regulating LpPLA$_2$ secretion and activity from HBCs *in vitro* could also have relevance *in vivo*, levels of these hormones and cytokines were determined in fetal plasma. Glucose levels were not measured, but insulin levels tended to be increased (+54%, p=0.06) in the GDM group. Leptin levels were increased in the GDM group (+84%, p=0.01).

TNFa levels could not be determined in the majority of samples, but ICAM-1 and VCAM-1 levels were both significantly increased in GDM plasma (+14%, p=0.02 and +10%, p=0.01; respectively). Levels of IL-4 were unchanged between Control and GDM group and IL-13 levels could unfortunately not be determined due to the detection limit of the ELISA. All ELISA results are summarized in Table 6.

Table 6 Fetal plasma levels of putative stimulators of $LpPLA_2$ activity.

Cytokine/ Hormones	Control (n≤21)	GDM (n≤21)	% change, p-value
Glucose	N/A	N/A	N/A
Insulin (IU/L)	9.14±4.7	14.1±8.5	+ 54%, p=0.06
Leptin (ng/ml)	6.0±3.2	11.2±6.9	+ 84%, p=0.01
TNFα (pg/ml)	N/A	N/A	N/A
ICAM-1 (pg/ml)	29.2±3.2	33.5±6.8	+ 14%, p=0.02
VCAM-1 (ng/ml)	176.0.0±16.1	192.0±17.4	+10%, p=0.006
IL-4 (pg/ml)	0.16±0.11	0.16±0.11	±0%, n.s.
IL-13 (pg/ml)	N/A	N/A	N/A

N-number is given as ≤21 per group as fetal plasma volume was a limiting factor. Cord blood plasma usually yields about 10ml. 8ml are needed for lipoprotein isolation, with the 2ml left all lipid profiling and ELISA diagnostics was performed. For some of the samples used there was not enough plasma left to conduct all ELISAs. However, for all ELISAs an equal number of samples per group was taken and sample size was never below 16 samples per group.

4.12 $LpPLA_2$ protein abundance and activity are inversely correlated with surrogate markers of oxidative stress

By Western Blot, the protein abundance of $LpPLA_2$ and proteins with an oxidized phosphocholine-backbone (detected by the E06 antibody, Avanti Polar Lipids) as surrogate of oxidized phospholipids were assessed. Whereas $LpPLA_2$ protein was more abundant in GDM placenta (Figure 20A), oxPL-modified proteins were less abundant (Figure 20B). Densitometric analysis revealed that these differences were statistically significant (Figure 20C and D). As it was tempting to speculate that reduced oxPL was a result of increased $LpPLA_2$ activity, correlation of the two was calculated. Although there was a trend (r= -0.36, p=0.09; Fig 20E), the relationship between the two was not significant. In placental tissue, no difference in the localization of $LpPLA_2$ and oxPL between Control and GDM placenta was found (data not shown), but a co-localization of the two was observed along the syncytial membrane of placental villi (Figure 20F), suggesting that $LpPLA_2$ might counteract oxidative de-stabilization of cell membranes in placental tissue.

Also in fetal plasma, a surrogate marker of oxidative stress, thiobarbituric acid substances (TBARS), was quantified. Similar to oxPL-modified proteins in placenta, it was found that TBARS were significantly decreased in fetal GDM plasma ($p<0.001$; Fig 20G). Moreover, TBARS were inversely correlated with fetal HDL-LpPLA2 activity ($r= -0.5$, $p=0.01$; Figure 20H), suggesting that LpPLA2 might limit oxidative stress.

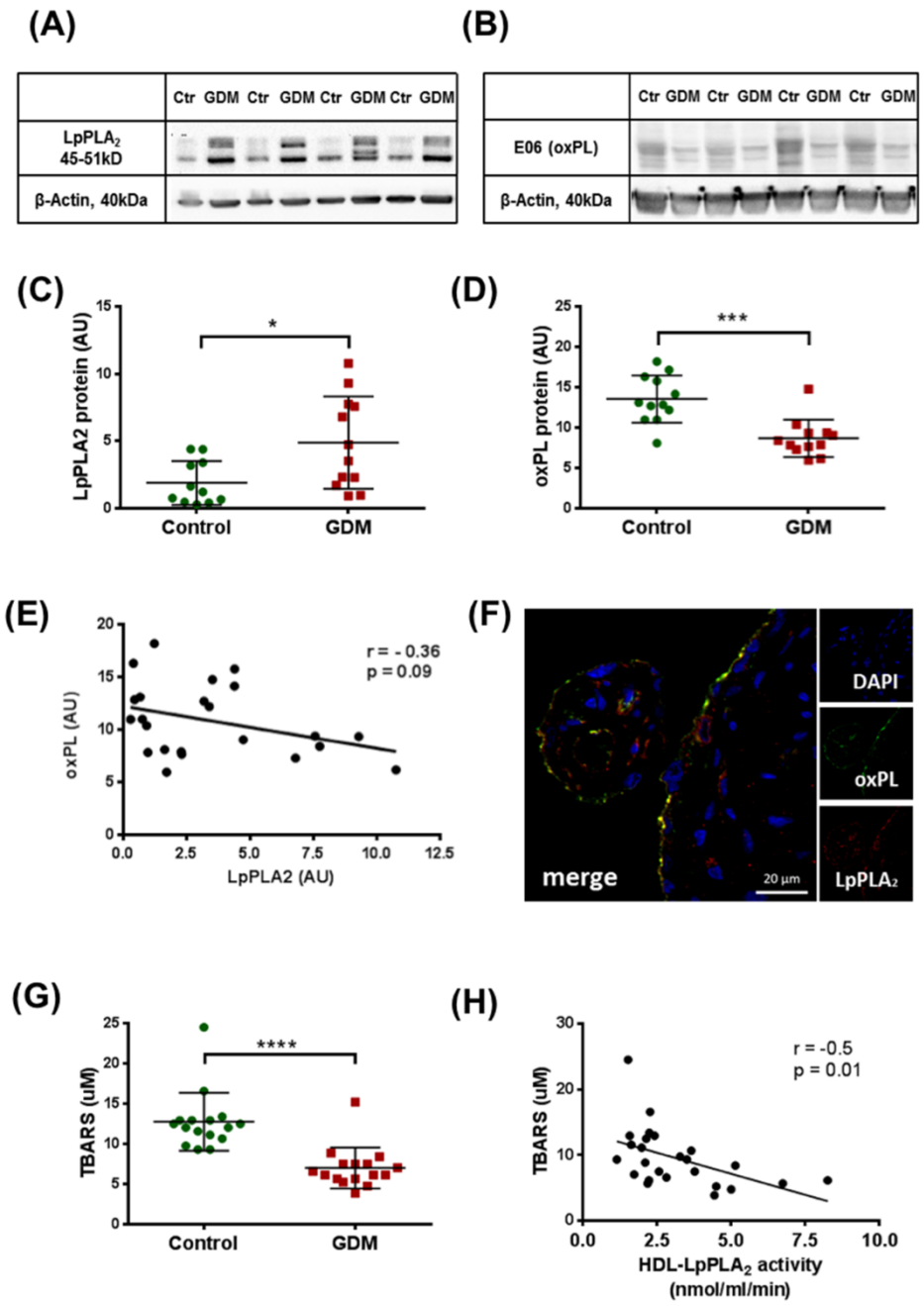

Figure 20: Inverse relationship between $LpPLA_2$ and surrogate markers of oxidative stress in placenta and fetus. A: Western Blot in Control and GDM placenta against $LpPLA_2$. B: Western Blot in Control and GDM placenta against oxPL-modified proteins. Pictures in A and B are representative of 3 individual experiments. β-Actin was used for normalization. C and D: Densitometric analysis of Western Blots against $LpPLA_2$ and oxPL, N=12/group, mean±SD, t-test. E: Pearson correlation between LpPLA2 and oxPL protein as measured by Western Blot. F: Immune-fluorescent co-localization of $LpPLA_2$ (red) with oxPL (green along) along membranes of placental villi. Nuclei were counterstained with DAPI (blue). G: TBARS levels in Control and GDM fetal plasma. N=16/group, mean±SD, t-test. H: Pearson correlation of TBARS in fetal plasma with HDL-associated $LpPLA_2$ activity.

4.13 HDL-associated $LpPLA_2$ contributes to the anti-inflammatory, athero-protective functions of HDL

4.13.1 Electrical Cell-substrate Impedance Sensing (ECIS)

ECIS exploits electrochemical properties of cells grown on culture dishes with embedded electrodes. In these experiments, human placental arterial endothelial cells (AECs) were grown on top of an electrode array, i.e. the culture dish contained more than 10 embedded electrodes. As endothelial cells require gelatin as extracellular matrix, electrodes had been coated with that matrix before addition of cells. The electrode array allows monitoring endothelial barrier function, i.e. how tight cells stick together or how much electrical current can pass between them. Cells were monitored to establish baseline impedance, and after five hours, compounds of interest were added to observe how impedance/barrier function is influenced by these compounds.

Compounds of interest were HDL, or HDL treated with Darapladib to inhibit $LpPLA_2$. DMSO was used as vehicle control for Darapladib. To also study the anti-oxidative function of HDL-LpPLA2, HDL was pre-incubated with 15ug/ml oxPL mixture before addition to the cells. In addition, cells were incubated with oxPL only, with Darapladib only (to test off-target effects of the inhibitor) or left untreated in Endothelial Basal Medium (EBM).
Figure 21A shows one representative ECIS experiment. No off-target effects of Darapladib (light blue) compared to untreated cells (EBM, red) were observed. OxPL only (green) abolished barrier function completely. Compared to oxPL only, barrier function was maintained in both oxPL-HDL-DMSO (dark blue) and oxPL-HDL-Darapladib (turquoise) treated cells; this indicates that HDL might exert protective functions against oxPL. However, oxPL-HDL-DMSO improved barrier function compared to untreated cells, whereas oxPL-HDL-Darapladib treated cells had reduced barrier function compared to untreated cells. This suggests that $LpPLA_2$ on HDL contributes to the anti-oxidative capacity of the HDL particle and endothelial barrier integrity.

Figure 21B represents data pooled from 5 individual ECIS experiments, conducted as described above. Delta impedance, which is the difference in impedance compared to impedance at the time of compound addition, was plotted against time, for better resolution of the treatment effects. Although the same tendencies and trends were observed in each experiment, intra-individual variance between AECs led to high variance between experiments which caused a lost in statistical power. Therefore, the effects demonstrated here, did not reach statistical significance. In addition to the cells themselves, also recovery and re-use of the electrodes might have influenced the experimental set-up.

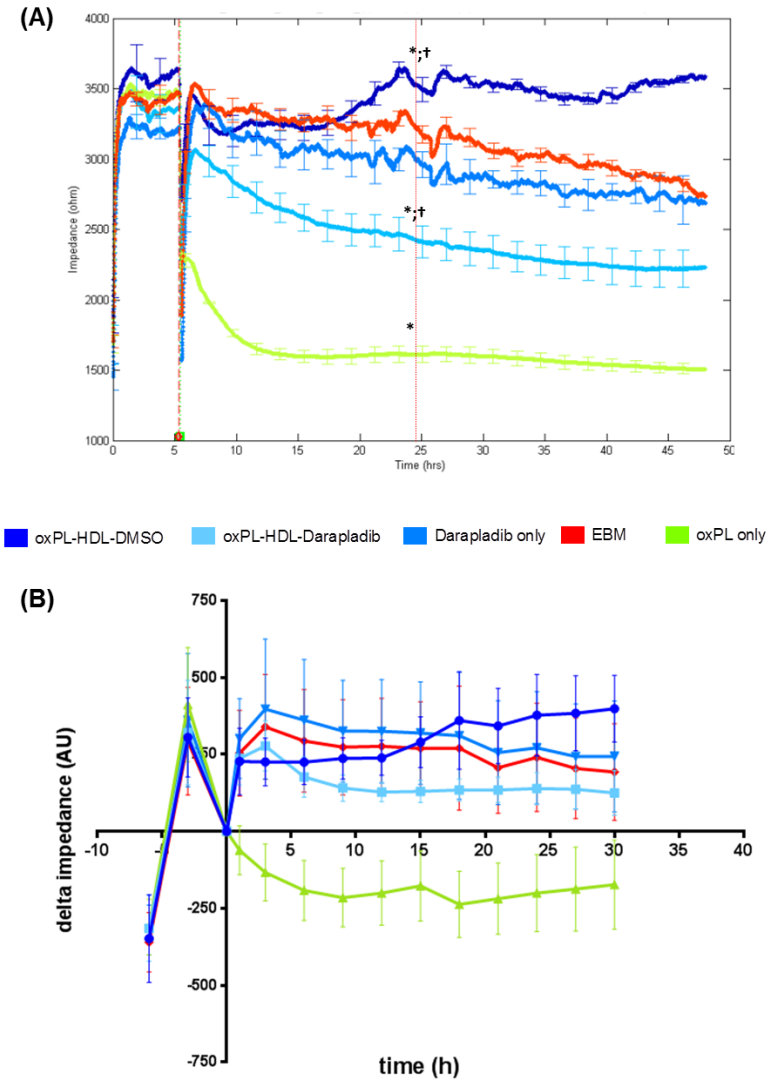

Figure 21: Endothelial barrier function in response to HDL and HDL treated with Darapladib. A: Representative ECIS image out of five individual experiments. The experiment was conducted in quadruplicates, all data mean±SD, two-way ANOVA; at 24h oxPL-HDL-DMSO, oxPL-HDL-Darapladib and oxPL only all significantly differed from EBM control (indicated by *). In addition, oxPL-HDL-DMSO and oxPL-HDL-Darapladib differed significantly from oxPL only (indicated by †). Differences persisted significantly until the end of the experiment. B: Impedance data pooled from 5 individual experiments, mean ±SD, delta impedance = difference in impedance at a given time point compared to the impedance at the time of compound addition.

4.13.2 Lipid Peroxidation assay

In another cell-based assay, the putative anti-oxidative properties of HDL-LpPLA$_2$ against lipid peroxidation were tested. Cells were plated onto chamber slides suitable for flurescence microscopy and pre-incubated with HDL or HDL plus Darapladib (final concentration of HDL 200ug/ml, Darapladib 250nM) from control and GDM pregnancies. Cells were subsequently incubated with the reagents provided in the ClickIT^{TM} Lipid peroxidation kit, so that peroxidized lipids in the cells were visualized in fluorescence microscopy. Additionally, cells were incubated with oxPL (20ug/ml) as positive control and with BSA (200ug/ml) as negative control. The fluorescent signal in HDL treated cells was

limited (Figure 22A, upper left) and similar to the BSA negative control (Figure 22A, lower right). The oxPL positive control (Figure 22A, upper right) showed a high degree of lipid peroxidation and cells were rounding up as if undergoing apoptosis. Cells treated with GDM-HDL (Figure 22A, upper center) presented with higher lipid peroxidation than those treated with Control-HDL. When LpPLA2 was inhibited on HDL and GDM-HDL, an increase in lipid peroxidation was observed in both control (Figure 22A, lower left) and GDM (Figure 22A, lower center) compared to respective native HDL. This suggests that lipid peroxidation in cells can be limited by HDL-$LpPLA_2$ and that inhibition of $LpPLA_2$ on fetal HDL particles is harmful to feto-placental cells.

4.13.3 Dihydrorhodamine 123 assay

Moreover, a cell-free assay measuring the anti-oxidative capacity (AOC) of HDL was carried out, using native HDL and GDM-HDL, and HDL and GDM-HDL treated with Darapladib to inhibit $LpPLA_2$, or with 2-hydroxyquinoline to inhibit Paraoxanase-1 (PON-1), another HDL associated anti-oxidative enzyme.
HDL supposedly protects Dihydrorhodamine-123 (DHR) against oxidation. While DHR oxidates, it develops an auto-fluorescence, which can be detected and used to calculate the degree of oxidation as percentage. As HDL will protect DHR from oxidation, the blank in this assay will usually have a higher fluorescence than the samples themselves. It was found, that HDL and GDM-HDL prevented DHR from oxidation to a similar degree (58% and 55%, respectively). Upon addition of Darapladib, more DHR became oxidized, 62% in Control-HDL plus Darapladib, and 64% in GDM-HDL plus Darapladib. Compared to respective native HDL, the anti-oxidative capacity of Control HDL was unchanged, but the AOC of GDM-HDL was significantly decreased (+9% oxidation, $p<0.001$). Upon addition of hydroxyquinoline, the AOC of both Control and GDM-HDL was significantly decreased (+7.5 and +8.5% oxidation, respectively; $p<0.001$ for both) compared to the native controls. While PON-1 activity seems to contribute to the total AOC of HDL and GDM-HDL in similar manner, the data suggest that $LpPLA_2$ activity is specifically important to the AOC of GDM-HDL particles.

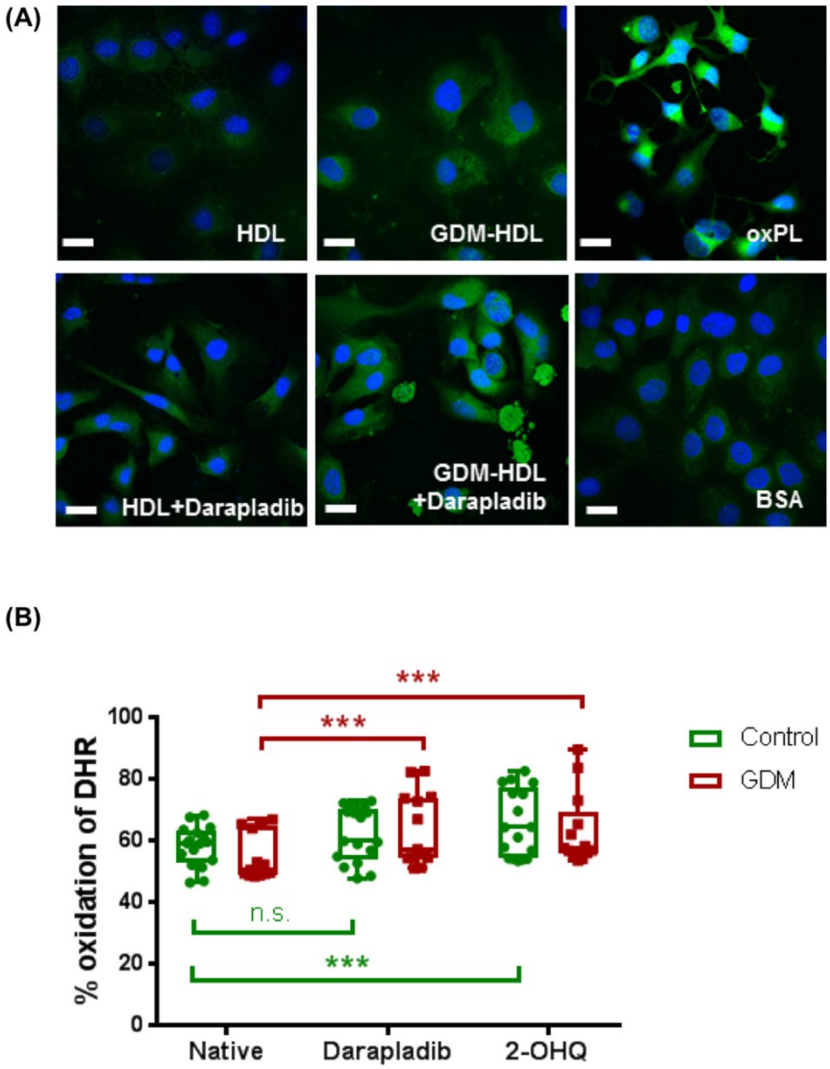

Figure 22: Anti-oxidative capacity of HDL and GDM-HDL. A: Cell-based fluorescent assay of lipid peroxidation. Representative pictures of two individual experiments with two different AEC isolations each (n=4) are shown. Scale bar = 20um. B: CEll-free assay employing dihydrirhodamine to measure the anti-oxidative capacity of HDL and GDM-HDL, in its native form, treated with Darapladib or with 2-hydroxyquinoline (2-OHQ). Boxes represent median and 25% and 75% percentile, data points shown are minimum-to-maximum; RM-ANOVA (two-way ANOVA) for paired measures.

5. Discussion

Gestational diabetes mellitus is a metabolic disorder in pregnancy, which affects 5-20% of all pregnancies, depending on the population looked at. As obesity is a major risk factor for the development of GDM and more and more women at child-bearing age are overweight or obese, the numbers of pregnancies affected by GDM will further rise in the future (195).

Several studies have shown that the pro-inflammatory, diabetic environment can alter the polarization of macrophages in *in vitro* models of pre-diabetes (196), atherosclerotic plaques (197), and in pancreatic islets (198). The human placenta is sensitive to maternal hyperglycemia and reacts to it by adaptation of inflammatory gene and protein expression (74), functional changes such as hypervascularization (191) and increased nutrient transport function (21). In the first part of this thesis, it was speculated if GDM also causes cellular adaptations by the microenvironment, i.e. a switch in the polarization of feto-placental macrophages. Hofbauer cells are generally described as M2 polarized cells in homeostasis, but are highly heterogeneous regarding their functions and phenotypes as a consequence of response to different tissue enviroments.

To study HBC polarization, cell surface markers in tissue and on isolated cells, as well as cytokine secretion from cells, and capability of HBCs to induce endothelial activation were considered. However, very little phenotypically differences between control and GDM HBCs were observed.

Major differences found between control and GDM HBCs, were 1) an increase in the proportion of the M2 markers CD209 and CD206 positive cells in GDM-HBCs, in FACS on isolated cells as well as *in situ* in immune histochemistry; 2) an increase in the M1 marker CD86 in FACS in GDM-HBCs, but not in immune histochemistry, and 3) increased release of M1 cytokines (IL-1β and IL-6) from GDM-HBCS, although this difference was not significant. As a matter of fact, more and more researchers realized that macrophage polarization might not be a uniform strict adaption process in tissues, i.e. M1 or M2 polarization; instead differentiation stages in between and beyond are possible. For example, for M2 macrophages, further subtypes, M2a until M2d, have been described (28). Research from our lab has suggested that in placenta HBCs of the M2a, M2b and M2c subtypes co-exist (43). The data presented here indicate that in GDM an increase in the M2a population, (reflected by the parallel increase in CD209 and CD206 positive cells) and an increase in the M2b population occurs. The M2b subset shares many features with the M1 phenotype, e.g. expression of CD86 and release of IL-1 and IL-6. Nevertheless, M1 and M2b macrophages can be distinguished with help of the ratio of IL-10 to IL-12 release (22). M1 macrophages are generally described as IL-10^{lo}/IL-12^{hi}; M2 macrophages are usually IL-10^{hi}/IL-12^{lo}. In the multiplex panel and by ELISA, it was observed that Control and GDM-HBCs released high levels of IL-10, compared to very low levels of IL-12. Therefore, GDM-HBCs can be claimed to be M2b, but not M1, polarized.
Whether a shift to mire M2a and M2b polarized HBCs point towards a decreased proportion of the M2c subset remains unclear. In immune histochemistry, a decrease in CD206 positive cells relative to CD209 positive cells was observed in GDM placenta. This might indicate a reduction of the M2c subset; in FACS, however, no such difference in the ratio of CD206 to CD209 positive cells was observed. Macrophages of the M2c phenotype appear to be

particularly important in tissue remodeling processes; regulation of such processes presumably belongs to the key functions of HBCs, e.g. the regulation of vascular growth (41,43). Therefore, in the present study, the effect of macrophage conditioned medium on activation of endothelial cells was examined. Conditioned medium from GDM-HBCS caused and increase in endothelial cells ICAM-1 expression, but five other endothelial adhesion molecules were unaffected. Thus, it remains inconclusive if local tissue derived signals casue a reduction in the tissue-remodeling M2c subset of HBCs in GDM placenta.

Independent of the method used (immune cytochemistry, histochemistry, FACS), simultaneous presence of M1 and M2 surface markers was observed in this study on HBCs. Similar findings have been reported by other researchers; for example presence of CD163 expression has been observed on 98% of all HBCs in a study by Young et al., while at the same time the proportion of CD40 positive cells ranged from 5-40% in FACS (199). The same study also demonstrated presence of CD163 and CD40 positive cells by IHC. In contrast to the observations made in this study, Young et al. reported an absence of CD11b positive cells in IHC and FACS. While we did not find CD11b staining in IHC, CD11b was present on isolated cells in cytochemistry and FACS. Such differences could be explained either by different antibody clones used for IHC and FACS, or by poor antigen retrieval and epitope loss after paraffin embedding, or differences could be due to the specific tissue microenvironment which might be lost during HBC isolation as compared to embedded tissue.

Although absent in IHC, we also found CD11c to be present on isolated HBCs using ICC or FACS. Whereas little is known about $CD11b^{+}/CD11c^{+}$ macrophages in placenta, these surface markers have been characterized in adipose tissue macrophages (196) (ATMs). Although most kinds of macrophages express CD11b, co-expression of CD11c has been suggested as sign of activation and switch towards M1 polarization. Furthermore, using ATMs, Zeyda et al. found that macrophages in inflamed adipose tissue show surface markers of the M2 phenotype, but secret M1-associated cytokines (200). Our data point in a similar direction, as GDM-HBCs express high CD209 and less CD206, but also release IL-1β, IL-6 and TNFα. Interestingly, in a study comparing HBCs and ATMs isolated from placenta and adipose tissue of pregnant women, similarities between the two macrophage populations have been found (201). Obesity, which has to be considered a confounding factor in most GDM studies, as many women suffering from GDM are also overweight or obese, has also been demonstrated to cause a switch in HBC gene expression, leading to increased TNFα, IL-1 and IL-6 mRNA levels, pointing towards M1 or M2b polarized HBCs (112).

Some studies have also indicated that independent of the polarization, a fluctuation in HBC cell numbers can occur in inflammatory pregnancy pathologies such as chorioamnionitis and villitis of unknown etiology (40) but also in obese (112) and GDM (202) pregnancies. In this study, however, no increased macrophage numbers in GDM placenta with respect to CD163 and CD68 positive cells was found. Also, calculating the yield of HBCs relative to tissue wet weight used for isolation no difference in HBC numbers was observed ($1.8\pm0.7 \times 10^{6}$ vs. $1.7\pm0.4 \times 10^{6}$ cells per gram tissue wet weight in Control vs. GDM, respectively).

A recent study proposed that Hofbauer cells of women and rats suffering from Type 1 Diabetes mellitus (T1DM) acquire a pro-inflammatory M1 phenotype (54). This is in contradiction to the findings presented here; however, one has to consider differences in study design.

T1DM is a type of diabetes substantially different from GDM, which in many respects resembles Type 2 diabetes mellitus (T2DM). T1DM is an auto-immune disease caused by the destruction of pancreatic beta cells and absolutely insulin-dependent. In contrast, T2DM and also GDM are associated with obesity and insulin-resistance, but can be managed by lifestyle interventions and don't necessarily require insulin treatment. Apart from the differences in the pathophysiology, Sisino and colleagues only measured mRNA levels of the M1 markers CD68 (more pan-macrophage than M1 marker), CCR7 and IL-1β, and mRNA levels of the M2 markers CD163, CD209 and IL-10. Our study, although small in sample size, measured surface markers and cytokine release on protein level and investigated a much larger panel of markers. Furthermore, the mentioned study used RPMI1640 medium to cultivate HBCs. RPMI1640 contains supra-physiological levels of L-arginine (2000mg/L) and is therefore not representative of the human tissue micro-environment. In rodent macrophages, arginine serves two competing metabolic pathways; the arginase-1 pathway, associated with M2 macrophages, and the nitric oxide synthesis (NOS) pathway associated with M1 macrophages (203). Although these pathways are poorly understood in human macrophages, excess L-arginine might have had influenced the HBC phenotype over the time in culture, and has been pointed out as a caveat in HBC culture (204). The present study used macrophage medium from ScienCell, which according to the manufacturer contains only 63mg/L L-arginine.

Placental HBCs are capable to induce placental endothelial cell migration and tube formation (43) and therefore promote feto-placental angiogenesis. Previous studies have indicated that only M2 polarized but not M1 polarized macrophages have pro-angiogenic functions (51,197). Interestingly, tumor-associated macrophages (TAMs) are tissue resident M2 polarized macrophages, which aid tumor angiogenesis (205,206). Strikingly, tumors and the placenta share a number of features (207): 1) both tumor and placental cell mass are build up extremely fast; 2) therefore build-up of an adequate vasculature supporting growth by continuous nutrient and oxygen supply is essential; and 3) evasion from the host or maternal immune system is desired for viability. In tumor patients, maintenance of an M2 macrophage phenotype is detrimental to the host, as the failure to activate macrophages aids the tumor to evade from the hosts immune system; at the same time it facilitates tumor angiogenesis and growth (206). In pregnancy, however, tolerance of the maternal immune system towards the fetus is a necessity to avoid miscarriage, and placental angiogenesis a prerequisite for fetal energy supply. It is tempting to speculate that HBCs are kept in their anti-inflammatory M2 state – even in such pathophysiologic situations as a GDM pregnancy – because (evolutionarily speaking) creating progeny might be just more important than an 'adequate' inflammatory response. This idea is underpinned by studies showing that macrophage activation in the second trimester is associated with spontaneous miscarriage (48), and that in general the fetal immune system is more determined to induce regulatory responses than inflammatory ones; this can be achieved by crosstalk of amnion mesenchymal cells and macrophages (208), and fetal dendritic cells and regulatory T-cells (209).

There are some obvious limitations to the study on macrophage polarization in GDM pregnancies. Only a small set of patients was enrolled in this study, which was therefore designated a pilot-study. This is relevant, as some potentially important but non-significant differences in the release of cytokines such as IL-1β and IL-6 were found between Control and GDM-HBCs.

Post-hoc power analysis however, revealed that specifically for these two parameters power was sufficient despite small sample size. Nevertheless, in a larger cohort, inter-individual differences between subjects would have been better dispersed, adding to better statistical power. Whereas power in the ELISA validation was sufficient, the results from the initial screening using the multiplexed cytokine array have to be interpreted cautiously due to low statistical power. Furthermore, the majority of the methods used in this study allow only for a descriptive characterization of HBCs; although the endothelial activation assay can be considered as one functional assay, more experiments on HBCs functionality (phagocytic activity, co-culture models with endothelial cells, etc.) could further add to a better characterization of these pleiotropic cells. Also, this study has to be considered ground-work basic research, making it hard to comment on any possible clinical impact.

Figure 23 summarizes the observations of the macrophage polarization study, grey and red dashed lines indicate where Control-HBCs (M2a and M2c) and GDM-HBCs (M2a and M2b) fit into the concept of macrophage polarization presented initially in the Introduction section (Figure 4).

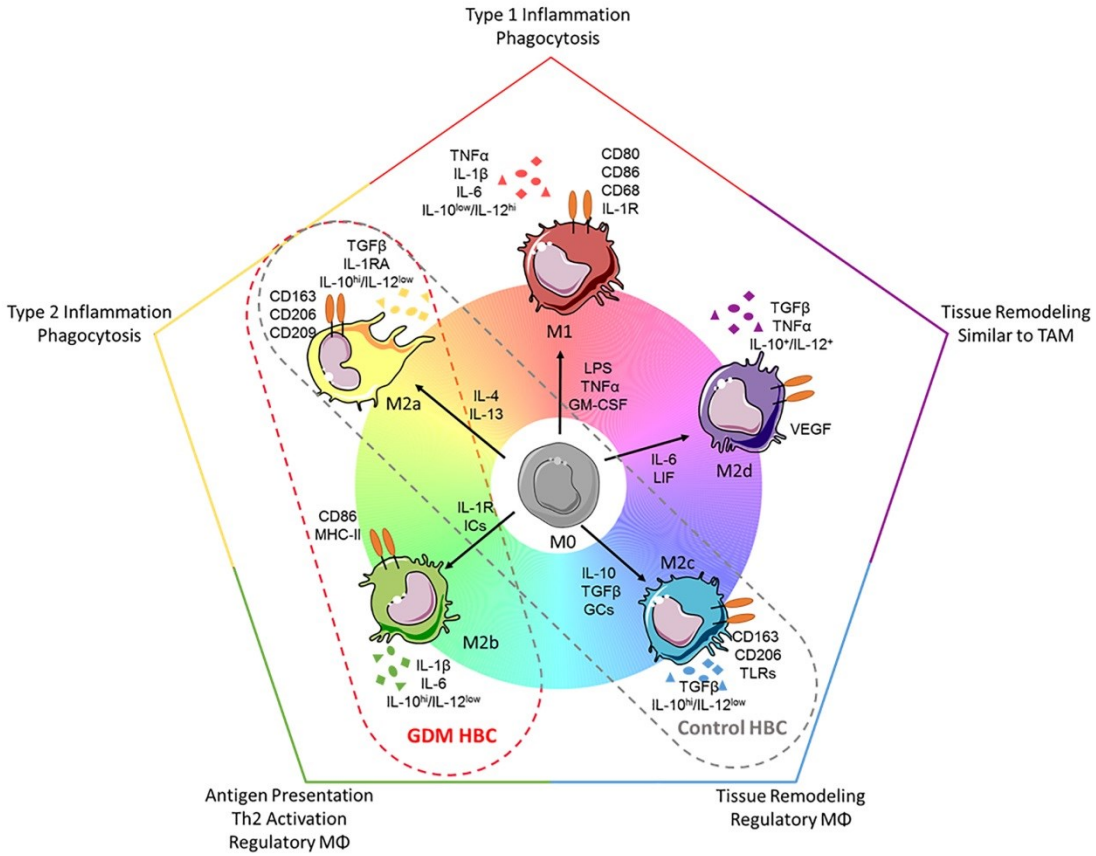

Figure 23: Phenotypes of Control and GDM-HBCs within the general concept of macrophage polarization. This figure has been published in (183).

The second part of this thesis was focused entirely on placental and fetal $LpPLA_2$ activity and its function. By chosing a unique study design which combines *in vitro* data on $LpPLA_2$ and its regulation in Hofbauer cells - which are of fetal origin- with *in vivo* data gained from fetal cord blood plasma, we tried to draw a 'big picture' of $LpPLA_2$ regulation and functional relevance in placenta and fetus.

$LpPLA_2$ is an enzyme produced exclusively by macrophages; however, previous reports have demonstrated that hepatocytes might also release $LpPLA_2$ activity (210). We tried to use HepG2 cells as positive control in initial experiments, but observed that $LpPLA_2$ activity released from these cells was more than 10-fold lower than in HBCs and therefore not a suitable control. To the best of our knowledge, this study is the first to investigate $LpPLA_2$ in human HBCs; previous studies have investigated $LpPLA_2$ in decidual macrophages (211–213), which are, however, said to be of maternal origin. We found that $LpPLA_2$ was increased on mRNA and protein level in GDM placenta compared to control placenta. HBCs were identified as the placental source of $LpPLA_2$ mRNA and protein by qPCR and immune histochemistry. $LpPLA_2$ activity in isolated HBCs could be completely inhibited by addition of its specific inhibitor, Darapladib, and was significantly higher in GDM-HBCs than those HBCs isolated form control placenta. Importantly, control and GDM-HBCs were cultured under identical conditions to measure their $LpPLA_2$ activity; divergent enzymatic activity between the two populations indicates that HBCs maintain their phenotypical properties despite removal from their natural tissue micro-environment over a course of several days in cell culture.

On fetal lipoproteins, a remarkable difference in the distribution of $LpPLA_2$ among LDL and HDL was observed compared to adults. Whereas several studies have demonstrated that LDL is the premier $LpPLA_2$-carrier in adults, as reflected by strong associations between $LpPLA_2$ activity and LDL-C and ApoB levels, in fetuses HDL appears to be the major carrier of $LpPLA_2$ activity. This is in line with LDL being the major lipoprotein fraction in adults, whereas in fetuses HDL comprises the major lipoprotein fraction (214). Many studies have suggested that the function of $LpPLA_2$ might depend on its lipoprotein carrier in plasma; LDL-$LpPLA_2$ is suggested to exert pro-inflammatory actions, whereas HDL-$LpPLA_2$ might exert beneficial anti-inflammatory actions (140,155,215). We also observed that HDL-$LpPLA_2$ was significantly increased in plasma of GDM fetuses and hypothesized about possible functional consequences of increased $LpPLA_2$ levels in placenta and fetal circulation.

As oxPL-species are the main substrates for $LpPLA_2$, the enzyme has long been associated with anti-oxidative functionality. In placental tissue, we found co-localization of oxPL in the syncytial membrane and $LpPLA_2$, hinting that $LpPLA_2$ might contribute to placental membrane integrity and stability. Also, placental $LpPLA_2$ and oxPL-levels were inversely associated, but this association was non-significant.
Performing functional assays with fetal HDL-$LpPLA_2$ was easier and provided more conclusive data. Similar to the inverse association of $LpPLA_2$ and oxPL in placenta, a highly significant inverse correlation between HDL-LpPLA2 activity and TBARS, as surrogate marker of oxidative stress in fetal plasma, was found. Moreover, HDL-$LpPLA_2$ seemed to have beneficial anti-oxidative effects in ECIS barrier function assay, and using Darapladib in this set-up demonstrated that barrier function was dependent on $LpPLA_2$. This indicates that HDL-$LpPLA_2$ has not only anti-oxidative but also vaso-protective functions.

The oxPL mixture used in the functional assays consisted of POV-PC [1-(palmitoyl)-2-(5-oxovaleroyl)-sn-glycero-3-phospatidylcholine], PAz-PC [1-O-hexadecanoyl-2-O-(9-carboxyoctanoyl)-sn-glycero-3-phospatidylcholine] and PGPC (1-palmitoyl-2-glutaryl-phospatidylcholine). These compounds have been identified as constituents of minimally modified/oxidized LDL particles (216), and $LpPLA_2$ has been suggested to detoxify oxPL species within oxLDL (156). Moreover, PGPC has been demonstrated to activate endothelial cells (217), which was beneficial in ECIS and peroxidation assays in order to demonstrate athero-protective functions of $LpPLA_2$. ECIS experiments were conducted with Control-HDL with and without Darapladib only, but not GDM-HDL, because in preliminary experiments no big differences in the effect of Control and GDM-HDL were observed. However, HDL and GDM-HDL were compared in a cell free assay employing Dihydrorhodamine; here, inhibition of $LpPLA_2$ affected the total anti-oxidative capacity of GDM-HDL more than that of Control-HDL, suggesting that $LpPLA_2$ might make a bigger contribution to the anti-oxidative functionality of fetal HDL in the setting of GDM. In summary, this data suggests that $LpPLA_2$ serves to counteract the increased oxidative stress observed in placenta and fetus in GDM (80,218) and obese (219) pregnancies. Furthermore, the vaso-protective action of HDL-$LpPLA_2$ on endothelial barrier function might be a mechanism to limit endothelial dysfunction commonly observed in GDM (190,191).

It was also sought to identify those factors within the low-grade pro-inflammatory, diabetic environment, that might regulate $LpPLA_2$ activity in HBCs *in vitro* and to determine if these factors might be relevant in the fetus *in vivo*. One key feature of GDM are elevated levels of glucose and insulin in fetal plasma; placental gene expression is regulated by fetal insulin, especially in the later stages of pregnancy (63), and particularly insulin receptors are highly abundant on HBCs (220). Glucose and insulin, therefore, were apparent candidates for regulating $LpPLA_2$ activity. Glucose did not have any effect on $LpPLA_2$ activity, but insulin regulated it positively. In addition, the major adipogenic hormone leptin seemed a likely candidate to regulate $LpPLA_2$ activity. Although not as strong as insulin, leptin was able to up-regulate $LpPLA_2$ activity. Insulin and Leptin were also significantly increased in the plasma of GDM fetuses, suggesting that these two hormones might contribute to the increased plasma $LpPLA_2$ activity observed in GDM fetuses. The pro-inflammatory cytokine TNFα, and the two adhesion molecules ICAM-1 and VCAM-1, up-regulated $LpPLA_2$ activity *in vitro*. While TNFα could not be reliably measured in the fetal circulation, both ICAM-1 and VCAM-1 were significantly increased in fetal plasma in the GDM group. Soluble ICAM-1 and VCAM-1 have been suggested as circulating markers of endothelial activation (111), and increased plasma levels in the GDM group might up-regulate $LpPLA_2$, which in turn might exert vaso-protective function.

Most importantly, as this is a very novel finding, anti-inflammatory cytokines such as IL-4 and IL-13 significantly decreased $LpPLA_2$ activity in vitro. The observed effects also were of higher magnitude compared to the effects of the pro-inflammatory cytokines, suggesting that anti-inflammatory cytokines are more potent regulators of $LpPLA_2$ activity. Furthermore, responsiveness to pro- and anti-inflammatory stimuli explains how $LpPLA_2$ expression – although under control of a constitutive promotor (132) – can adapt to the tissue micro-environment, e.g. during and after the acute phase response (221). While previous studies on $LpPLA_2$ were mostly clinical and linked the enzymes activity/mass with other clinical parameters in an associative fashion, the study presented here tried to identify putative causal regulators of $LpPLA_2$ activity *in vitro*.

However, it was not a goal of this study to investigate the signal transduction pathways in-depth, by which these regulators achieve $LpPLA_2$ regulation. Of course, this can be regarded a limitation of the study at hand. Research on signal transduction mechanisms which regulate $LpPLA_2$ activity is scarce, but has indicated that it is mostly dependent on the p38 and PI3K kinases within the MAPK pathway (135,222). From current knowledge about those signaling mechanisms activated by pro-inflammatory cytokines (223), insulin and leptin (224), one might assume that these stimuli also regulate $LpPLA_2$ activity through p38 or PI3K kinases.

BMI has already been mentioned as an important confounding factor of this study, and needs to be thoroughly discussed. Morbid obesity but also overweight are a major predisposing factor for the development of GDM. The cohort used for HDL isolation in this study could not be matched for maternal pre-gravid BMI and BMI at term, and the maternal BMI in the GDM group was significantly higher. Other studies have faced similar problems (173,175). Consequently, we had to take into account that the observed differences in fetal cord blood HDL-$LpPLA_2$ were not related to maternal hyperglycemia, but –at least in part - to maternal obesity. We did find a highly significant correlation between HDL-$LpPLA_2$ activity in the fetus with maternal pre-gravid BMI, and a more moderate correlation with BMI at term. This is logical, as gestational weight gain in the overweight GDM group was significantly lower, making pre-gravid BMI a better measure of the extent of maternal obesity. This is also underpinned by the inverse correlation of fetal HDL-$LpPLA_2$ with maternal gestational weight gain. Interestingly, when groups were split for the correlation analysis, the lean control group did not show any association with fetal HDL-$LpPLA_2$ activity, but the overweight GDM group still did.

Given this data, it remains inconclusive if maternal hyperglycemia or overweight contribute more to the changes observed in fetal $LpPLA_2$ activity. If maternal blood had been available in this study, one could have tried to correlate fetal $LpPLA_2$ activity with such maternal blood parameters as glucose and insulin levels, or HbA1c ore AGEs levels as a measure of the degree of insulin resistance. If such data had been available, we might have been able to distinguish whether hyperglycemia or adiposity did affect fetal $LpPLA_2$ more prominently. With the current data, however, it is only possible to state that our study was flawed by a considerable co-effect of obesity along with hyperglycemia.

Of note, maternal GDM and adiposity affect not only the long-term health of the mother, but also their children. At time of birth, children born to GDM pregnancies are often macrosomic, which increases e.g. the peri-partum risk for shoulder dystocia. Studies have shown that GDM also alters the body composition of the fetuses, the fat tissue mass is increased compared to controls – independent of macrosomia. Furthermore, the risk to develop T2DM or metabolic syndrome later in life is increased. With respect to $LpPLA_2$ activity in children and adolescents, several studies have shown that increased $LpPLA_2$ activity is correlated with BMI and waist circumference (225,226), and is a predictor for the development of T2DM (227). In order to elucidate if increased $LpPLA_2$ activity in GDM fetuses could be causally connected to obesity and T2DM later in life, or if it could at least serve as a risk predictor, consequent prospective follow-up studies of such children would be needed.

Finally, one study recent study from Gao and colleagues (173) needs to be mentioned here, as their study showed some results contradicting our findings on $LpPLA_2$ in the fetal circulation. This study was investigating $LpPLA_2$ in GDM pregnancies, comparing maternal and fetal $LpPLA_2$ levels. Whereas the group did find differences in maternal $LpPLA_2$ levels comparing GDM mothers to pregnant controls, no differences in fetal $LpPLA_2$ levels were found. Also, the majority of fetal $LpPLA_2$ was attached to fetal LDL. Differences in study design and methodology used might explain these divergent observations. First of all, Gao et al. included only mothers with a BMI <25kg/m2 in their study (although noteworthy, BMI in the GDM group was significantly higher than in the control group). Second, fetal cord blood was drawn exclusively from the umbilical vein. The umbilical vein transports oxygenated nutrient-rich blood to the fetus; the two umbilical arteries contain deoxygenated, nutrient-depleted blood back to the placenta for exchange. In the present study, mixed cord blood from vein and arteries was used, as we assume that this might replicate the systemic fetal situation more diligently. Also, the method for lipoprotein isolation differed; whereas we used density gradient ultracentrifugation, their study used precipitation of ApoB containing lipoproteins. As a consequence, their study assessed $LpPLA_2$ activity in total plasma and in the 'non-ApoB-fraction', and calculated LDL-$LpPLA_2$ as the difference between the two. Our study on the other hand, isolated both LDL and HDL and measured $LpPLA_2$ activity directly on the respective particle. Also, the quality of the obtained LDL and HDL was measured by means or the ratio of cholesterol to protein, and the content of ApoB and ApoA1. Lastly, the assay by which $LpPLA_2$ activity was measured was distinct: Goa and colleagues used an in-house assay requiring trichloroacetic acid precipitation and a radioactive tracer. TCA precipitation could substantially affect enzymatic activity. In this study, a commercially available colorimetric kit was used, and LDL and HDL were added natively.

Figure 24 depicts an idea, of how the maternal and fetal environment might affect placental and fetal $LpPLA_2$ expression and enzymatic activity and relates it to the data obtained in this study.

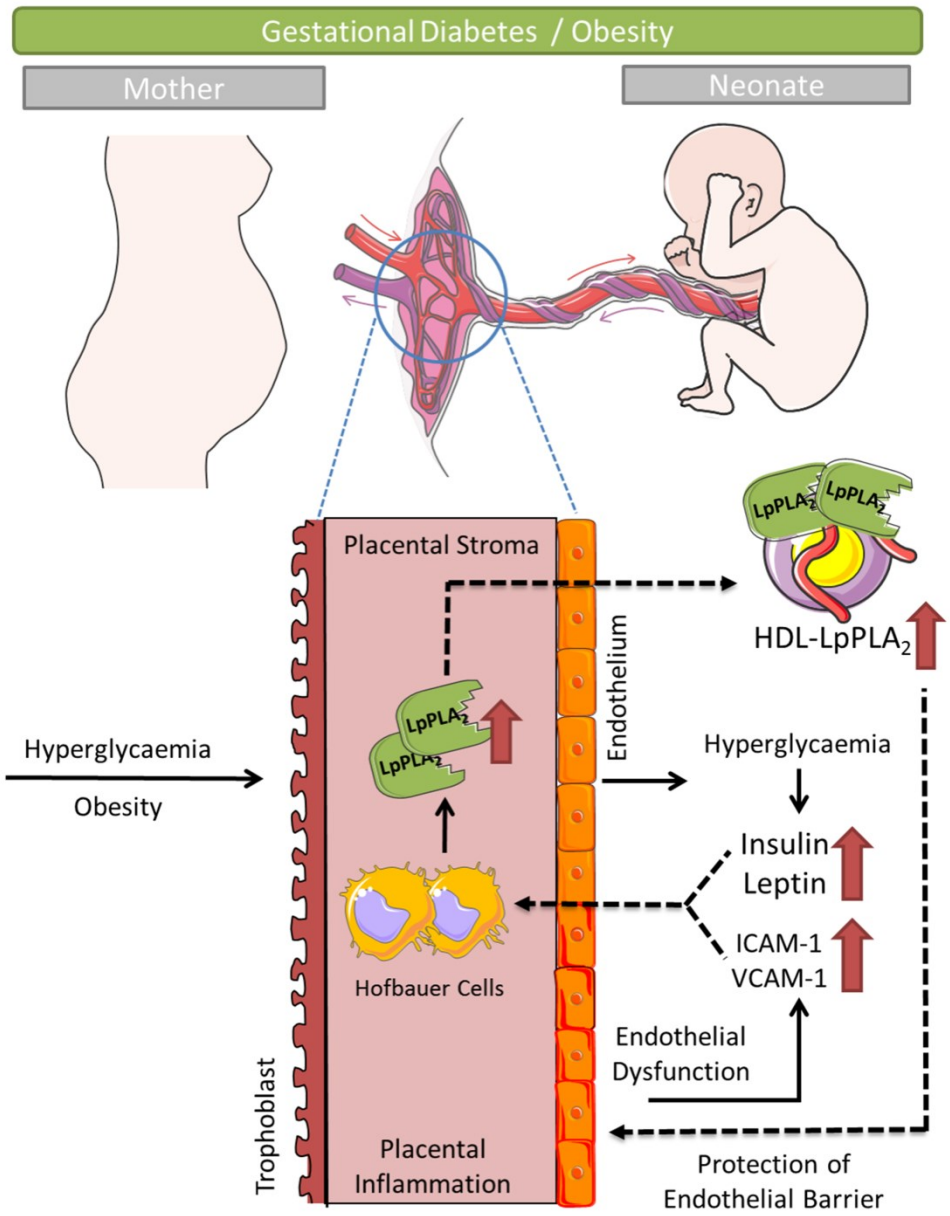

Figure 24: Summary of the role of $LpPLA_2$ in placenta and neonate. Maternal hyperglycemia and obesity are known to cause hyperglycemia in the unborn, reflected by high cord plasma insulin and leptin levels. Also, GDM is known to cause placental (and fetal) endothelial dysfunction, mirrored by ICAM-1 and VCAM-1 activation. We found that insulin, leptin, ICAM-1, and VCAM-1 levels were increased in our study population and all these factors caused increased $LpPLA_2$ activity in HBCs *in vitro*. HBCs are derived from monocytes recruited from the fetal circulation. It is not understood yet, how $LpPLA_2$ is transferred onto HDL after secretion from macrophages, i.e. HBCs. Nevertheless, we found increased $LpPLA_2$ levels both in HBCs and on HDL in neonatal plasma and demonstrated that HDL-$LpPLA_2$ exerts anti-oxidative, protective functions on endothelial cells. Solid arrows represent established effects of GDM and obesity; dashed arrows were used to relate our findings within the concept. Bold red arrows represent elevated levels of respective parameters in our study cohort.

6. Conclusion

In summary, the obtained data indicate that:

1. Feto-placental Hofbauer cells maintain their phenotypic polarization despite the presence of maternal hyperglycemia. As the fetal immune system appears to 'prefer' regulatory responses over inflammatory responses in general, we believe that this stable phenotype could be part of an evolutionarily important mechanism which ensures maternal tolerance against the fetus despite pathophysiology to avoid miscarriage.

2. Insulin, leptin and TNFα up-regulate $LpPLA_2$ activity *in vitro*, IL-4 and IL-13 down-regulate LpPLA2 activity. In the recent past, LDL-$LpPLA_2$ in atherosclerosis and cardiovascular disease patients was mainly tried to be managed by Darapladib as specific inhibitor of the enzyme. However, no direct benefit for the patient was observed upon $LpPLA_2$-inhibition (165). Our data indicate that $LpPLA_2$ activity could be regulated by other means, e.g. life style interventions to lower insulin and leptin, as well as BMI and LDL-cholesterol and reducing (adipose and/or endothelial) tissue inflammation at the same time.

3. $LpPLA_2$ activity in placenta, HBCs, and fetus was increased by Gestational Diabetes. In placenta and fetus, inverse relationships between $LpPLA_2$ levels and oxidative stress markers were observed. Inhibition of $LpPLA_2$ on fetal HDL affected endothelial carrier function and the anti-oxidative capacity of HDL *in vitro*. Therefore, we concluded that HDL-associated $LpPLA_2$ activity exerts anti-oxidative and vaso-protective functions, which might be beneficial to placenta and fetus in the setting of GDM.

7. References

1. Benirschke K, Kaufmann P, Baergen R. Pathology of the Human Placenta - 5th Edition. 2006.
2. Huppertz B. The anatomy of the normal placenta. J Clin Pathol. 2008 Dec;61(12):1296–302.
3. Kaufmann P, Huppertz B, Frank HG. The fibrinoids of the human placenta: origin, composition and functional relevance. Ann Anat. 1996 Dec;178(6):485–501.
4. Lang I, Schweizer A, Hiden U, Ghaffari-Tabrizi N, Hagendorfer G, Bilban M, et al. Human fetal placental endothelial cells have a mature arterial and a juvenile venous phenotype with adipogenic and osteogenic differentiation potential. Differentiation. 2008;76(10):1031–43.
5. Chen DB, Zheng J. Regulation of Placental Angiogenesis. Microcirculation. 2014;21(1):15–25.
6. Demir R, Kaufmann P, Castellucci M, Erbengi T, Kotowski A. Fetal Vasculogenesis and Angiogenesis in Human Placental Villi. Cells Tissues Organs. 1989;136(3):190–203.
7. Hahn T, Hartmann M, Blaschitz A, Skofitsch G, Graf R, Dohr G, et al. Localisation of the high affinity facilitative glucose transporter protein GLUT 1 in the placenta of human, marmoset monkey (Callithrix jacchus) and rat at different developmental stages. Cell Tissue Res. 1995 Apr;280(1):49–57.
8. Hahn D, Blaschitz A, Korgun ET, Lang I, Desoye G, Skofitsch G, et al. From maternal glucose to fetal glycogen: expression of key regulators in the human placenta. Mol Hum Reprod. 2001 Dec;7(12):1173–8.
9. Xing AY, Challier JC, Lepercq J, Caüzac M, Charron MJ, Girard J, et al. Unexpected expression of glucose transporter 4 in villous stromal cells of human placenta. J Clin Endocrinol Metab. 1998 Nov;83(11):4097–101.
10. Cetin I, de Santis MSN, Taricco E, Radaelli T, Teng C, Ronzoni S, et al. Maternal and fetal amino acid concentrations in normal pregnancies and in pregnancies with gestational diabetes mellitus. Am J Obstet Gynecol. 2005 Feb;192(2):610–7.
11. Schneider H, Möhlen KH, Challier JC, Dancis J. Transfer of glutamic acid across the human placenta perfused in vitro. Br J Obstet Gynaecol. 1979 Apr;86(4):299–306.
12. Cariappa R, Heath-Monnig E, Smith CH. Isoforms of amino acid transporters in placental syncytiotrophoblast: plasma membrane localization and potential role in maternal/fetal transport. Placenta. 2003 Aug;24(7):713–26.
13. Herrera E, Amusquivar E, López-Soldado I, Ortega H. Maternal Lipid Metabolism and Placental Lipid Transfer. Horm Res Paediatr. 2006;65(suppl 3(Suppl. 3):59–64.
14. Sattar N, Greer IA, Louden J, Lindsay G, Mcconnell M, Shepherd J, et al. Lipoprotein subfraction changes in normal pregnancy: Threshold effect of plasma triglyceride on appearance of small, dense low density lipoprotein. J Clin Endocrinol Metab. 1997;82(8):2483–91.
15. Lindegaard MLS, Olivecrona G, Christoffersen C, Kratky D, Hannibal J, Petersen BL, et al. Endothelial and lipoprotein lipases in human and mouse placenta. J Lipid Res. 2005;46(11):2339–46.
16. McArdle HJ, Andersen HS, Jones H, Gambling L. Copper and iron transport across the placenta: regulation and interactions. J Neuroendocrinol. 2008 Apr;20(4):427–31.
17. Brunette MG. Calcium transport through the placenta. Can J Physiol Pharmacol. 1988;66:1261–9.

18. Watson ED. Development of Structures and Transport Functions in the Mouse Placenta. Physiology. 2005;20(3):180–93.
19. Malone JI. Vitamin passage across the placenta. Clin Perinatol. 1975;2(2):295–307.
20. Hirschmugl B, Desoye G, Catalano P, Klymiuk I, Scharnagl H, Payr S, et al. Maternal obesity modulates intracellular lipid turnover in the human term placenta. Int J Obes (Lond). 2017 Feb 22;41(2):317–23.
21. Desoye G, Gauster M, Wadsack C. Placental transport in pregnancy pathologies. Am J Clin Nutr. 2011;94(6):1896–902.
22. Mosser DM, Edwards JP. Exploring the full spectrum of macrophage activation. Nat Rev Immunol. 2008;8(12):958–69.
23. Dey A, Allen J, Hankey-Giblin P a. Ontogeny and Polarization of Macrophages in Inflammation: Blood Monocytes Versus Tissue Macrophages. Front Immunol. 2015;5(January):1–15.
24. Valentin JE, Stewart-Akers AM, Gilbert TW, Badylak SF. Macrophage participation in the degradation and remodeling of extracellular matrix scaffolds. Tissue Eng Part A. 2009;15(7):1687–94.
25. Ferrante CJ, Leibovich SJ. Regulation of Macrophage Polarization and Wound Healing. Adv wound care. 2012;1(1):10–6.
26. Baer C, Squadrito ML, Iruela-Arispe ML, De Palma M. Reciprocal interactions between endothelial cells and macrophages in angiogenic vascular niches. Exp Cell Res. 2013;319(11):1626–34.
27. Zajac E, Schweighofer B, Kupriyanova T a, Juncker-Jensen A, Minder P, Quigley JP, et al. Angiogenic capacity of M1- and M2-polarized macrophages is determined by the levels of TIMP-1 complexed with their secreted proMMP-9. Blood. 2013;122(25):4054–67.
28. Rőszer T. Understanding the Mysterious M2 Macrophage through Activation Markers and Effector Mechanisms. Mediators Inflamm. 2015;2015:1–16.
29. Italiani P, Boraschi D. From monocytes to M1/M2 macrophages: Phenotypical vs. functional differentiation. Front Immunol. 2014;5(Oct):1–22.
30. Tang Z, Tadesse S, Norwitz E, Mor G, Abrahams VM, Guller S. Isolation of Hofbauer Cells from Human Term Placentas with High Yield and Purity. Am J Reprod Immunol. 2011; 4;66(4):336–48.
31. Ingman K, Cookson VJKW, Jones CJP, Aplin JD. Characterisation of Hofbauer cells in first and second trimester placenta: incidence, phenotype, survival in vitro and motility. Placenta. 2010 Jun;31(6):535–44.
32. Selkov SA, Selutin A V, Pavlova OM, Khromov-Borisov NN, Pavlov O V. Comparative phenotypic characterization of human cord blood monocytes and placental macrophages at term. Placenta. 2013;34(9):836–9.
33. Vinnars M-TN, Rindsjö E, Ghazi S, Sundberg A, Papadogiannakis N. The Number of CD68+ (Hofbauer) Cells is Decreased in Placentas with Chorioamnionitis and with Advancing Gestational Age. Pediatr Dev Pathol. 2009; 23;13(4):300–4.
34. Yamaguchi M, Ohba T, Tashiro H, Yamada G, Katabuchi H. Human chorionic gonadotropin induces human macrophages to form intracytoplasmic vacuoles mimicking hofbauer cells in human chorionic villi. Cells Tissues Organs. 2013;197(2):127–35.
35. Simoni MK, Jurado KA, Abrahams VM, Fikrig E, Guller S. Zika virus infection of Hofbauer cells. Am J Reprod Immunol. 2017 Feb;77(2) e12613.
36. Rosenberg AZ, Yu W, Hill DA, Reyes CA, Schwartz DA. Placental Pathology of Zika

Virus: Viral Infection of the Placenta Induces Villous Stromal Macrophage (Hofbauer Cell) Proliferation and Hyperplasia. Arch Pathol Lab Med. 2017 Jan;141(1):43–8.
37. Johnson EL, Chu H, Byrareddy SN, Spearman P, Chakraborty R. Placental Hofbauer cells assemble and sequester HIV-1 in tetraspanin-positive compartments that are accessible to broadly neutralizing antibodies. J Int AIDS Soc. 2015;18:19385.
38. Johnson EL, Chakraborty R. Placental Hofbauer cells limit HIV-1 replication and potentially offset mother to child transmission (MTCT) by induction of immunoregulatory cytokines. Retrovirology. 2012;9(1):101.
39. Ben Amara A, Gorvel L, Baulan K, Derain-Court J, Buffat C, Vérollet C, et al. Placental macrophages are impaired in chorioamnionitis, an infectious pathology of the placenta. J Immunol. 2013;191:5501–14.
40. Kim J, Romero R, Kim M, Kim M, Friel L, Espinoza J, et al. Involvement of Hofbauer cells and maternal T cells in villitis of unknown etiology. Histopathology. 2008;52(4):457–64.
41. Seval Y, Korgun ET, Demir R. Hofbauer Cells in Early Human Placenta: Possible Implications in Vasculogenesis and Angiogenesis. Placenta. 2007;28(8–9):841–5.
42. Anteby EY, Natanson-Yaron S, Greenfield C, Goldman-Wohl D, Haimov-Kochman R, Holzer H, et al. Human placental Hofbauer cells express sprouty proteins: A possible modulating mechanism of villous branching. Placenta. 2005;26(6):476–83.
43. Loegl J, Hiden U, Nussbaumer E, Schliefsteiner C, Cvitic S, Lang I, et al. Hofbauer cells of M2a, M2b and M2c polarization may regulate feto-placental angiogenesis. Reprod. 2016 Nov;152(5):447–55.
44. Tang Z, Buhimschi IA, Buhimschi CS, Tadesse S, Norwitz E, Niven-Fairchild T, et al. Decreased Levels of Folate Receptor-β and Reduced Numbers of Fetal Macrophages (Hofbauer Cells) in Placentas from Pregnancies with Severe Preeclampsia (PE). Am J Reprod Immunol. 2014 Aug 11;70(2):104–15.
45. Erlebacher A. Immunology of the maternal-fetal interface. Annu Rev Immunol. 2013 Jan;31:387–411.
46. Malassine A, Frendo J-L, Evain-Brion D. A comparison of placental development and endocrine functions between the human and mouse model. Hum Reprod Update. 2003;9(6):531–9.
47. Svensson-Arvelund J, Mehta RB, Lindau R, Mirrasekhian E, Rodriguez-Martinez H, Berg G, et al. The Human Fetal Placenta Promotes Tolerance against the Semiallogeneic Fetus by Inducing Regulatory T Cells and Homeostatic M2 Macrophages. J Immunol. 2015;194:1534–44.
48. Matsubara S, Takayama T, Yamada T, Usui R, Izumi A, Watanabe T, et al. Hofbauer Cell Activation and its increased Glucose-6-Phosphate Dehydrogenase Activity in Second Trimester-spontaneous Abortion: an Ultrastructural Dual Staining Enzyme-cytochemical Study. Am J Reprod Immunol. 2003 Apr 1;49(4):202–9.
49. Bockle BC, Solder E, Kind S, Romani N, Sepp NT. DC-SIGN+ CD163+ Macrophages Expressing Hyaluronan Receptor LYVE-1 Are Located within Chorion Villi of the Placenta. Placenta. 2008;29(2):187–92.
50. Svensson J, Jenmalm MC, Matussek A, Geffers R, Berg G, Ernerudh J. Macrophages at the fetal-maternal interface express markers of alternative activation and are induced by M-CSF and IL-10. J Immunol. 2011;187(7):3671–82.
51. Jetten N, Verbruggen S, Gijbels MJ, Post MJ, De Winther MPJ, Donners MMPC. Anti-inflammatory M2, but not pro-inflammatory M1 macrophages promote angiogenesis in vivo. Angiogenesis. 2014;17(1):109–18.

52. Kim SY, Romero R, Tarca AL, Bhatti G, Kim CJ, Lee J, et al. Methylome of Fetal and Maternal Monocytes and Macrophages at the Feto-Maternal Interface. 2012;68(1):8–27.
53. Joerink M, Rindsjö E, van Riel B, Alm J, Papadogiannakis N. Placental macrophage (Hofbauer cell) polarization is independent of maternal allergen-sensitization and presence of chorioamnionitis. Placenta. 2011 May;32(5):380–5.
54. Sisino G, Bouckenooghe T, Aurientis S, Fontaine P, Storme L, Vambergue A. Diabetes during pregnancy influences Hofbauer cells, a subtype of placental macrophages, to acquire a pro-inflammatory phenotype. Biochim Biophys Acta - Mol Basis Dis. 2013;1832(12):1959–68.
55. Eades CE, Cameron DM, Evans JMM. Prevalence of gestational diabetes mellitus in Europe: A meta-analysis. Diabetes Res Clin Pract. 2017 Jul;129:173–81.
56. Yeung RO, Savu A, Kinniburgh B, Lee L, Dzakpasu S, Nelson C, et al. Prevalence of gestational diabetes among Chinese and South Asians: A Canadian population-based analysis. J Diabetes Complications. 2017 Mar;31(3):529–36.
57. Sletner L, Jenum AK, Yajnik CS, Mørkrid K, Nakstad B, Rognerud-Jensen OH, et al. Fetal growth trajectories in pregnancies of European and South Asian mothers with and without gestational diabetes, a population-based cohort study. PLoS One. 2017;12(3):e0172946.
58. Huynh J, Yamada J, Beauharnais C, Wenger JB, Thadhani RI, Wexler D, et al. Type 1, type 2 and gestational diabetes mellitus differentially impact placental pathologic characteristics of uteroplacental malperfusion. Placenta. 2015;36(10):1161–6.
59. Jirkovská M, Kubínová L, Janáček J, Moravcová M, Krejčí V, Karen P. Topological properties and spatial organization of villous capillaries in normal and diabetic placentas. J Vasc Res. 2002;39(3):268–78.
60. Babawale MO, Lovat S, Mayhew TM, Lammiman MJ, James DK, Leach L. Effects of gestational diabetes on junctional adhesion molecules in human term placental vasculature. Diabetologia. 2000 Sep;43(9):1185–96.
61. Arany E, Hill DJ. Fibroblast growth factor-2 and fibroblast growth factor receptor-1 mRNA expression and peptide localization in placentae from normal and diabetic pregnancies. Placenta. 19(2–3):133–42.
62. Marini M, Vichi D, Toscano A, Thyrion GDZ, Bonaccini L, Parretti E, et al. Effect of impaired glucose tolerance during pregnancy on the expression of VEGF receptors in human placenta. Reprod Fertil Dev. 2008;20(7):789–801.
63. Hiden U, Maier A, Bilban M, Ghaffari-Tabrizi N, Wadsack C, Lang I, et al. Insulin control of placental gene expression shifts from mother to foetus over the course of pregnancy. Diabetologia. 2006;49(1):123–31.
64. Freinkel N. Banting Lecture 1980. Of pregnancy and progeny. Diabetes. 1980 Dec;29(12):1023–35.
65. Widness JA, Susa JB, Garcia JF, Singer DB, Sehgal P, Oh W, et al. Increased erythropoiesis and elevated erythropoietin in infants born to diabetic mothers and in hyperinsulinemic rhesus fetuses. J Clin Invest. 1981 Mar;67(3):637–42.
66. Lassance L, Miedl H, Absenger M, Diaz-Perez F, Lang U, Desoye G, et al. Hyperinsulinemia stimulates angiogenesis of human fetoplacental endothelial cells: A possible role of insulin in placental hypervascularization in diabetes mellitus. J Clin Endocrinol Metab. 2013;98(9):1438–47.

67. Osmond DT, King RG, Brennecke SP, Gude NM. Placental glucose transport and utilisation is altered at term in insulin-treated, gestational-diabetic patients. Diabetologia. 2001 Sep;44(9):1133–9.
68. Colomiere M, Permezel M, Riley C, Desoye G, Lappas M. Defective insulin signaling in placenta from pregnancies complicated by gestational diabetes mellitus. Eur J Endocrinol. 2009 Apr;160(4):567–78.
69. Dicke JM, Henderson GI. Placental amino acid uptake in normal and complicated pregnancies. Am J Med Sci. 1988 Mar;295(3):223–7.
70. Nandakumaran M, Al-Shammari M, Al-Saleh E. Maternal-fetal transport kinetics of L-Leucine in vitro in gestational diabetic pregnancies. Diabetes Metab. 2004 Sep;30(4):367–74.
71. Couch SC, Philipson EH, Bendel RB, Wijendran V, Lammi-Keefe CJ. Maternal and cord plasma lipid and lipoprotein concentrations in women with and without gestational diabetes mellitus. Predictors of birth weight? J Reprod Med. 1998 Sep;43(9):816–22.
72. Magnusson AL, Waterman IJ, Wennergren M, Jansson T, Powell TL. Triglyceride hydrolase activities and expression of fatty acid binding proteins in the human placenta in pregnancies complicated by intrauterine growth restriction and diabetes. J Clin Endocrinol Metab. 2004 Sep;89(9):4607–14.
73. Radaelli T, Lepercq J, Varastehpour A, Basu S, Catalano PM, Hauguel-De Mouzon S. Differential regulation of genes for fetoplacental lipid pathways in pregnancy with gestational and type 1 diabetes mellitus. Am J Obstet Gynecol. 2009 Aug;201(2):209.e1-209.e10.
74. Radaelli T, Varastehpour A, Catalano P, Mouzon SH. Gestational Diabetes Induces Placental Genes for Chronic Stress and Inflammatory Pathways. Diabetes. 2003;52(April):2951–8.
75. Mrizak I, Grissa O, Henault B, Fekih M, Bouslema A, Boumaiza I, et al. Placental infiltration of inflammatory markers in gestational diabetic women. Gen Physiol Biophys. 2014;33(2):169–76.
76. Gomes CP, Torloni MR, Gueuvoghlanian-Silva BY, Alexandre SM, Mattar R, Daher S. Cytokine Levels in Gestational Diabetes Mellitus: A Systematic Review of the Literature. Am J Reprod Immunol. 2013;69:545–57.
77. Dubé M-C, Morisset A-S, Tchernof A, Weisnagel SJ. Cord blood C-peptide levels relate to the metabolic profile of women with and without gestational diabetes. Acta Obstet Gynecol Scand. 2012 Dec;91(12):1469–73.
78. Atègbo JM, Grissa O, Yessoufou A, Hichami A, Dramane KL, Moutairou K, et al. Modulation of adipokines and cytokines in gestational diabetes and macrosomia. J Clin Endocrinol Metab. 2006;91(10):4137–43.
79. Hara C de CP, França EL, Fagundes DLG, de Queiroz AA, Rudge MVC, Honorio-França AC, et al. Characterization of Natural Killer Cells and Cytokines in Maternal Placenta and Fetus of Diabetic Mothers. J Immunol Res. 2016;2016:7154524.
80. Coughlan MT, Vervaart PP, Permezel M, Georgiou HM, Rice GE. Altered placental oxidative stress status in gestational diabetes mellitus. Placenta. 2004 Jan;25(1):78–84.
81. Biri A, Onan A, Devrim E, Babacan F, Kavutcu M, Durak I. Oxidant status in maternal and cord plasma and placental tissue in gestational diabetes. Placenta. 2006 Jan;27(2–3):327–32.
82. Rayanagoudar G, Hashi AA, Zamora J, Khan KS, Hitman GA, Thangaratinam S. Quantification of the type 2 diabetes risk in women with gestational diabetes: a

systematic review and meta-analysis of 95,750 women. Diabetologia. 2016 Apr;59:1403–11.
83. Linné Y, Barkeling B, Rössner S. Natural course of gestational diabetes mellitus: long term follow up of women in the SPAWN study. BJOG. 2002 Nov;109(11):1227–31.
84. Zhu Y, Zhang C. Prevalence of Gestational Diabetes and Risk of Progression to Type 2 Diabetes: a Global Perspective. Curr Diab Rep. 2016;16(1):1–11.
85. Shah BR, Retnakakaran R, Booth G. Increased Risk of Cardiovascular Disease in Young Women Following Gestational Diabetes Mellitus. Diabetes Care. 2008;31(May):1668–9.
86. Banerjee M, Anderson SG, Malik R a, Austin CE, Cruickshank JK. Small artery function 2 years postpartum in women with altered glycaemic distributions in their preceding pregnancy. Clin Sci (Lond). 2012 Jan;122(2):53–61.
87. Hwu L-J, Sung F-C, Mou C-H, Wang I-K, Shih H-H, Chang Y-Y, et al. Risk of Subsequent Hypertension and Diabetes in Women With Hypertension During Pregnancy and Gestational Diabetes. Mayo Clin Proc. 2016 Sep;91(9):1158–65.
88. Durnwald C, Huston-Presley L, Amini S, Catalano P. Evaluation of body composition of large-for-gestational-age infants of women with gestational diabetes mellitus compared with women with normal glucose tolerance levels. Am J Obstet Gynecol. 2004 Sep;191(3):804–8.
89. Michael Weindling A. Offspring of diabetic pregnancy: Short-term outcomes. Semin Fetal Neonatal Med. 2009;14(2):111–8.
90. Kc K, Shakya S, Zhang H. Gestational diabetes mellitus and macrosomia: A literature review. Ann Nutr Metab. 2015;66:14–20.
91. Lawlor DA, Lichtenstein P, Långström N. Association of maternal diabetes mellitus in pregnancy with offspring adiposity into early adulthood: Sibling study in a prospective cohort of 280 866 men from 248 293 families. Circulation. 2011;123(3):258–65.
92. Crume TL, Ogden L, West NA, Vehik KS, Scherzinger A, Daniels S, et al. Association of exposure to diabetes in utero with adiposity and fat distribution in a multiethnic population of youth: The Exploring Perinatal Outcomes among Children (EPOCH) study. Diabetologia. 2011;54(1):87–92.
93. Dabelea D, Hanson RL, Lindsay RS, Pettitt DJ, Imperatore G, Gabir MM, et al. Intrauterine exposure to diabetes conveys risks for type 2 diabetes and obesity: A Study of Discordant Sibships. Diabetes. 2000;49(12):2208–11.
94. Burgio E, Lopomo A, Migliore L. Obesity and diabetes: from genetics to epigenetics. Mol Biol Rep. 2015;42(4):799–818.
95. Chen Y, Quick WW, Yang W, Zhang Y, Baldwin A, Moran J, et al. Cost of gestational diabetes mellitus in the United States in 2007. Popul Health Manag. 2009;12(3):165–74.
96. Petersen M. Economic costs of diabetes in the U.S. in 2012. Diabetes Care. 2016;39(7):1033–46.
97. Huang ES, Basu A, O'Grady M, Capretta JC. Projecting the future diabetes population size and related costs for the U.S. Diabetes Care. 2009;32(12):2225–9.
98. Sebire NJ, Jolly M, Harris JP, Wadsworth J, Joffe M, Beard RW, et al. Maternal obesity and pregnancy outcome: a study of 287,213 pregnancies in London. Int J Obes Relat Metab Disord. 2001 Aug;25(8):1175–82.
99. Boney CM, Verma A, Tucker R, Vohr BR. Metabolic Syndrome in Childhood: Association With Birth Weight, Maternal Obesity, and Gestational Diabetes Mellitus. Pediatrics. 2005;115(3):e290–6.

100. Berghoefer A, Pischon T, Reinhold T, Apovian CM, Sharma AM, Willich SN, et al. Obesity prevalence from a European perspective: a systematic review. BMCPublic Heal. 2008;8(1):200–10.
101. Heslehurst N, Rankin J, Wilkinson JRR, Summerbell CDD. A nationally representative study of maternal obesity in England, UK: trends in incidence and demographic inequalities in 619 323 births, 1989-2007. Int J Obes. 2010;34(3):420–8.
102. Hotamisligil GS, Shargill NS, Spiegelman BM. Adipose expression of tumor necrosis factor-alpha: direct role in obesity-linked insulin resistance. Science. 1993 Jan 1;259(5091):87–91.
103. Maffei M, Halaas J, Ravussin E, Pratley RE, Lee GH, Zhang Y, et al. Leptin levels in human and rodent: Measurement of plasma leptin and ob RNA in obese and weight-reduced subjects. Nat Med. 1995 Nov;1(11):1155–61.
104. Arita Y, Kihara S, Ouchi N, Takahashi M, Maeda K, Miyagawa J, et al. Reprint of "Paradoxical Decrease of an Adipose-Specific Protein, Adiponectin, in Obesity." Biochem Biophys Res Commun. 2012;425(3):560–4.
105. Juge-Aubry CE, Somm E, Pernin A, Alizadeh N, Giusti V, Dayer JM, et al. Adipose tissue is a regulated source of interleukin-10. Cytokine. 2005;29(6):270–4.
106. Apovian CM, Bigornia S, Mott M, Meyers MR, Ulloor J, Gagua M, et al. Adipose macrophage infiltration is associated with insulin resistance and vascular endothelial dysfunction in obese subjects. Arterioscler Thromb Vasc Biol. 2008 Sep;28(9):1654–9.
107. Ramsay JE, Ferrell WR, Crawford L, Michael Wallace A, Greer IA, Sattar N. Maternal obesity is associated with dysregulation of metabolic, vascular, and inflammatory pathways. J Clin Endocrinol Metab. 2002;87(9):4231–7.
108. Roberts KA, Riley SC, Reynolds RM, Barr S, Evans M, Statham A, et al. Placental structure and inflammation in pregnancies associated with obesity. Placenta. 2011 Mar;32(3):247–54.
109. Christian LM, Porter K. Longitudinal changes in serum proinflammatory markers across pregnancy and postpartum: Effects of maternal body mass index. Cytokine. 2014;70(2):134–40.
110. Stewart FM, Freeman DJ, Ramsay JE, Greer IA, Caslake M, Ferrell WR. Longitudinal assessment of maternal endothelial function and markers of inflammation and placental function throughout pregnancy in lean and obese mothers. J Clin Endocrinol Metab. 2007;92(3):969–75.
111. Videm V, Albrigtsen M. Soluble ICAM-1 and VCAM-1 as markers of endothelial activation. Scand J Immunol. 2008 May 1;67(5):523–31.
112. Challier J, Basu S, Bintein T, Hotmire K, Minium J, Catalano P, et al. Obesity in pregnancy stimulates macrophage accumulation and inflammation in the placenta. Placenta. 2008;29(3):274–81.
113. Scifres CM, Chen B, Nelson DM, Sadovsky Y. Fatty acid binding protein 4 regulates intracellular lipid accumulation in human trophoblasts. J Clin Endocrinol Metab. 2011 Jul;96(7):E1083-91.
114. Varastehpour A, Radaelli T, Minium J, Ortega H, Herrera E, Catalano P, et al. Activation of Phospholipase A2 is associated with generation of placental lipid signals and fetal obesity. J Clin Endocrinol Metab. 2006;91(1):248–55.
115. Martino J, Sebert S, Segura MT, García-Valdés L, Florido J, Padilla MC, et al. Maternal Body Weight and Gestational Diabetes Differentially Influence Placental and Pregnancy Outcomes. J Clin Endocrinol Metab. 2016;101(1):59–68.

116. Saben J, Lindsey F, Zhong Y, Thakali K. Maternal obesity is associated with a lipotoxic placental environment. Placenta. 2014 Mar;35(3):171–7.
117. Roberts VHJ, Jessica Smith, BS, Stacey A. McLea, Angela B. Heizer, BS, Jade L. Richardson, MD, and Leslie Myatt P, Department. Effect of Increasing Maternal Body Mass Index on Oxidative and Nitrative Stress in the Human Placenta. Placenta. 2010;30(2):169–75.
118. Pantham P, Aye ILMH, Powell TL. Inflammation in maternal obesity and gestational diabetes mellitus. Placenta. 2015;36(7):709–15.
119. Denison FC, Roberts K a, Barr SM, Norman JE. Obesity, pregnancy, inflammation, and vascular function. Reproduction. 2010 Sep;140(3):373–85.
120. Herskind AM, McGue M, Iachine IA, Holm N, Sørensen TI, Harvald B, et al. Untangling genetic influences on smoking, body mass index and longevity: a multivariate study of 2464 Danish twins followed for 28 years. Hum Genet. 1996 Oct;98(4):467–75.
121. Godfrey KM, Inskip HM, Hanson MA. The long-term effects of prenatal development on growth and metabolism. Semin Reprod Med. 2011;29(1526–4564 (Electronic)):257–65.
122. Blank ML, Lee T, Fitzgerald V, Snyder F. A specific acetylhydrolase for 1-alkyl-2-acetyl-sn-glycero-3-phosphocholine (a hypotensive and platelet-activating lipid). J Biol Chem. 1981 Jan 10;256(1):175–8.
123. Tjoelker LW, Eberhardt C, Trong H Le, Zimmerman G a, Mcintyre TM, Stafforini DM, et al. Protein Chemistry and Structure : Plasma Platelet-activating Factor Acetylhydrolase Is a Secreted Phospholipase A 2 with a Catalytic Triad Plasma Platelet-activating Factor Acetylhydrolase Is a Secreted Phospholipase A 2 with a Catalytic Triad *. J Biol Chem. 1995;270(43):25481–25487.
124. Akiyama M, Sugatani J, Suzuki T, Suzuki Y, Miwa M. Identification of a major PAF acetylhydrolase in human serum/plasma as a 43 kDa glycoprotein containing about 9 kDa asparagine-conjugated sugar chain(s). J Biochem. 1998;123(5):786–9.
125. Tselepis A, Karabina S. N-linked glycosylation of macrophage-derived PAF-AH is a major determinant of enzyme association with plasma HDL. J Lipid Res. 2001;42(10):1645–54.
126. McCall MR, La Belle M, Forte TM, Krauss RM, Takanami Y, Tribble DL. Dissociable and nondissociable forms of platelet-activating factor acetylhydrolase in human plasma LDL: implications for LDL oxidative susceptibility. Biochim Biophys Acta. 1999 Jan 29;1437(1):23–36.
127. Karabina SA, Elisaf MC, Goudevenos J, Siamopoulos KC, Sideris D, Tselepis AD. PAF-acetylhydrolase activity of Lp(a) before and during Cu(2+)-induced oxidative modification in vitro. Atherosclerosis. 1996 Aug 23;125(1):121–34.
128. Stafforini DM, Tjoelker LW, Mccormick SPA, Vaitkus D, McIntyre TM, Gray PW, et al. Molecular Basis of the Interaction between Plasma Platelet-activating Factor Acetylhydrolase and Low Density Lipoprotein Molecular Basis of the Interaction between Plasma Platelet- activating Factor Acetylhydrolase and Low Density Lipoprotein. J Biol Chem. 1999;274(11):7018–24.
129. Gardner A a, Reichert EC, Alexander TS, Topham MK, Stafforini DM. Novel mechanism for regulation of plasma platelet-activating factor acetylhydrolase expression in mammalian cells. Biochem J. 2010 Jun;428(2):269–79.

130. Elstad MR, Stafforini DM, McIntyre TM, Prescott SM, Zimmerman GA. Platelet-activating factor acetylhydrolase increases during macrophage differentiation. A novel mechanism that regulates accumulation of platelet-activating factor. J Biol Chem. 1989 May;264(15):8467–70.
131. Stafforini DM. Biology of platelet-activating factor acetylhydrolase (PAF-AH, lipoprotein associated phospholipase A2). Cardiovasc Drugs Ther. 2009 Feb;23(1):73–83.
132. Wu X, McIntyre TM, Zimmerman GA, Prescott SM, Stafforini DM. Molecular characterization of the constitutive expression of the plasma platelet-activating factor acetylhydrolase gene in macrophages. Biochem J. 2003 Oct;375(Pt 2):351–63.
133. Cao Y, Stafforini DM, Zimmerman GA, McIntyre TM, Prescott SM. Expression of plasma platelet-activating factor acetylhydrolase is transcriptionally regulated by mediators of inflammation. J Biol Chem. 1998;273(7):4012–20.
134. Okumura KK, Sagawa N, Ihara Y, Kobayashi F, Itoh H, Mori T. Cortisol and TGF-beta inhibit secretion of platelet-activating factor-acetylhydrolase in a monocyte-macrophage model system [corrected]. Mol Hum Reprod. 1997 Nov;3(11):927–32.
135. Howard KM, Abdel-Al M, Ditmyer M, Patel N. Lipopolysaccharide and platelet-activating factor stimulate expression of platelet-activating factor acetylhydrolase via distinct signaling pathways. Inflamm Res. 2011 Aug;60(8):735–44.
136. MacRitchie AN, Gardner A a, Prescott SM, Stafforini DM. Molecular basis for susceptibility of plasma platelet-activating factor acetylhydrolase to oxidative inactivation. FASEB J. 2007 Apr;21(4):1164–76.
137. Huang YH, Schäfer-Elinder L, Wu R, Claesson HE, Frostegård J. Lysophosphatidylcholine (LPC) induces proinflammatory cytokines by a platelet-activating factor (PAF) receptor-dependent mechanism. Clin Exp Immunol. 1999 May;116(2):326–31.
138. Liu-Wu Y, Hurt-Camejo E, Wiklund O. Lysophosphatidylcholine induces the production of IL-1β by human monocytes. Atherosclerosis. 1998 Apr;137(2):351–7.
139. Gonçalves I, Edsfeldt A, Ko NY, Grufman H, Berg K, Björkbacka H, et al. Evidence supporting a key role of Lp-PLA2-generated lysophosphatidylcholine in human atherosclerotic plaque inflammation. Arterioscler Thromb Vasc Biol. 2012;32(6):1505–12.
140. Tsimihodimos V, Karabina S-AP, Tambaki AP, Bairaktari E, Miltiadous G, Goudevenos J a, et al. Altered distribution of platelet-activating factor- acetylhydrolase activity between LDL and HDL as a function of the severity of hypercholesterolemia. J Lipid Res. 2002 Feb;43(2):256–63.
141. Vickers KC, Maguire CT, Wolfert R, Burns AR, Reardon M, Geis R, et al. Relationship of lipoprotein-associated phospholipase A2 and oxidized low density lipoprotein in carotid atherosclerosis. J Lipid Res. 2009 Sep;50(9):1735–43.
142. Ammirati E, Moroni F, Norata GD, Magnoni M, Camici PG. Markers of Inflammation Associated with Plaque Progression and Instability in Patients with Carotid Atherosclerosis. Mediators Inflamm. 2015;2015(ID 718329).
143. Wegner M, Araszkiewicz A, Pioruńska-Mikołajczak A, Zozulińska-Ziółkiewicz D, Wierusz-Wysocka B, Pioruńska-Stolzmann M. The evaluation of IL-12 concentration, PAF-AH, and PLA(2) activity in patients with type 1 diabetes treated with intensive insulin therapy. Clin Biochem. 2009 Nov;42(16–17):1621–7.

144. Serban M, Tanaseanu C, Kosaka T, Vidulescu C, Stoian I, Marta DS, et al. Significance of platelet-activating factor acetylhydrolase in patients with non-insulin-dependent (type 2) diabetes mellitus. J Cell Mol Med. 2002;6(4):643–7.
145. Kudolo GB, Bressler P, DeFronzo R a. Plasma PAF acetylhydrolase in non-insulin dependent diabetes mellitus and obesity: effect of hyperinsulinemia and lovastatin treatment. J Lipid Mediat Cell Signal. 1997 Nov;17(2):97–113.
146. Miwa M, Miyake T, Yamanaka T, Sugatani J, Suzuki Y, Sakata S, et al. Characterization of serum platelet-activating factor (PAF) acetylhydrolase. Correlation between deficiency of serum PAF acetylhydrolase and respiratory symptoms in asthmatic children. J Clin Invest. 1988 Dec 1;82(6):1983–91.
147. Stafforini DM, Satoh K, Atkinson DL, Tjoelker LW, Eberhardt C, Yoshida H, et al. Platelet-activating factor acetylhydrolase deficiency: A missense mutation near the active site of an anti-inflammatory phospholipase. J Clin Invest. 1996;97(12):2784–91.
148. Ito S, Noguchi E, Shibasaki M, Yamakawa-Kobayashi K, Watanabe H, Arinami T. Evidence for an association between plasma platelet-activating factor acetylhydrolase deficiency and increased risk of childhood atopic asthma. J Hum Genet. 2002;47(2):99–101.
149. Yamada Y, Yoshida H, Ichihara S, Imaizumi T, Satoh K, Yokota M. Correlations between plasma platelet-activating factor acetylhydrolase (PAF-AH) activity and PAF-AH genotype, age, and atherosclerosis in a Japanese population. Atherosclerosis. 2000;150(1):209–16.
150. Hiramoto M, Yoshida H, Imaizumi T, Yoshimizu N, Satoh K. A Mutation in Plasma Platelet-Activating Factor Acetylhydrolase (Val→Phe) is a Genetic Risk Factor for Stroke. Stroke. 1997 Dec 1;28(12):2417 LP-2420.
151. Tetta C, Bussolino F, Modena V, Montrucchio G, Segoloni G, Pescarmona G, et al. Release of platelet-activating factor in systemic lupus erythematosus. Int Arch Allergy Appl Immunol. 1990;91(3):244–56.
152. Serebruany VL, Gurbel PA, Murugesan SR, Lowry DR, Sturm E, Svetlov SI. Depressed plasma platelet-activating factor acetylhydrolase in patients presenting with acute myocardial infarction. Cardiology. 1998 Oct;90(2):127–30.
153. Graham RM, Stephens CJ, Silvester W, Leong LL, Sturm MJ, Taylor RR. Plasma degradation of platelet-activating factor in severely ill patients with clinical sepsis. Crit Care Med. 1994 Feb;22(2):204–12.
154. Vadas P, Gold M, Perelman B, Liss GM, Lack G, Blyth T, et al. Platelet-activating factor, PAF acetylhydrolase, and severe anaphylaxis. N Engl J Med. 2008;358(1):28–35.
155. Tellis CC, Tselepis AD. The role of lipoprotein-associated phospholipase A2 in atherosclerosis may depend on its lipoprotein carrier in plasma. Biochim Biophys Acta. 2009 May;1791(5):327–38.
156. Watson AD, Navab M, Hama SY, Sevanian A, Prescott SM, Stafforini DM, et al. Effect of platelet activating factor-acetylhydrolase on the formation and action of minimally oxidized low density lipoprotein. J Clin Invest. 1995 Feb;95(2):774–82.
157. Theilmeier G. HDL-associated PAF-AH reduces endothelial adhesiveness in apoE-/- mice. FASEB J. 2000 Oct 1;14(13):2032–9.
158. Quarck R, De Geest B, Stengel D, Mertens A, Lox M, Theilmeier G, et al. Adenovirus-mediated gene transfer of human platelet-activating factor-acetylhydrolase prevents injury-induced neointima formation and reduces spontaneous atherosclerosis in apolipoprotein E-deficient mice. Circulation. 2001 May;103(20):2495–500.

159. Filippatos TD, Rizos EC, Tsimihodimos V, Gazi IF, Tselepis AD, Elisaf MS. Small high-density lipoprotein (HDL) subclasses are increased with decreased activity of HDL-associated phospholipase A2 in subjects with prediabetes. Lipids. 2013;48(6):547–55.
160. Lagos KG, Filippatos TD, Tsimihodimos V, Gazi IF, Rizos C, Tselepis a D, et al. Alterations in the high density lipoprotein phenotype and HDL-associated enzymes in subjects with metabolic syndrome. Lipids. 2009 Jan;44(1):9–16.
161. Kiechl S, Willeit J, Mayr M, Viehweider B, Oberhollenzer M, Kronenberg F, et al. Oxidized phospholipids, lipoprotein(a), lipoprotein-associated phospholipase A2 activity, and 10-year cardiovascular outcomes: prospective results from the Bruneck study. Arterioscler Thromb Vasc Biol. 2007 Aug;27(8):1788–95.
162. Persson M, Hedblad B, Nelson JJ, Berglund G. Elevated Lp-PLA2 levels add prognostic information to the metabolic syndrome on incidence of cardiovascular events among middle-aged nondiabetic subjects. Arterioscler Thromb Vasc Biol. 2007;27(6):1411–6.
163. Sabatine MS, Morrow DA, O'Donoghue M, Jablonksi KA, Rice MM, Solomon S, et al. Prognostic utility of lipoprotein-associated phospholipase A2 for cardiovascular outcomes in patients with stable coronary artery disease. Arterioscler Thromb Vasc Biol. 2007;27(11):2463–9.
164. Opal S, Laterre PF, Abraham E, Francois B, Wittebole X, Lowry S, et al. Recombinant human platelet-activating factor acetylhydrolase for treatment of severe sepsis: results of a phase III, multicenter, randomized, double-blind, placebo-controlled, clinical trial. Crit Care Med. 2004;32(2):332–41.
165. Roberts A. Coronary artery disease: Darapladib fails to improve the STABILITY of CAD. Nat Rev Cardiol. 2014 Jun;11(6):310.
166. ML O, Braunwald E, HD W, al et. Effect of darapladib on major coronary events after an acute coronary syndrome: The solid-timi 52 randomized clinical trial. JAMA. 2014 Sep 10;312(10):1006–15.
167. Wilensky RL, Shi Y, Mohler ER, Hamamdzic D, Burgert ME, Li J, et al. Inhibition of lipoprotein-associated phospholipase A2 reduces complex coronary atherosclerotic plaque development. Nat Med. 2008;14(10):1059–66.
168. Hu M, Zhang J, Wang W, Wu W, Ma Y, Chen W, et al. The inhibition of lipoprotein-associated phospholipase A2 exerts beneficial effects against atherosclerosis in LDLR-deficient mice. Acta Pharmacol Sin. 2011 Oct;32(10):1253–8.
169. Mor G, Cardenas I, Abrahams V, Guller S. Inflammation and pregnancy: the role of the immune system at the implantation site. Ann N Y Acad Sci. 2011 Mar;1221(1):80–7.
170. Miyaura S, Maki N, Byrd W, Johnston JM. The hormonal regulation of platelet-activating factor acetylhydrolase activity in plasma. Lipids. 1991 Dec;26(12):1015–20.
171. Tiemann U. The role of platelet-activating factor in the mammalian female reproductive tract. Reprod Domest Anim. 2008 Dec;43(6):647–55.
172. Fan P, Liu X-H, He G-L, Zhang S, Zhang J-X, Bai H. Maternal and fetal plasma platelet-activating factor acetylhydrolase activity and distribution in pre-eclampsia. Pediatr Res. 2012 Oct;72(4):426–31.
173. Gao Q, He G-L, Zhang L, Bai H, Liu X-H, Fan P. Activity and distribution of plasma platelet- activating factor acetylhydrolase in women with gestational diabetes mellitus and their neonates. Diabetes Metab Res Rev. 2016;32:634–42.
174. Okumura K, Sagawa N, Kobayashi F, Nanno H, Matsumoto T, Itoh H, et al. Activity of platelet-activating-factor-acetylhydrolase and the nitric oxide metabolite level in the plasma of women who develop transient pregnancy hypertension during later pregnancy. Reprod Fertil Dev. 1999;11(2):75–9.

175. Mai C, Wang B, Wen J. Lipoprotein-associated phospholipase A2 and AGEs are associated with cardiovascular risk factors in women with history of gestational diabetes mellitus. Gynecol Endocrinol. 2014 Mar;30(3):241–4.
176. Derbent A, Kargili A, Koca C, Gümüs I, Sevgili S, Simavli S, et al. Serum platelet-activating factor acetylhydrolase activity: relationship with metabolic snydrome in women with a history of gestational diabetes mellitus. Gynecol Endocrinol. 2011;27(2):128–33.
177. Ginsburg BE, Zetterström R. Serum cholesterol concentrations in newborn infants with gestational ages of 28-42 weeks. Acta Paediatr Scand. 1980 Sep;69(5):587–92.
178. Carlson SE. Plasma cholesterol and lipoprotein levels during fetal development and infancy. Ann N Y Acad Sci. 1991;623:81–9.
179. Sreckovic I, Birner-Gruenberger R, Obrist B, Stojakovic T, Scharnagl H, Holzer M, et al. Distinct composition of human fetal HDL attenuates its anti-oxidative capacity. Biochim Biophys Acta - Mol Cell Biol Lipids. 2013;1831(4):737–46.
180. Sreckovic I, Birner-Gruenberger R, Besenboeck C, Miljkovic M, Stojakovic T, Scharnagl H, et al. Gestational diabetes mellitus modulates neonatal high-density lipoprotein composition and its functional heterogeneity. Biochim Biophys Acta. 2014 Nov;1841(11):1619–27.
181. American Diabetes Association. 12. Management of Diabetes in Pregnancy. Diabetes Care. 2014;38(Supplement_1):S77–9.
182. Caughey A, Valent A. When to Deliver Women with Diabetes in Pregnancy? Am J Perinatol. 2016 Jul 19;33(13):1250–4.
183. Schliefsteiner C, Peinhaupt M, Kopp S, Lögl J, Lang-Olip I, Hiden U, et al. Human Placental Hofbauer Cells Maintain an Anti-inflammatory M2 Phenotype despite the Presence of Gestational Diabetes Mellitus. Front Immunol. 2017;8(July):1–17.
184. Cervar M, Blaschitz A, Dohr G, Desoye G. Paracrine regulation of distinct trophoblast functions in vitro by placental macrophages. Cell Tissue Res. 1999;295(2):297–305.
185. Rodero MP, Khosrotehrani K. Skin wound healing modulation by macrophages. Int J Clin Exp Pathol. 2010;3(7):643–53.
186. Witkowska a M, Borawska MH. Soluble intercellular adhesion molecule-1 (sICAM-1): an overview. Eur Cytokine Netw. 2004;15(2):91–8.
187. Gho YS, Kleinman HK, Sosne G. Angiogenic activity of human soluble intercellular adhesion molecule-1. Cancer Res. 1999;59(20):5128–32.
188. Dorey FJ. In brief: Statistics in brief: Statistical power: What is it and when should it be used? Clin Orthop Relat Res. 2011;469(2):619–20.
189. Sprague AH, Khalil RA. Inflammatory Cytokines in Vascular Dysfunction and Vascular Disease. Biochem Pharmacol. 2010;78(6):539–52.
190. Mordwinkin NM, Ouzounian JG, Yedigarova L, Montoro MN. Alteration of endothelial function markers in women with gestational diabetes and their fetuses. J Matern Fetal Neontal Med. 2013;26(5):507–12.
191. Sobrevia L, Abarzúa F, Nien JK, Salomón C, Westermeier F, Puebla C, et al. Review: Differential placental macrovascular and microvascular endothelial dysfunction in gestational diabetes. Placenta. 2011;32(SUPPL. 2):S159–64.
192. Bielicki JK, Knoff LJ, Tribble DL, Forte TM. Relative sensitivities of plasma lecithin:cholesterol acyltransferase, platelet-activating factor acetylhydrolase, and paraoxonase to in vitro gas-phase cigarette smoke exposure. Atherosclerosis. 2001;155(1):71–8.

193. Maki N, Hoffman DR, Johnston JM. Platelet-activating factor acetylhydrolase activity in maternal, fetal, and newborn rabbit plasma during pregnancy and lactation. Proc Natl Acad Sci U S A. 1988;85(3):728–32.
194. Kominiarek MA, Peaceman AM. Gestational weight gain. Am J Obstet Gynecol. 2017 May;S0002-9378(17):30651-8.
195. Devlieger R, Benhalima K, Damm P, Van Assche A, Mathieu C, Mahmood T, et al. Maternal obesity in Europe: where do we stand and how to move forward?: A scientific paper commissioned by the European Board and College of Obstetrics and Gynaecology (EBCOG). Eur J Obstet Gynecol Reprod Biol. 2016 Jun;201:203–8.
196. Torres-Castro I, Arroyo-Camarena ÚD, Martínez-Reyes CP, Gómez-Arauz AY, Dueñas-Andrade Y, Hernández-Ruiz J, et al. Human monocytes and macrophages undergo M1-type inflammatory polarization in response to high levels of glucose. Immunol Lett. 2016 Aug;176:81–9.
197. Roma-Lavisse C, Tagzirt M, Zawadzki C, Lorenzi R, Vincentelli A, Haulon S, et al. M1 and M2 macrophage proteolytic and angiogenic profile analysis in atherosclerotic patients reveals a distinctive profile in type 2 diabetes. Diabetes Vasc Dis Res. 2015 Jul 1;12(4):279–89.
198. Cucak H, Grunnet LG, Rosendahl A. Accumulation of M1-like macrophages in type 2 diabetic islets is followed by a systemic shift in macrophage polarization. J Leukoc Biol. 2014 Jan;95(1):149–60.
199. Young OM, Tang Z, Niven-Fairchild, Tracy Tadesse S, Krikun G, Norwitz ER, Mor G, et al. Toll-like Receptor-Mediated Responses by Placental Hofbauer Cells (HBCs): A Potential Pro-Inflammatory Role for Fetal M2 Macrophages*. Am J Clin Obs. 2015;73(1):22–35.
200. Zeyda M, Farmer D, Todoric J, Aszmann O, Speiser M, Györi G, et al. Human adipose tissue macrophages are of an anti-inflammatory phenotype but capable of excessive pro-inflammatory mediator production. Int J Obes. 2007;31:1420–8.
201. Bari MF, Weickert MO, Sivakumar K, James SG, Snead DRJ, Tan BK, et al. Elevated Soluble CD163 in Gestational Diabetes Mellitus: Secretion from Human Placenta and Adipose Tissue. PLoS One. 2014 Jan;9(7):e101327.
202. Yu J, Zhou Y, Gui J, Li A, Su X, Feng L. Assessment of the number and function of macrophages in the placenta of gestational diabetes mellitus patients. J Huazhong Univ Sci Technol. 2013;33(5):725–9.
203. Rath M, Müller I, Kropf P, Closs EI, Munder M. Metabolism via Arginase or Nitric Oxide Synthase: Two Competing Arginine Pathways in Macrophages. Front Immunol. 2014;5(October):1–10.
204. Brown MB, von Chamier M, Allam AB, Reyes L. M1/M2 Macrophage Polarity in Normal and Complicated Pregnancy. Front Immunol. 2014;5(November):1–10.
205. Khan MA, Assiri AM, Broering DC. Complement and macrophage crosstalk during process of angiogenesis in tumor progression. J Biomed Sci. Journal of Biomedical Science; 2015;22(1):58.
206. Mantovani A, Schioppa T, Porta C, Allavena P, Sica A. Role of tumor-associated macrophages in tumor progression and invasion. Cancer Metastasis Rev. 2006;25(3):315–22.
207. Zhao H, Ozen M, Wong RJ, Stevenson DK. Heme oxygenase-1 in pregnancy and cancer: Similarities in cellular invasion, cytoprotection, angiogenesis, and immunomodulation. Front Pharmacol. 2015;6(Jan):1–10.
208. Magatti M, Vertua E, De Munari S, Caro M, Caruso M, Silini A, et al. Human amnion

favours tissue repair by inducing the M1-to-M2 switch and enhancing M2 macrophage features. J Tissue Eng Regen Med. 2016;4(7):524–31.
209. McGovern N, Shin A, Low G, Low D, Duan K, Yao LJ, et al. Human fetal dendritic cells promote prenatal T-cell immune suppression through arginase-2. Nature. 2017 Jun 14;546(7660):662–6.
210. Tabet F, Vickers K, Torres L, Wiese C. HDL-transferred microRNA-223 regulates ICAM-1 expression in endothelial cells. Nat Commun. 2014;5(3292).
211. Kawano Y, Narahara H, Johnston JM. Inhibitory effect of interleukin-8 on the secretion of platelet-activating factor acetylhydrolase by human decidual macrophages. J Soc Gynecol Investig. 1999;6(6):328–32.
212. Narahara H, Mine SI, Kawano Y, Johnston JM, Miyakawa I. Effects of colony-stimulating factors on the secretion of platelet-activating factor acetylhydrolase by human decidual macrophages. Am J Obstet Gynecol. 2003;188(1):157–61.
213. Narahara H, Nishioka Y, Johnston JM. Secretion of platelet-activating factor acetylhydrolase by human decidual macrophages. J Clin Endocrinol Metab. 1993 Nov;77(5):1258–62.
214. Averna MR, Barbagallo CM, Di Paola G, Labisi M, Pinna G, Marino G, et al. Lipids, lipoproteins and apolipoproteins AI, AII, B, CII, CIII and E in newborns. Biol Neonate. 1991;60(3–4):187–92.
215. Kujiraoka T, Iwasaki T, Ishihara M, Ito M, Nagano M, Kawaguchi A, et al. Altered distribution of plasma PAF-AH between HDLs and other lipoproteins in hyperlipidemia and diabetes mellitus. J Lipid Res. 2003 Oct;44(10):2006–14.
216. Watson AD, Leitinger N, Navab M, Faull KF, Hörkkö S, Witztum JL, et al. Structural identification by mass spectrometry of oxidized phospholipids in minimally oxidized low density lipoprotein that induce monocyte/endothelial interactions and evidence for their presence in vivo. J Biol Chem. 1997 May 23;272(21):13597–607.
217. Leitinger N, Tyner TR, Oslund L, Rizza C, Subbanagounder G, Lee H, et al. Structurally similar oxidized phospholipids differentially regulate endothelial binding of monocytes and neutrophils. Proc Natl Acad Sci U S A. 1999;96(21):12010–5.
218. Grissa O, Atègbo JM, Yessoufou A, Tabka Z, Miled A, Jerbi M, et al. Antioxidant status and circulating lipids are altered in human gestational diabetes and macrosomia. Transl Res. 2007;150(3):164–71.
219. Negro S, Boutsikou T, Briana DD, Tataranno ML, Longini M, Proietti F, et al. Maternal obesity and perinatal oxidative stress: the strength of the association. J Biol Regul Homeost Agents. 31(1):221–7.
220. Desoye G, Hartmann M, Jones CJP, Wolf HJ, Kohnen G, Kosanke G, et al. Location of insulin receptors in the placenta and its progenitor tissues. Microsc Res Tech. 1997;38(1–2):63–75.
221. Memon R, Fuller J, Moser AH, Feingold K, Grunfeld C. In vivo regulation of plasma platelet-activating factor acetylhydrolase during the acute phase response. Am J Physiol Regul Intgr Comp Physiol. 1999;277:R94–103.
222. Wang W-Y, Li J, Yang D, Xu W, Zha R, Wang Y. OxLDL stimulates lipoprotein-associated phospholipase A2 expression in THP-1 monocytes via PI3K and p38 MAPK pathways. Cardiovasc Res. 2010 Mar 1;85(4):845–52.
223. Turner MD, Nedjai B, Hurst T, Pennington DJ. Cytokines and chemokines: At the crossroads of cell signalling and inflammatory disease. Biochim Biophys Acta - Mol Cell Res. 2014;1843(11):2563–82.

224. Benoit SC, Clegg DJ, Seeley RJ, Woods SC. Insulin and leptin as adiposity signals. Recent Prog Horm Res. 2004;59:267–85.
225. Okada T, Miyashita M, Kuromori Y, Iwata F, Harada K, Hattori H. Platelet-activating factor acetylhydrolase concentration in children with abdominal obesity. Arterioscler Thromb Vasc Biol. 2006 May;26(5):e40-1.
226. Sakka S, Siahanidou T, Voyatzis C, Pervanidou P, Kaminioti C, Lazopoulou N, et al. Elevated circulating levels of lipoprotein-associated phospholipase A2 in obese children. Clin Chem Lab Med. 2015 Jan 1;53(7):1119.
227. Nelson TL, Biggs ML, Kizer JR, Cushman M, Hokanson JE, Furberg CD, et al. Lipoprotein-associated phospholipase A2 (Lp-PLA2) and future risk of type 2 diabetes: results from the Cardiovascular Health Study. J Clin Endocrinol Metab. 2012 May;97(5):1695–701.

8. Picture Credits

To create Figures 2, 3, 4, and 24 shapes and drawings obtained from the Powerpoint image bank of the 'Servier Medical Art Server' have been used and modified. Servier provides these illustrations under a Creative Commons Attribution 3.0 unported license, allowing modification, reproduction and redistribution in any format.
http://www.servier.com/Powerpoint-image-bank
https://creativecommons.org/licenses/by/3.0/

Figure 3 was adapted with permission of the authors from: Desoye G, Gauster M, Wadsack C. Placental transport in pregnancy pathologies. *Am J Clin Nutr* (2011) **94**:1896–1902.

In Figure 5, Ac-Dil-LDL staining was kindly provided by Jelena Lögl and the ultrastructural TEM picture by Michael Gruber, both whose work is gratefully acknowledged.

9. Acknowledgements

Last but not least, I want to take the time to say thank you to all those, who accompanied me throughout the past 5 years.

First of all, I am grateful to my supervisors Gernot Desoye and Christian Wadsack, who believed in me and my capabilities right from the start. They encouraged me to follow up on my ideas for new experiments and helped broaden my technical skills and knowledge. Both also motivated me to embark on a new adventure, my stay abroad in Nashville, TN. I am grateful to Christian, who always had an open door and ear, and helped my scientific development until here and hopefully also from here on.

None of the work described here would have been possible without the help from our study nurses, Bettina Amtmann and Petra Winkler, who continuously enroll patients in the delivery ward. They do an amazing job.

I want to thank Susanne Kopp, Jasmin Strutz and Ate Michlmaier for their technical support; without them, the lab would most possible break down. Susi taught me many protocols used in the lab so I could work independently but also carried out all histochemical experiments for me, so I could work on other things – I am really grateful for that. Jasmin is providing an endless supply of endothelial cells for all of us, we couldn't work without her, but I also wouldn't want to miss her as a friend, travel-buddy and co-gardener. Ate always isolated trophoblasts in parallel with me isolating HBCs and I just loved our Radio-Wien-Cell Culture-Parties.

My fellow PhD students in the lab, in particular Alejandro, Fran, Birgit and Michi, are more friends than colleagues. I want to thank them for their friendship, steady support and sharing all the heights and depths of a PhD study program. I really enjoyed coming to work every single day, and I want to thank everybody in the lab for the great teamwork we have.

I also want to thank our collaborator at Vanderbilt University, Dr. Kasey C. Vickers, for giving me the opportunity to start an entirely new project under his supervision and developing the needed skills, and I also want to thank my colleagues in Nashville, who helped at work and also showed me around the town.

This thesis is dedicated to my husband Paul. I probably would never have thought about getting my PhD if he hadn't brought it up, and although my daily reports about what I did in the lab sounded mostly like Chinese to him, he never stopped listening and tried to follow. I am so grateful and happy that he is there for me every single day.

10. Appendix

The following Tables include all reagents, kits, antibodies, instruments and software packages used during the thesis project for data generation and analysis. Detailed information about suppliers, dilutions etc. is provided here and was omitted in the Material and Methods section for other fluent legibility.

Table 7: Hofbauer cell isolation: Reagents and consumables used and their suppliers.

Chemicals	**Supplier**
Trypsin 2.5%	Gibco, Carlsbad, CA, USA
MgSO4	Sigma, Steinheim, DE
CaCl2	Sigma, Steinheim, DE
Dnase I	Roche, Basel, CH
Collagenase A	Roche, Basel, CH
HBSS 1x	Gibco, Carlsbad, CA, USA
HBSS 10x	Gibco, Carlsbad, CA, USA
RPMI 1640 w/o phenol red	Gibco, Carlsbad, CA, USA
Percoll Density Solution	Sigma, Steinheim, DE
Dynabeads anti goat-IgG	Invitrogen, Carlsbad, CA, USA
anti EGFR antibody	NeoMarkers, Fremont, CA, USA
anti CD10 antibody	Abcam, Cambridge, UK
MaM macrophage medium + supplements	ScienCell, Carlsbad, CA, USA
Amicon Ultra Centrifual Concentrators MwCo 3kD	Merck Millipore, Billerica, CA, USA

Table 8: Reagents used to regulate LpPLA2 activity in HBC cell culture in vitro.

Chemicals	**Supplier**
Darapladib	MedChemExpress, Sollentuna, SE
D-Glucose	Sigma, Steinheim, DE
L-Glucose	Sigma, Steinheim, DE
Leptin	Sigma, Steinheim, DE
Insulin	Calbiochem, San Diego, CA, USA
TNFa	Sigma, Steinheim, DE
IL-4	Sigma, Steinheim, DE
IL-13	Sigma, Steinheim, DE
ICAM-1	Sigma, Steinheim, DE
VCAM-1	Sigma, Steinheim, DE
POV-PC	Cayman Chemical, Ann Arbor, MA, USA
Paz-PC	Cayman Chemical, Ann Arbor, MA, USA
PG-PC	Cayman Chemical, Ann Arbor, MA, USA

Table 9: Media and supplements used for cultivation of Endothelial Cells and Trophoblast.

Chemicals	Supplier
EBM Endothelial Basal Medium	Lonza, Basel, CH
EBM EGM-V Bullet Kit	Lonza, Basel, CH
Dulbeccos Modified Eagel Medium	Gibco, Carlsbad, CA, USA
Fetal Bovine Serum	Lonza, Basel, CH
Penicillin/Streptomycin 5%	Gibco, Carlsbad, CA, USA

Table 10: Reagents used for Immune Cyto-/Histochemistry and Immune Fluorescence Staining

Chemicals	Supplier
Antibody Diluent	Dako, Santa Clara, CA, USA
Antibody Enhancer	Dako, Santa Clara, CA, USA
Larg HRP Polymer	Dako, Santa Clara, CA, USA
AEC Chromogen Solution	Dako, Santa Clara, CA, USA
Hydrogen Peroxide Block	Dako, Santa Clara, CA, USA
UltraV Block	Dako, Santa Clara, CA, USA
Haemalaun	Sigma, Steinheim, DE
Prolong Gold Antifade with DAPI	Invitrogen, Carlsbad, CA, USA

Table 11: Reagents used for preparation of HBCs for FACS.

Chemicals	Supplier
TrypLE Select	Gibco, Carlsbad, CA, USA
Bovine Serum Albumin	Sigma, Steinheim, DE
HBSS 1x	Gibco, Carlsbad, CA, USA
Phosphate buffered saline - Tablets	Thermo Scientific, Waltham, CA, USA

Table 12: Reagents and Taqman Assays used for RNA isolation, cDNA transcription and RT-qPCR.

Chemicals	Supplier
RNeasy Mini kit	Qiagen, Hilden, DE
Superscript Reverse Transcriptase II	Invitrogen, Carlsbad, CA, USA
Random Hexamer Primers	Thermo Scientific, Waltham, CA, USA
Universal MasterMix for Taqman	Roche, Basel, CH
PLA2G7 Taqman assay, ID: Hs00965837_m1	Life Technologies, Darmstadt, DE
RL30 Taqman assay, ID: Hs02800695_m1	Life Technologies, Darmstadt, DE
PPIA Taqman assay, ID: Hs04194521_s1	Life Technologies, Darmstadt, DE

Table 13: Reagents and Consumables used for Polyacrylamide Gel Electrophoresis and Western Blotting.

Chemicals	Supplier
10x Tris-Glycine SDS Running Buffer	Biorad, Hercules, CA, USA
Mini Protean TGX Gels 4-20%	Biorad, Hercules, CA, USA
2x Laemmli Buffer	Sigma, Steinheim, DE
Page Ruler Plus Prestained Protein Marker	Invitrogen, Carlsbad, CA, USA
TransBlot Turbe Mini Nitrocellulose Membranes	Biorad, Hercules, CA, USA
Non-fat dry milk powder	Biorad, Hercules, CA, USA
TBE Buffer	In-house Pharmacy, General Hospital Graz, AT
Tween 100	Sigma, Steinheim, DE
West Pico/Femto ECL Reagent	Pierce, Waltham, MA, USA

Table 14: Consumables and Reagents used in Assays of HDL functionality (ECIS, ClickIT™Lipid Peroxidation assay, DHR-Assay).

Chemicals	Supplier
8W10E+ electrode slides	ibidi, Munich, DE
ClickIT Lipid Peroxidation Kit	Invitrogen, Carlsbad, CA, USA
12-well chamber slides for fluorescence microscopy	ibidi, Munich, DE
Dihydrorhodamine 123	Sigma, Steinheim, DE
Chelex 100	Sigma, Steinheim, DE
Darapladib	MedChemExpress, Sollentuna, SE
2-hydroxyquinoline	Sigma, Steinheim, DE
DMSO	Sigma, Steinheim, DE
Ethanol 100%	Sigma, Steinheim, DE
Bovine Serum Albumin	Sigma, Steinheim, DE
POV-PC	Cayman Chemical, Ann Arbor, MA, USA
Paz-PC	Cayman Chemical, Ann Arbor, MA, USA
PG-PC	Cayman Chemical, Ann Arbor, MA, USA

Table 15: Consumables and Reagents used for Isolation and Characterization of adult and fetal lipoproteins.

Chemicals	Supplier
Vacuette® EDTA blood collection tube	Greiner Bio-One, Kremsmünster, AT
Potassium bromide	Sigma, Steinheim, DE
PD10 de-salting columns	GE Healthcare, Little Chalfont, UK
Vivaspin Centrifuge Concentrators (MwCO 5kDa)	Sartorius, Goettingen, DE
Cholesterol FS kit	Greiner Diagnostic Group, Bahlingen, DE
Bichinonic Acid Kit	Pierce, Waltham, MA, USA

Table 16: Multiplex panels and ELISA kits used, their suppliers, as well as sample type and dilution of sample used. * Panel contained antibodies against: MCP-1, MCP-3, IL-1α, IL-1β, IL-4, IL-6, IL-8, IL-10, IL-12p70, IL-13, IL-1RA, ICAM-1, VCAM-1, VEGF, MPO, M-CSF, TNFα, and INFγ. ** Panel contained antibodies against: EGF; FGF, PDGF-AB, TGFα, Leptin. † diluted from the Supernatant originally concentrated 4:1 for multiplex assay; # panel contained antibodies against ICAM-1, VCAM-1, P-Selectin, E-Selectin, VE-Cadherin, M-CSF.

Kit	Manufacturer	Sample Type	Dilution used
Aimplex Custom 18-plex array*	YSL Bioprocess Dev. Co., Pasadena, CA, USA	HBC supernatant	4:1
Aimplex Custom 5-plex array**	YSL Bioprocess Dev. Co., Pasadena, CA, USA	HBC supernatant	4:1
TGFβ Ready Set Go ELISA	eBioscience, San Diego, CA, USA	HBC supernantant	1:3†
IL-1β Ready Set Go ELISA	eBioscience, San Diego, CA, USA	HBC supernantant	1:2†
IL-1RA Mini ABTS Development kit	Peprotech, Rocky Hill, NJ, USA	HBC supernantant	1:50†
IL-4 Mini ABTS Development kit	Peprotech, Rocky Hill, NJ, USA	HBC supernantant	1:2†
IL-6 Mini ABTS Development kit	Peprotech, Rocky Hill, NJ, USA	HBC supernantant	1:2†
IL-10 Mini ABTS Development kit	Peprotech, Rocky Hill, NJ, USA	HBC supernantant	1:2†
IL-12 Mini ABTS Development kit	Peprotech, Rocky Hill, NJ, USA	HBC supernantant	1:2†
IL-13 Ready Set Go ELISA	eBioscience, San Diego, CA, USA	HBC supernantant	1:2†
ICAM-1 Mini ABTS Development kit	Peprotech, Rocky Hill, NJ, USA	HBC supernantant	undiluted†
VCAM-1 Quantikine ELISA	RnD Systems, Minneapolis, MN, USA	HBC supernantant	undiluted†
TNFα Mini ABTS Development kit	Peprotech, Rocky Hill, NJ, USA	HBC supernantant	1:3†
MCP-1 Mini ABTS Development kit	Peprotech, Rocky Hill, NJ, USA	HBC supernantant	1:50†
VEGF Mini ABTS Development kit	Peprotech, Rocky Hill, NJ, USA	HBC supernantant	1:4†
Quantibody Custom array#	Raybiotech, Norcross, GA, USA	pAECs lysate	1:5
Insulin ELISA for Siemens Advia	Siemens Healthcare, Vienna, AT	Neonatal plasma	undiluted
Leptin ELISA	Merck Millipore, Billerica, MA, USA	Neonatal plasma	undiluted
TNFα Mini ABTS Development kit	Peprotech, Rocky Hill, NJ, USA	Neonatal plasma	undiluted
IL-4 Mini ABTS Development kit	Peprotech, Rocky Hill, NJ, USA	Neonatal plasma	1:2
IL-13 Ready Set Go ELISA	eBioscience, San Diego, CA, USA	Neonatal plasma	undiluted
ICAM-1 Mini ABTS Development kit	Peprotech, Rocky Hill, NJ, USA	Neonatal plasma	1:2
VCAM-1 Quantikine ELISA	RnD Systems, Minneapolis, MN, USA	Neonatal plasma	1:2

TNFα Mini ABTS Development kit	Peprotech, Rocky Hill, NJ, USA	Neonatal plasma	undiluted
TBARS Assay Kit	Cayman Chemical, Ann Arbor, MA, USA	Neonatal plasma	undiluted
PAF-AH Assay Kit	Cayman Chemical, Ann Arbor, MA, USA	HBC supernantant	undiluted
PAF-AH Assay Kit	Cayman Chemical, Ann Arbor, MA, USA	Neonatal plasma	undiluted

Table 17 Antibodies used in this study, their suppliers, purpose and dilution used.

Antibodies	Supplier	used for	Dilution
α-human-CD163 APC	Biolegend	FACS	1:50
mouse α-human-CD163	Thermo Fisher	IHC	1:1000
mouse α-human-CD163	Thermo Fisher	ICC	1:50
mouse α-human-CD163	Thermo Fisher	IF	1:25
mouse α-human-CD163	Thermo Fisher	Western Blot	1:750
mouse-α-human-CD68	Dako	IHC	1:100
mouse-α-human-CD68	Dako	ICC	1:500
mouse-α-human CD14	BD Pharmingen	ICC	1:500
α CD11b Horizon V450	BD Pharmingen	FACS	1:20
rabbit-α-human CD11b	Abcam	IHC	1:250
rabbit-α-human CD11b	Abcam	ICC	1:500
α CD11c PE	BD Pharmingen	FACS	1:50
mouse-α-human CD11c	Abcam	IHC	1:250
mouse-α-human CD11c	Abcam	ICC	1:500
α CD206 FITC	BD Pharmingen	FACS	1:10
mouse-α-human CD206	NovusBio	IHC	1:50
mouse-α-human CD206	NovusBio	IF	1:100
α CD209 PerCPCy5.5	BD Pharmingen	FACS	1:10
mouse-α-human CD209	NovusBio	IHC	1:50
mouse-α-human CD209	NovusBio	ICC	1:200
mouse-α-human CD209	NovusBio	IF	1:100
α CD40 - FITC	BD Pharmingen	FACS	1:20
rabbit-α-human CD40	Abcam	IHC	1:50
α CD45 PE	BD Pharmingen	FACS	1:10

mouse-α-human CD45	Abcam	IF	1:50
α CD80 Horizon V450	BD Pharmingen	FACS	1:20
mouse-α-human CD80	Abcam	IF	1:100
α CD86 Horizon V450	BD Pharmingen	FACS	1:20
mouse-α-human CD86	NovusBio	IF	1:100
mouse-α-human CD90 PE	Biolegend	FACS	1:50
mouse-α-human CD90	Dianova	ICC	1:1000
mouse-α-human SMA	Dako	ICC	1:300
mouse-α-human Desmin	Dako	ICC	1:300
rabbit-α human PAF-AH	Cayman Chemical	ICC	1:300
rabbit-α human PAF-AH	Cayman Chemical	IF	1:100
rabbit-α human PAF-AH	Cayman Chemical	Western Blot	1:750
rabbit-α-human vWF	Dako	ICC	1:250
mouse-α-human vWF	Thermo Fisher	IF	1:100
mouse-α-human CK7	Dako	ICC	1:750
rabbit-α-human CK7	Abgent	IF	1:50
mouse-α-oxPL E06	Avanti Polar Lipids	IF	1:200
mouse-α-oxPL E06	Avanti Polar Lipids	Western Blot	1:1000
mouse-α-human β-Actin	Abcam	Western Blot	1:10000
2^{nd} goat anti mouse IgG	Biorad	Western Blot	respective to primary Ab
2^{nd} goat anti rabbit IgG	Biorad	Western Blot	respective to primary Ab
Negative Control for Mouse IgG	NeoMarkers	ICC	1:250
Negative Control for Rabbit IgG	NeoMarkers	ICC	1:250
DyLight Alexa 488	Thermo Fisher	IF	1:50
DyLight Alexa 555	Thermo Fisher	IF	1:100
Dylight Alexa 633	Thermo Fisher	IF	1:50